AN ABSTRACT OF THE DISSERTATION OF

Scott R. Waichler for the degree of Doctor of Philosophy in Bioresource Engineering presented on August 31, 2000. Title: Simulation of Vegetation and Hydrology for Climate Change Analysis of a Mountain Watershed.

Redacted for Privacy

Abstract approved: _____
Richard H. Cuenca

Climate change is expected to have both direct and indirect effects on water resources. Hydrologic impacts of two indirect effects, vegetation density and stomatal conductance, are evaluated for the American River, a 200 km^2 watershed in the Cascade Range of Washington state. First, a set of distributed hydrology-biogeochemistry model structures are created by coupling DHSVM (Distributed Hydrology-Soil-Vegetation Model) and Biome-BGC (BioGeochemistry Cycles). The model structures are applied to idealized hillslopes and current and future climate scenarios for the watershed. Eleven model structures, differing in vertical 1-D hydrology parameterization, lateral water routing, timestep, slope and aspect, are tested. Sensitivity of hydrology and vegetation density (as measured by leaf area index, LAI) is evaluated with respect to model structure, lapsed climate (elevation), climate change, and soil thickness and nitrogen input rate. Lapsed climate accounts for the largest range in LAI, but choice of model structure is also significant, highlighting opportunities and problems in model development. LAI is water-limited at low elevations, temperature-limited at high elevations, and solar-limited at all elevations. All model structures predict increased LAI under the future scenario that includes reduced stomatal conductance—the conifer forest grows denser. Next, climate scenarios and LAI results from the idealized hillslope simulations are input to the hydrology model DHSVM for hydrologic analysis of the full American River watershed. Basin-average annual precipitation, streamflow, and evapotranspiration all increase under the future climate scenario. The direct effect of increased temperature causes the major hydrologic impact, reduced snowpack and altered seasonal timing of

streamflow and ET. Indirect effects of altered LAI and stomatal conductance on hydrology are minor in comparison to the direct effects. Future streamflow and ET are essentially the same between the simplest treatment of climate change, involving fixed LAI and physical climate change only, and the most detailed treatment, involving variable LAI and reduced stomatal conductance in addition to physical climate change.

Simulation of Vegetation and Hydrology for Climate Change Analysis of a Mountain Watershed

by

Scott R. Waichler

A dissertation
submitted to
Oregon State University,
Corvallis, Oregon

in partial fulfillment of
the requirements for the
degree of

Doctor of Philosophy

Presented August 31, 2000
Commencement June 2001

Doctor of Philosophy dissertation of Scott R. Waichler presented on August 31, 2000.

APPROVED:

Redacted for Privacy

Major Professor, representing Bioresource Engineering

Redacted for Privacy

Head of Department of Bioresource Engineering

Redacted for Privacy

Dean of Graduate School

I understand that my dissertation will become part of the permanent collection of Oregon State University libraries. My signature below authorizes release of my dissertation to any reader upon request.

Redacted for Privacy

Scott R. Waichler, Author

ACKNOWLEDGMENTS

I wish to thank Dr. Ron Neilson for bringing me into the project and ensuring excellent funding and facility support in the Forestry Sciences Laboratory. Project funding was provided by the EPA Regional Hydrologic Vulnerability to Climate Change Program, and the U.S. Forest Service. Major funding was also provided by the Dept. of Bioresource Engineering Graduate Fellowship.

I was given much important guidance by Richard Cuenca, Mark Wigmosta, John Selker, and Ron Neilson. Thank you for helping me in my intellectual and professional adventure at OSU.

Valuable technical assistance was provided by Mark Wigmosta, Ed Llewellyn, Marcela Brugnach, Peter Thornton, Bill Perkins, Ray Drapek, Glynis Bower, Pascal Storck, and Bart Nijssen. All of them contributed gold nuggets of help along the way.

Finally, I am deeply grateful to my wife, Wendy Sims Waichler, for believing in me and encouraging me when the going got tough. Wendy also assumed much of our household and family workload, allowing me to focus on this project. I could not have succeeded without her moral and tangible support.

TABLE OF CONTENTS

TABLE OF CONTENTS (Continued)

LIST OF FIGURES

LIST OF FIGURES (Continued)

LIST OF TABLES

LIST OF ACRONYMS

AVHRR	Advanced Very High Resolution Radiometer
Biome-BGC	BioGeochemical Cycles Model
CCM3	Community Climate Model 3
DEM	Digital elevation model
DHB	Distributed Hydrology-Biogeochemistry Model
DHSVM	Distributed Hydrology-Soil-Vegetation Model
ET	Evapotranspiration
GCM	Global Climate Model
HSI	Hydrologic similarity index (from TOPMODEL)
LAI	Leaf area index
MAPSS	Mapped Atmosphere-Plant-Soil System
MC1	MAPSS-Century version 1
NCAR	National Center for Atmospheric Research
NPP	Net primary productivity
PNW	Pacific Northwest
OTTER	Oregon Transect Ecosystem Research
PRMS	Precipitation-Runoff Modeling System
PSN	Net photosynthesis
RCM	Regional climate model
RHESSys	Regional Hydrological-Ecological Simulation System
SHE	Systeme Hydrologique Europeen
SWC	Soil water holding capacity
TOPMODEL	Topography Based Hydrological Model
TOPOG	Topography Based Hydrologic Modeling Package
USFS	U.S. Forest Service
VEMAP	Vegetation/Ecosystem Modeling and Analysis Project
WUE	Water use efficiency
VIC	Variable Infiltration Capacity Model

SIMULATION OF VEGETATION AND HYDROLOGY FOR CLIMATE CHANGE ANALYSIS OF A MOUNTAIN WATERSHED

1 INTRODUCTION

Modeling is the process of simplifying a real system to its fundamental components and conducting associated experiments. Computer simulation is the only feasible form of modeling when the real phenomena occur over large spatial or temporal scales. Today natural resources management often places a priority on problems and solutions that don't involve engineered structures, many of which extend to an entire watershed and require an integrated approach across disciplines, space, and time. Numerical modeling provides a powerful tool for assessment and decision support under such requirements. This thesis presents a new model for analysis of interrelated vegetation and hydrology phenomena, and applies it to a case study involving climate change in a Cascade watershed.

The remaining sections of Chapter 1 give some background information relevant to the thesis topic:

- Potential climate change impacts in the Pacific Northwest region
- Review of climate change applications of previous models
- Objectives for this study
- Overview of the American River watershed.

Chapters 2 and 3 are written for submittal to journals and are the core of the thesis. Chapter 2 describes the development and testing of a prototype, grid-based watershed model. The Distributed Hydrology-Biogeochemistry model (DHB) introduced here is a strategic coupling of the hydrology model DHSVM (Distributed Hydrology-Soil-Vegetation Model, Wigmosta et al. 1994) and biogeochemistry model BIOME-BGC (BioGeochemistry Cycles, Running and Gower 1991; Thornton 1998). It integrates the logic of the original component models to simulate vegetation and hydrology dynamically. The model is applied to an idealized hillslope representing conditions in the American River watershed. In Chapter 3, leaf area index (LAI)

results from the idealized hillslope simulations are used with DHSVM to perform a climate change analysis on the full watershed. Chapter 4 presents a summary and further discussion of the key findings from chapters 2 and 3. The Bibliography includes a comprehensive reference list for the entire thesis. The Appendix contains additional information on development of DHB.

1.1 Potential Impacts of Climate Change on the Pacific Northwest

1.1.1 Water Resources

Global climate change is likely to result in shifting regional means and increasing variability of precipitation, streamflow, and evapotranspiration (Houghton et al. 1996). Impacts to the water resources and ecology of the Pacific Northwest (PNW) that are outside historical experience could occur within the lifetimes of our children. Although the PNW as a region is thought to be relatively less vulnerable to climate change than other regions in the U.S., notably the southwest and south (Hurd et al. 1999), the region could still have significant problems, especially east of the Cascade climate divide. The most important risk factors of the PNW region are its large consumption of water resources relative to supply, natural variability, seasonal drought and flooding, and flow and thermal stress to ecosystems (Hurd et al. 1999). All of these factors are closely related to timing of runoff, which in turn depends on snow hydrology.

Global climate change models (GCMs) predict modest increases in precipitation for the PNW, but with more winter rainfall and faster spring snowmelt as a result of increased temperature (Hamlet and Lettenmaier 1999). An average of two GCM predictions (Canadian Centre for Cliamte Modeling and Analysis GCM, Hadley Centre for Climate Prediction and Research GCM) yielded the following changes from 1961-90 to 2090-2099 for the PNW: +16% winter precipitation, +4 C winter temperature, and –76% snow water content on April 1 (McCabe and Wolock 1999).

The same two GCMs differed substantially in estimating evapotranspiration, with the result that one predicted an increase in annual streamflow, and the other predicted a decrease (Wolock and McCabe 1999). If more precipitation falls as rain, winter flooding could increase. If snowmelt occurs earlier in the year, spring flow peaks could be increased, and summer low flows decreased, intensifying seasonal drought. Because supply and demand for water resources reach their peaks in different seasons, mountain snowpacks and baseflow are critical for meeting demand. Understanding the water balance in mountainous areas is a critical part of assessing larger, regional impacts of climate change in the PNW.

1.1.2 Conifer Forests

Summer drought and winter chilling are key characteristics of PNW conifer forests, so alterations of soil moisture, water use efficiency (WUE), and temperature regimes may impact their density and distribution. Existing local and regional gradients of species composition and ecosystem functioning result largely from moisture and temperature regime differences (Franklin et al. 1992). Where vegetation is temperature-limited, boundaries between types are expected to shift upward in latitude and elevation. Density of existing temperature-limited vegetation types is expected to increase overall. Thus, assuming soil depth and nitrogen are not limiting, alpine grassland could convert to forest, and currently sparse high-altitude conifer savannah and forest could grow more dense. However, where vegetation types are water-limited, direction of change in distribution and density of vegetation depends on relative changes in temperature and precipitation, and the role of CO_2 physiological effects (IPCC 1998). If CO_2 effects are minimal and future temperatures are relatively hot, biogeography models indicate a reduction in LAI of the PNW. Conversely, if CO_2 effects favor increased growth, and temperatures are not too warm, then the PNW would experience overall increase in LAI. Predicted changes in vegetation depend largely on choice of climate scenario and vegetation model (IPCC 1998).

Under future scenarios of physical climate change only (no CO_2 effects), a suite of biogeography and biogeochemical models indicate modest changes in existing vegetation types in the PNW. Some existing cool conifer forest could convert to warm mixed forest of similar density, while in other areas conifer forest could convert to less dense mixed or conifer woodland. Arid shrubland could expand in some areas and be replaced by woodland in other areas. If CO_2 effects are included, then modeling experiments are in greater agreement and predict an overall greening, reflecting warmer temperatures and increased WUE. Cooler forests could shift to warmer ones, and less dense vegetation types could shift to more dense types. An overall increase in net primary productivity (NPP) is indicated for the PNW, although a slight decrease could take place west of the Cascades (IPCC 1998). More recent simulations involving transient climate also support a greening over most of the PNW when a higher WUE is assumed (Neilson and Drapek 1998). However, it is possible that an initial greening period of increasing LAI could occur during the early stages of climate change, followed by LAI decreases as temperatures and potential evapotranspiration continue to increase towards $2xCO_2$ equilibrium levels. Direction of vegetation change is sensitive to magnitude of temperature and precipitation changes, and the assumed effect of CO_2 on WUE (Neilson and Drapek 1998). Simulations involving second-order effects such as changed disturbance regimes could further alter the degree and even direction of predicted vegetation response to altered climate.

1.2 Use of Process Models to Investigate Watershed Change

In this section general considerations for watershed modeling are discussed, followed by a review of climate change applications of select models. The models themselves are described more fully in Chapter 2.

1.2.1 Overview

One use of process-based watershed models is to conduct experiments involving comparison of watershed characteristics under past, present, and future states. Typically one of the states involves either a land cover change, for example forest clear-cutting, or a climate change, for example a $2xCO_2$ scenario derived from a global climate model (GCM). To date, most research of landscape-scale hydrologic impacts has focused on land use rather than climate as the agent of change. In PNW forests, the impacts of timber harvesting and road construction on peak flows and sediment transport have been a focus of much field and modeling effort (e.g., Jones and Grant 1996; Wemple et al. 1996; Wright et al. 1990). More recently, low flows and the importance of "refugia" for instream wildlife, especially salmonids, have received increased attention (Keppeler and Ziemer 1990; Hicks et al. 1991). Concern for plant communities and forest structure has also trained interest on vegetation and its connection to the water balance.

Two main techniques have been used to assess how different climates or land use practices affect watershed-scale hydrology and ecology: paired watershed field experiments, and numerical modeling. Field experiments are able to quantify effects of land use practices, but assume climate is stationary. It is also difficult to manipulate age of vegetation, which is an important influence on how CO_2 enrichment changes vegetation function and development (Eamus 1996a). Distributed, process-based models can address impacts of changed boundary conditions, and also indicate geographic variation of fluxes and states within the watershed.

Precipitation is the largest hydrologic flux, and has the largest effect on streamflow. Most watershed modeling concerned with climate change has focused on the physical climate change, particularly precipitation and temperature regimes. After precipitation, evapotranspiration (ET) from vegetation and soil is the most important flux affecting streamflow and subsurface storage. Vegetation is represented in most watershed hydrology models as a prescribed land surface with little variation in either

space or time. To advance our understanding of climate change impacts on watershed hydrology, the role of changing vegetation must also be included.

Simulation of vegetation under climate change has typically been addressed with vegetation models that incorporate relatively simple hydrology schemes. The two main types that are relevant to the watershed scale are biogeochemistry and biogeography models. Biogeochemistry models simulate cycling of carbon, nitrogen, and water in soil and vegetation, with fluxes to and from the atmosphere (VEMAP 1995). Simulated leaf- and plot-scale hydrology and plant physiology govern the growth and senescence of vegetation in response to environmental conditions. Vegetation functional type is prescribed (e.g. evergreen needleleaf), but density changes in response to transient conditions. Outputs from biogeochemistry models include major organic fluxes (e.g., net primary productivity, nitrogen mineralization), in addition to hydrologic fluxes (e.g., ET, soil drainage).

Biogeography models predict the dominant plant life form or biome type based on ecophysiological constraints, and resource limitations (VEMAP 1995). In contrast to biogeochemistry models, biogeography models predict the type as well as density of vegetation. The first generation of biogeography models ran under an equilibrium assumption, wherein climate is stationary and the model iterates to find the vegetation state that satisfies constraints such as growing degree days and winter minimum temperatures, as well as resource limitations such as plant-available soil water and solar radiation. Recently, biogeography principles have been incorporated into biogeochemistry models to simulate vegetation type as well as density in a transient mode [e.g., MC1 (MAPSS-Century version 1), Daly et al. 2000]. Biogeography models have been applied mainly at continental and global scales. Transient, non-equilibrium biogeochemistry models are most similar to hydrology models in structure, and are the most appropriate starting point for introducing dynamic vegetation to watershed modeling. Biogeographical processes are best introduced to the watershed scale after the fundamental processes at short time scales are addressed.

Land surface modeling can be conceptually regarded in three dimensions: temporal, vertical, and horizontal. All three dimensions are present in watershed

hydrology models, while the horizontal dimension is often missing from ecologic and land surface/atmosphere interaction models. The temporal dimension in watershed models ranges from storm events through decades, with a range in time step size from minutes to 24 hours. The vertical dimension usually includes from the canopy top to the bottom of the saturated soil or unconfined aquifer, with a division of 2 or more layers to represent the vegetation and soil regimes. Within the vertical dimension, the primary exchange of mass and energy take place between the atmosphere and the land surface. The horizontal dimension includes the variation in soil and vegetation properties, and mass exchange between adjacent areas. Horizontal exchange is a key process in the case of water. It is less important for carbon at short timescales, but processes such as fire, seed dispersal, and landslides alter carbon and nitrogen states laterally and are important at decadal or longer timescales. For analyzing direct climate change impacts on vegetation, it is possible to capture essential processes without a horizontal dimension. However, the water balance at a watershed scale requires both vertical and horizontal dimensions.

The main differences among distributed, process-based watershed models are the type of spatial representation, and the degree of detail in the process parameterizations. Selection of appropriate spatial representation and parameterization depends on data availability, investigation goals, and computing power. Watershed models have followed three styles of spatial representation. The first style uses topographic knowledge to define a distribution of wetness index values within a watershed, and simulates water routing within the watershed implicitly [e.g., TOPMODEL (Topography Based Hydrological Model, Beven and Kirkby 1979; Beven 1997)]. No channel flow per se is simulated within the watershed, but outflow from separate watersheds can be linked and routed using a separate algorithm. The second style involves defining irregularly-shaped, internally homogeneous subareas (patches) of a basin, then explicitly routing water vertically within a patch and horizontally between patches [e.g., PRMS (Precipitation-Runoff Modeling System, Leavesley et al. 1983)]. The third style also embraces an explicit approach to routing, but is based on a regular grid [e.g., DHSVM (Wigmosta et al. 1994)]. DHB, presented

here, is grid-based. RHESSys (Regional Hydrological-Ecological Simulation System, Band et al. 1993; Mackay and Band 1997), another hydrology-biogeochemistry model, is based on the implicit routing approach of TOPMODEL, though substitution of an explicit routing approach has recently been explored (Tague and Band 2000a).

After selecting a model based on topic and available resources, the next major strategic decision is how to calibrate and validate the model—getting it to work on the application, and objectively demonstrating it to others. Calibration is a difficult problem with a model that has many internal parameters whose values are unknown even though they may be measurable in principle. (For this discussion, "parameters" refers to properties that govern the internal behavior of the system and are constant. "Boundary conditions" are the external forcing conditions that drive the system, e.g. climate.) Typically it has not been addressed with the same rigor for distributed watershed models as has been done, say, for groundwater flow models. This is partly due to the much smaller number of parameters in most groundwater models, and the lack of distributed data for watershed models. In groundwater models, the fundamental purpose is to simulate hydraulic head, for which data are usually available in the relevant application; but analogous observations of surface hydrologic properties other than streamflow are much rarer, particularly in mountainous areas. Most evaluation of watershed models has focused on streamflow because data are available and it integrates the results of the other major fluxes. However, remote sensing estimates of shallow soil moisture, snow cover, LAI, and phenology dates can also be used to validate distributed watershed models if these data are available.

Most distributed, process-based watershed modelers have either tuned a limited number of parameters (e.g., Wigmosta et al. 1994), or have chosen to not tune at all, instead using only measured values or literature estimates and simply reporting how good (or bad) the results are (e.g., Beven and Binley 1992). Limited tuning typically involves one or two of the most sensitive parameters, such as hydraulic conductivity and soil depth. In any case, quantitative measures of goodness-of-fit such as R^2 and model efficiency should always be reported even if other aspects of the simulation are justifiably the center of attention.

1.2.2 Applications of DHSVM

In the paper that introduced the model, Wigmosta et al. (1994) described an application to the Middle Fork Flathead, Montana watershed. This 2900 km^2 basin was simulated for a 4-year historical period, at spatial and temporal resolutions of 180 m and 3 hrs, respectively. Single-layer vegetation types were obtained from an AVHRR 1-km classification, and included aspen, grass, subalpine fir, and pine. A two-season LAI scheme was used for aspen and grass, while other types had constant LAI. The first calibration action involved comparing annual simulated and observed streamflows, and uniformly increasing precipitation input by 16 percent so that streamflows would match on an annual basis. The alteration of the precipitation data was justified as being a reasonable undercatch factor. The model was then calibrated to daily streamflow by adjusting uniform values of soil thickness and hydraulic conductivity. Correlation coefficients (R^2) of 0.95 and 0.91 were obtained for calibration and verification periods, respectively. Snow cover from AVHRR images on several dates indicated the model had a slight tendency to lag actual snowmelt. The authors concluded that better distributions of wind speed, precipitation, and air temperature would be needed to significantly improve model performance; and distributed surface energy and flux data were needed to better test the model.

Storck et al. (1998) reviewed the niche of DHSVM among watershed models; highlighted its important grid- and GIS-related characteristics, and described some new parameterizations for snow mass and energy balance in the canopy. Next they presented an analysis of the effects of timber harvesting on the peak flows in three Cascade watersheds in Washington. Each watershed was simulated at a 3 hr timestep for up to a year, but analysis focused on storm events. Land use impacts on peak flows were presented as maximum differences between response in mature, unmanaged and managed forest. In the west side North Fork Snowqualmie, the effect of a hypothetical clearcutting was tested for two rain-on-snow events. Flows for the two events were 31 and 10 percent larger in the clearcut case, with most of the difference owing to snowmelt contribution from lower elevations. In these areas, the clearcut simulation predicted more antecedent snow on the ground because there was

no canopy to intercept snowfall in previous small storms. The clearcut simulation also involved greater latent heat transfer to the snowpack without the sheltering effect of the canopy. The second case study involved snowmelt peaks in the east-side Little Naches River. Flow increases were only 3 percent for the basin overall, but were up to 30 percent for the higher elevation areas. The last case study involved presence and absence of roads in west-side Hard and Ware Creeks. Average flow increase over four events with roads present was 16 percent. The authors noted that DHSVM did not need recalibration when applying it to a new basin with similar geomorphology, except for land cover characteristics that are very sensitive to climate, such as LAI.

Leung and Wigmosta (1999) presented an analysis of climate change on two watersheds in the Pacific Northwest, the American and the Middle Fork Flathead. They used output from a GCM, the Community Climate Model 3 (CCM3) to drive a regional climate model (RCM), which in turn was used to drive DHSVM. A highlight of the RCM is a subgrid parameterization to describe orographic precipitation, which provides vertical lapsing to complement horizontal variation across the regional grid. Climate scenarios were generated for current climate ("control"), and $2xCO_2$ conditions. Scenarios were seven years long and DSHVM was run at a 3 hr timestep for each. The $2xCO_2$ scenario was 2.7 degrees warmer and had 7 percent more precipitation than the control. In the cold continental climate of the Middle Fork, the resulting changes in hydrology were modest because temperatures are still mostly below freezing. However, the American River with its much warmer maritime climate was more susceptible to the temperature increase, particularly for low- to mid-elevations. Less precipitation fell as snow, and snowmelt occurred about two months earlier in the year. Mean annual snow water content was reduced by 61 percent with the climate change, and the spring and summer streamflows were greatly reduced. Evapotranspiration was essentially unchanged.

Chapter 3 is essentially a follow-up study to the Leung and Wigmosta (1999) paper. The main differences lie in the handling of climate and LAI inputs to the model. Leung and Wigmosta used climate output from the RCM/GCM model to directly drive the watershed model. In this study, a delta approach is used. The

$2xCO_2$ scenario is created by computing monthly mean differences between the control and $2xCO_2$ scenarios, then applying the differences to the historic ("current") climate scenario. There are tradeoffs with both approaches. Using the RCM scenarios directly allowed Leung and Wigmosta to directly drive the hydrology model without further manipulation of the climate input. A drawback of their approach, however, is that the control climate has significant bias compared to the observed climate for WY1990-96, with the result that the average annual hydrographs are markedly different. The delta approach applied here is the standard way of implementing a climate change scenario. It doesn't take full advantage of the horizontal (e.g., rainshadow) gradients in the RCM output because the current climate scenario is based on vertical lapsing from a single station, but it does have the advantage of permitting a direct comparison between observed streamflow and simulated streamflow. It also preserves variability in the historic record. The delta approach has also been used for the whole Columbia Basin, for the same reasons given above (Hamlet and Lettenmaier 1999). A second future scenario is also used. It has the same physical change as the first scenario, but also includes a programmed 20 percent reduction in stomatal conductance to represent a possible effect of atmospheric enrichment on vegetation function (Pan et al. 1998).

The other respect in which Chapter 3 differs from Leung and Wigmosta is in the LAI input to the hydrology model. They used a uniform value both spatially and across climates. This study compares that approach with one involving LAI that varies as a function of terrain position and climate. The variable LAI scenarios are derived in Chapter 2.

1.2.3 Applications of BIOME-BGC

Nemani and Running (1989) applied an early version of the model (FOREST-BGC) to a variety of conifer forest sites in Montana and found good correlation between observed, simulated, and remotely sensed LAI. They elaborated on the hydrologic equilibrium theory, which states that leaf area adjusts to a level where

plant-available water in soil is used up but not exceeded, on average. In environments with seasonal drought, climate and soil water holding capacity (SWC) set an upper limit on leaf area through growing season length and evaporative demand during the growing season. Trees must strike a balance between maximizing photosynthesis and avoiding internal water stress, so restrictions of transpiration to preserve water come at a cost of reduced carbon fixation.

Running and Nemani (1991) applied climate change scenarios to a 1500 km^2 area around Flathead Lake, Montana. They used a delta approach, where the direct (climate) effect was defined by adding +4 C to each daily minimum and maximum temperature; and +10% was added to each precipitation event. For a physiological effect, -30% was subtracted from canopy stomatal conductance, and +30% was added to maximum net canopy photosynthesis. For current LAI, they used AVHRR estimates; future LAI was derived from their previously developed hydrologic equilibrium theory. LAI was predicted to increase from a current range of 2 to 15 to a range of 4 to 18 under both direct and physiological effects. They noted that canopy evaporation would be favored over transpiration in the future scenario because LAI and canopy interception are greater, and there is more rain instead of snow. Final snowmelt occurred 19 and 69 days earlier at 1000 and 2000 m, respectively. Conversely, the growing season was lengthened by 63 to 92 days for mountain and valley sites, respectively. The physical scenario alone increased ET by 11% at Missoula, primarily because of the number of growing season days increased, and snow completely ablated earlier. Net primary productivity (NPP) decreased by 9% because of a longer soil drought and increased nighttime respiration. Addition of the physiology effect caused NPP to jump +88% because of substantial improvement in water use efficiency.

Running (1994) tested BGC performance against the Oregon Transect Ecological Research (OTTER) climatic gradient in Oregon and evaluated some related validation issues. The OTTER transect consists of seven sites, ranging from the mild and wet coast, to drier valley sites, to cold and wet mountain sites, to cold and dry east-slope sites. He used the same generic set of tree physiology parameters for all sites, varying

only specific leaf area and leaf turnover rate, and these only for the evergreen needleleaf-deciduous broadleaf distinction. He found good correlation between observed and simulated aboveground net primary productivity, stem biomass, and leaf nitrogen concentration. Poorer correlation was obtained for pre-dawn leaf water potential and LAI, which he attributed to inadequate definition of the rooting zone soil water holding capacity. By using known LAI, climate, and the maximum forest ET rate of around 6 mm/day, it was possible to estimate SWC and canopy conductance in areas with seasonal drought. He stated that if SWC is wrong, canopy water stress would be mistimed seasonally. If canopy conductance is wrong, either the ET limit will be exceeded, or the length of soil drought will be wrong. If LAI is unknown, it must be estimated inversely by matching model output to stream outflow or snowpack duration. In a temperate climate, the water balance is the primary climatic control on LAI.

Kremer et al. (1996) used BGC to examine the effects of natural climatic variation and climate change on a sagebrush-steppe ecosystem. They used four years of extreme climate extracted from a 1931-1989 climate record to represent extreme minimum and maximum daily air temperature, and minimum and maximum annual precipitation. They used a single year to represent an average year. For the climate change scenarios, they added +2 C to daily temperatures, and +10% to precipitation magnitudes or frequencies. Under one climate scenario based on an average year, sagebrush failed to survive but grass did survive. Under a different climate input that included natural variation, sagebrush was able to survive the $2xCO_2$ GCM scenario.

Pan et al. (1998) compared the response of three biogeochemical models, including BGC, to a $2xCO_2$ atmosphere. They noted that changing CO_2 concentrations directly affects the canopy conductance function, intercellular CO_2 concentration, leaf nitrogen concentration, and indirectly affects LAI. The observation that leaf-scale stomatal conductance is reduced by elevated CO_2 was represented by prescribing a linear reduction of up to 20% for doubled CO_2 concentration. The same linear reduction was applied for leaf nitrogen concentration. BGC simulated an

increase in NPP of 11 percent for the continental U.S. under the future climate scenario.

1.2.4 Applications of RHESSys

The Regional HydroEcological Simulation System (RHESSys) is a merger of TOPMODEL and BGC. It was developed to merge the hydrology of variable terrain with dynamic vegetation processes. Its overall purpose and biogeochemistry component are very similar to the new model described in Chapter 2. The main difference lies in the treatment of watershed hydrology. TOPMODEL does an implicit routing of water and is based on computation of a wetness index over the watershed DEM. In contrast, DHSVM routes water explicitly between grid cells defined by the DEM. TOPMODEL by itself is very fast and can be efficiently used in Monte Carlo techniques. RHESSys is also relatively efficient, though spin-up for the carbon states in BGC can be slow (Christina Tague, personal communication), as was found with DHB (Chapter 2). Another difference between RHESSys and DHSVM is that the former allows only one lifeform type at a given location, while DHSVM allows up to two vegetation layers, which can be distinct lifeform types.

In the seminal paper for RHESSys, Band et al. (1993) simulated Soup Creek, a 15 km^2 watershed located on the west slope of the Swan Mountain Range in northwestern Montana. It has a coniferous canopy, with crown closure ranging from 30-70%. In the first model version, LAI was a fixed variable, and the basin was selected primarily because LAI data were available from previous remote sensing and ground surveys. LAI inputs were computed as the mean observed LAI over a given hydrologic similarity index (HSI) interval. HSI is defined as the logarithm of the ratio of upslope contributing area divided by slope: $HSI = \ln(a/\tan \beta)$, where a=upslope area and β=local slope angle. Higher values of HSI indicate terrain areas that are wetter, either because there is more flow contributed from upslope, or the hydraulic gradient is less, or both. They ran the model for one year, 1988, without tuning, to see if hydrograph shape rather than specific flux magnitudes matched with observed

runoff patterns. They found that lateral redistribution of subsurface water had the effect of reducing ET slightly in drier areas, by introducing drought earlier, but buffering wetter areas from drought (as compared to BGC's point model hydrology). At the highest HSI (wettest) intervals, annual ET was not limited by soil moisture, and was up to three times greater than at the lowest intervals. Annual ET and runoff were shown to be fairly sensitive to the parameter that controls the distribution of soil moisture within the HSI values. Overall, basin averaged soil water potential, ET, and photosynthesis were higher with TOPMODEL hydrology than with BGC's bucket model hydrology. Topographic variation was greatest during periods of intermediate soil moisture, as distinct from very dry or very wet conditions. The authors concluded that it is important to preserve parameter covariance, such as between LAI and SWC, to adequately represent microenvironment variation and resultant differences in flux rates.

Nemani et al. (1993) used RHESSys to independently evaluate LAI maps derived from two remote sensing methods. They compared the different LAI distributions in a heterogeneous 13 km^2 western Montana watershed and examined the differences in ET and PSN output from RHESSys. They found the equilibrium LAI estimates to be strongly controlled by microclimate and soil water conditions, with lower values near ridgelines, and large values near hollows and streams.

Band et al. (1996) applied RHESSys to a climate change problem. They examined the effects of temperature and precipitation change, increased CO_2 concentration, and changes in forest cover on water and carbon fluxes. The case study used a 66 ha subwatershed of the Turkey Lakes Watershed in central Ontario. Topographic relief in the subwatershed is moderate (244-644 m), soils are typically 2 m or less, and forest cover is almost entirely deciduous. To investigate climate change effects, they used three successive steps: 1) adjust the daily temperature and precipitation records; 2) include the physiological effect of elevated CO_2; and 3) include the increase in LAI. The direct effects of 1) were incorporated by increasing daily temperature between 3.0-4.0 C, using one value for each of four seasons. Precipitation was adjusted by +10 percent (winter) or –10 percent (summer) weekly

totals, followed by apportioning the change among days with daily rainfall. The physiological effect was incorporated by decreasing canopy conductance 30 percent, and increasing mesophyll conductance 30 percent. The LAI effect was defined by increasing the growing season value 30 percent. By prescribing each of the effects, they were able to separate their impacts on the hydrology and ecology. However, their approach negated some of the dynamic capabilities of the models, and did not include a dynamic interaction between climate, physiology, and LAI.

Some results from Band et al. (1996) follow. Snowpack was reduced on average compared to control because of the higher temperatures resulting in reduced snowfall and earlier melt. LAI had little effect on snowmelt because the canopy was deciduous. ET response was complicated. Growing season length and water stress tended to be competing outcomes of the physical climate change. Decreased stomatal conductance and increased LAI also tended to be competing outcomes. ET decreased because of reduced stomatal conductance, but was partially offset by a longer growing season, within the constant constraint of SWC. Each of the climate change response scenarios produced a distinct watershed response, and addition of more feedback mechanisms would have further increased the variance of the results. Overall, climate change impacts to long-term average hydrologic response was less than previous climate change thinking predicted, in their opinion.

Mckay and Band (1997) expanded the RHESSys approach to include dynamic simulation of LAI. They identified root zone depth as an important source of model uncertainty, given the importance of water limitations on vegetation response. A new annual allocation scheme in the BGC component was used to grow LAI dynamically. Carbon was allocated to leaves according to the minimum of photosynthate, water, and nitrogen limitations. Leaf-out and leaf-fall were prescribed, and both the Onion Creek, California and Turkey Lakes, Ontario watersheds were assumed to consist of one lifeform type. By comparing remote sensing LAI values with the HSI, Onion Creek was characterized as water limited, while Turkey Lakes was water-saturated, with a decrease in LAI at the highest values of HSI.

Mackay and Band's (1997) experimental design compared prescribed canopy and dynamic canopy factors. Prescribed canopy comprised both uniform basin mean LAI and a spatially variable LAI (both cases had the same watershed total leaf biomass). The spatial pattern of LAI was determined from the remote sensing work, and the resultant LAI inputs were used without further change in the model. They also used shallow and deep rooting zone depths as a further factor (2 x 2 under Prescribed Canopy). With spatially variable LAI, higher LAI near streams tended to slow down snowmelt, while lower LAI higher up in the watershed tended to increase snowmelt. This resulted in snowmelt occurring simultaneously over the entire watershed rather than in steps. Distributing the LAI also had the effect of increasing summer low flows, because LAI was reduced at the dominant runoff-producing upper elevations. A deeper rooting zone increased total transpiration, and the effect was greater under the distributed LAI input. In contrast, the Turkey Lakes watershed has a more humid climatology, and streamflow discharge was not sensitive to LAI distribution. They used a very short spin-up period for their experiments (10 years), and the 100-year simulations showed asymptotic adjustment of the vegetation state variables. In summary, they found rooting depth to be a significant parameter, and suggested that local rooting depth may be more related to long-term average soil water deficits than total soil depth. Since TOPMODEL assumes a spatially uniform recharge rate, variability of vertical recharge is an important source of uncertainty. Elevation bands of recharge rate could be utilized, but then lateral routing has to be more explicit, and the whole enterprise tends toward a spatially explicit model like DHB described in Chapter 2.

Fagre et al. (1997) and White et al. (1998) presented an application of RHESSys to Glacier National Park, Montana. Fagre et al. introduced the project and focused on initial application of the model to the Lake McDonald watershed for climate years 1993 and 1994. Validation focused on snow water equivalent, streamflow, and stream temperature. They also discussed implications for changing stream temperature on distribution of caddisfly populations in streams. White et al. presented a more comprehensive assessment of the model's ability to simulate vegetation properties.

They validated the model under current climate against extensive field measurements, then evaluated sensitivity to a climate change scenario by repeating a three-year sequence comprised of extreme wet year-average year-extreme dry year. Overall, the upper and lower treelines rose, and NPP decreased slightly between climate scenarios.

1.2.5 Applications of Other Models

For application of watershed models to questions of climate change, coupling between the atmosphere, vegetation, snow, soil, and streams is required for a realistic analysis. The multidisciplinary nature of these various realms, differing development agendas for the respective models, and contrasting time and length scales have hindered progress in coupling them, but the situation is gradually improving. Ideally, the strengths and key characteristics of each model type would be preserved and enhanced by coupling with other model types. The first degree of coupling involves first-order effects, but not interactive, second-order effects. For example, contrasting climate scenarios from a GCM are imposed on a watershed model, with no changes in the land cover. Or, a future state of vegetation is prescribed, but feedback to climate at a regional scale is not considered. In both cases, the "direct effect" of climate or land cover change is investigated, but without consideration of their mutual evolution or inherent consistency.

Kite (1998) provided an example of this type of watershed analysis. He applied $1xCO_2$ and $2xCO_2$ climate scenarios, a $2xCO_2$ vegetation distribution based on $2xCO_2$ temperature, and a $2xCO_2$ stomatal conductance reduction to the Kootenay Basin, British Columbia. The major hydrologic change was the occurrence of more high flows, earlier in the year, with a 10 percent reduction in ET due to the new vegetation scenario, and a further 25 percent reduction in ET due to decreased stomatal conductance. After presenting his coupling of models, which really amounted to driving a hydrologic model with different climate and vegetation inputs, Kite argued for greater coupling of atmospheric, hydrologic, and biologic models.

Neilson and Running (1996) proposed a framework for understanding and coupling biogeochemistry and biogeographical models. Biogeographical models address establishment, disturbance and survival of types, while biogeochemical models address growth and persistence, given knowledge of what lives there. In a limited experiment of running MAPSS on the American River with a similar climate change scenario as used in Chapter 2, little change in vegetation types occurred (Ray Drapek, personal communication).

1.3 Study Objectives

The overall objectives of this study are to create a coupled hydrology-biogeochemistry model and use it to analyze potential impacts of climate change on a Cascades watershed.

The specific method objectives are:

- Evaluate compatibility of DHSVM and BGC
- Couple DHSVM and BGC to create a new Distributed Hydrology Biogeochemistry (DHB) model for dynamic vegetation and hydrology simulation
- Evaluate the effects of coupling and compare them to landscape factors including elevation, slope, and aspect.

The specific application objectives are:

- Develop a new future climate scenario for the American River watershed, Washington, from existing scenarios
- Use DHB to develop scenarios of leaf area index (LAI) under current and future climate scenarios
- Evaluate sensitivity of LAI to selected DHB inputs
- Evaluate sensitivity of the American River hydrology to the LAI and climate scenarios using stand-alone DHSVM

- Evaluate relative importance of physical climate, CO_2, and LAI factors on American River hydrology.

1.4 Case Study Watershed: American River, Washington

The American River basin is a 200 km^2 watershed that heads along the Pacific Crest near Mt. Rainier in central Washington and extends eastward. The order of tributaries in the regional river system is American-Naches-Yakima-Columbia. The basin ranges in elevation from 850 to 2100 m. Land use is primarily wilderness area, with a highway corridor traversing the middle. Land cover is primarily mature conifer forest. Mean annual basin precipitation is approximately 1800 mm, and hydrology is snow dominated. This gauged watershed has been the focus of previous modeling efforts by Mark Wigmosta and colleagues at Pacific Northwest Laboratory (Leung and Wigmosta 1999). General characteristics of the American and adjacent Bumping watersheds were recently assessed by the US Forest Service as part of its resource management activities (Naches Ranger District 1998).

2 A GRID-BASED HYDROLOGY-BIOGEOCHEMISTRY MODEL

Scott R. Waichler

For submittal to Hydrological Processes

2.1 Abstract

A set of grid-based hydrology-biogeochemistry models, produced from coupling the previously published Distributed Hydrology-Soil-Vegetation Model (DHSVM) and BioGeochemical Cycles (Biome-BGC), combine an explicit 3-D hydrology scheme with a dynamic vegetation scheme for watershed analysis. Carbon, nitrogen and vegetation functions from BGC are identical in all model structures. Sensitivities of leaf area index (LAI) and hydrologic variables are evaluated for model structure effects including 1-D vertical hydrology parameterization, 2-D water routing and timestep; and landscape features including lapsed climate, climate change, aspect, nitrogen input rate and soil thickness. The test case for evaluating the model set consists of a simple grid representing an idealized hillslope, and climate inputs corresponding to current and $2xCO_2$ scenarios in a Cascade Range watershed. Based on hydrology and LAI results, the best model structure is based on DHSVM 1-D hydrology and 2-D water routing operating at a 3-hour timestep. This model structure produces a 15 percent decrease in LAI under a future climate scenario of meteorologic change only; and a 7 percent increase in LAI under the future scenario with reduction of stomatal conductance in response to increased CO_2. Most model structures exhibit significant variation of soil water content, LAI and evapotranspiration with terrain position and climate, but validation of these effects and their significance for mean watershed hydrology are still needed.

2.2 Introduction

Process-based, distributed models are favored tools for investigating potential impacts of land use and climate change on watersheds. One class of landscape models is focused on physical hydrology [e.g. TOPMODEL (Topography Based Hydrological Model, Beven and Kirkby 1979; Beven 1997); DHSVM (Distributed Hydrology-Soil-Vegetation Model, Wigmosta et al. 1994); TOPOG (Topography Based Hydrologic

Modeling Package, Vertessy et al. 1994); PRMS (Precipitation-Runoff Modeling System/Modular Modeling System, Leavesley et al. 1983); SHE (Systeme Hydrologique Europeen, Abbott 1986a,b)], while another is focused on biogeochemistry with hydrology included [e.g. Biome-BGC (BioGeochemical Cycles, Running and Gower 1991); Century (Parton et al. 1987); MC1 (MAPSS-Century version 1, Daly et al. 2000)]. A weakness of hydrology models is their lack of dynamic vegetation properties, particularly leaf area index (LAI), a critical mediator for land surface fluxes. A weakness of biogeochemistry models is their less sophisticated hydrology, particularly in the lateral movement of water. By linking models with complementing strengths in the hydrology and ecology realms it is possible to create comprehensive new models.

RHESSys (Band et al. 1993; Mackay and Band 1997) is one such linkage, and is based on TOPMODEL and Biome-BGC. TOPMODEL uses elevation data to define a distribution of wetness index values within a watershed, typically at the pixel scale of the DEM. The watershed is then represented with a distribution of index values, and water routing within the watershed is done implicitly. No channel flow per se is simulated within the watershed, but outflow from separate watersheds can be linked and routed using a separate algorithm. Because vertical flux calculations are carried out on classes of wetness index values rather than individual pixels, this approach has the advantage of low computational demand compared to an explicit grid-based model like DHSVM and the one developed here. A subsequent version of RHESSys has incorporated some aspects of DHSVM to explore effects of explicit water routing, respectively (Tague and Band 2000).

This paper presents a coupling of DHSVM and Biome-BGC4.1 (BGC) in a new grid-based model, Distributed Hydrology-Biogeochemistry (DHB). Like RHESSys, DHB is intended to address the interaction between hydrology and biogeochemistry across hillslopes and watersheds in a fully dynamic way. Unlike RHESSys, DHB retains all of the information provided in the watershed DEM, so that all computations are based on the DEM grid. A grid-based structure has large computational cost, but has several advantages, including image-type representations of land surface

conditions (Storck et al. 1998), straightforward climate mapping by horizontal and vertical location, and explicit water routing and runoff generation (Tague and Band 2000), all of which allow variability and local controls within the watershed to be readily portrayed and understood. A merger of two models that have overlapping functions requires choosing which parameterizations will be retained and which will be discarded. Rather than make these decisions before simulation, the approach taken here explores the sensitivity to model structure, including choice of hydrology parameterization, as well as climate and terrain effects. To minimize introduction of new sources of error associated with coupling, DHB retains as much as possible of the original DHSVM and BGC codes.

The emphasis of this paper is on model development and not validation to field data. Some comparisons are made to values in the literature to provide a general sense of model performance, but the primary purpose is to investigate methodology issues associated with landscape modeling.

The model application is a small, idealized hillslope grid that represents conditions in a Cascade Range watershed. By integrating the original codes in small steps and applying them to a simplified test bed, it is possible to identify the relative importance of terrain features and model structure on the model's output. DHB is used to simulate conditions on the idealized hillslope under three climate conditions: 1) current climate; 2) future climate, physical effect only; and 3) future climate, physical and CO_2 effects. Both future climate scenarios derive from global 2x CO_2 scenarios. The first future scenario includes only changes to the meteorology variables. The second future scenario also includes increased CO_2 concentration, to investigate the impact of a potential decrease in stomatal conductance.

2.2.1 DHSVM

DHSVM (Wigmosta et al. 1994) is a process-based hydrology model that computes vertical 1-D fluxes and 2-D water routing in a grid structure (Table 2.1). Major processes simulated are canopy interception, evaporation, transpiration, canopy

and ground snow accumulation and melt, vertical unsaturated water flow, and horizontal saturated groundwater flow. Major inputs are regular grids of elevation, soil type, soil thickness, and vegetation type; look-up tables of soil and vegetation biophysical parameter values; and time series tables of the climate variables air temperature, precipitation, wind speed, relative humidity, solar radiation, and longwave radiation from one or more stations. In the version used here, local climate data are mapped to each cell during the model run using lapse rates for vertical distribution of temperature and precipitation. Horizontal distribution using inverse-distance weighting is used when multiple climate stations are available. Incoming solar radiation is adjusted according to topographic slope and aspect.

Canopy evapotranspiration is simulated for each cell with a Penman-Monteith scheme that utilizes local aerodynamic and canopy resistances. An explicit energy-balance approach is used for snow accumulation and ablation, on both the canopy and on the ground. Infiltration rate is assumed to be unlimited for unsaturated soil (a reasonable assumption for Cascade climate and soils). Unsaturated soil water movement is downward only and driven by a unit gradient with hydraulic conductivity as a function of soil moisture content, using the Brooks-Corey equation. Lateral saturated soil water movement is simulated with Darcy's Law and hydraulic gradient based on either land surface or water table elevations. Surface overland flow is generated where the water table intersects the land surface. Streamflow is generated by channel interception of surface and subsurface runoff.

Vegetation may be represented with up to two layers. An overstory, if present, may cover all or some fraction of the cell. An understory, if present, is assumed to cover the entire cell. Vegetation types ranging from bare soil to low-lying vegetation to closed-canopy forests with understory may be specified. Climate variables are specified at some distance above the top of the vegetation. Wind speed and solar radiation are attenuated down through the vegetation layers based on fractional area covered, vegetation height, and LAI. Stomatal resistance is computed separately for each root zone-vegetation layer combination, using soil moisture (Feddes et al. 1978), and air temperature, vapor pressure deficit, solar radiation (Dickinson et al. 1991).

Property	DHSVM	BGC
General		
Spatial extent	Grid	Point
Looping	Space inside time	Time only
Timestep	15 min – 24 hrs	24 hrs
Spin-up essential?	No	Yes
Outputs	Water	Water, C, N
Lines of code	29,000	
Constant parameters	90	80
State variables (per cell)	20	100
Flux variables (per cell)	50	360
Vegetation		
Layers	Multiple	1
LAI	Prescribed	Dynamic
Radiation balance	Includes fractional canopy coverage	Includes separate sun, shade fractions within canopy
Evapotranspiration	Penman-Monteith	Penman-Monteith
Soil		
Layers	Multiple	1
Layer types	Root zones + 2-D saturated flow zone	Root zones only
Texture and hydraulic properties	Volumetric contents; Brooks-Corey Kh, Kv	Matric potentials; regression eqs. to convert from %sand, silt, clay
Subsurface flow		
Lateral flow	Yes (no macropore flow)	No
Vertical flow	Darcy's law with unit gradient, $K=f(\theta)$; force saturation from bottom up	"Bucket" model with exponential decrease in drainage below field capacity

Table 2.1 Comparison of DHSVM and BGC properties.

2.2.2 BIOME-BGC v4.1

BIOME-BGC is an ecosystem process model that computes water, carbon, and nitrogen cycles at a plot scale (Running and Coughlan 1988; Running and Gower 1991). The overall assumption behind the model is that climate and LAI integrate most of the defining characteristics of ecosystems. In addition to the major 1-D hydrology fluxes, the model simulates the major biological processes that govern

vegetation growth and senescence: photosynthesis, respiration, allocation, litterfall, decomposition, and nitrogen mineralization. Generic vegetation types (e.g. evergreen needleaf) and associated biophysical parameters are defined. Its "point" model structure simulates only vertical 1-D processes, and assumes horizontal homogeneity. Therefore, single plots or grids with individual cells that are larger in scale than hillslopes are the ideal applications (Waring and Running 1998).

LAI is the principal state variable for canopy processes in BGC. The canopy is treated as a homogeneous, three-dimensional green "sponge", or "big leaf" with a thickness given by the LAI. Live carbon pools are defined for leaves, roots, and stems. Leaves serve as carbon sources, stems are inert, and roots are carbon sinks. Dead carbon pools are defined for leaves, stems, roots, and soil. Nitrogen pool types parallel those for carbon. Carbon and nitrogen budgets are dynamic and interacting so that leaf/root allocation is controlled by carbon, nitrogen, and water availability.

The model was designed around a daily time step because that is the most widely available resolution for climate data. Meteorology to drive BGC consists of daily minimum and maximum air temperature, short-wave radiation, vapor pressure deficit, and precipitation. Average daytime and nighttime air temperatures are computed and used for processes that occur during only part of the day, for example photosynthesis, and nighttime respiration.

2.2.3 Opportunity and Challenges for Coupling DHSVM and BGC

DHSVM and BGC have complementary strengths. DHSVM offers a detailed treatment of the water balance, in the vertical dimension from the top of the vegetation canopy to the saturated soil zone that defines the lower extent, and in the horizontal dimension with respect to subsurface, surface, and channel routing of water. Land elevation, soil types, and vegetation types are defined for each grid cell. Grid resolution is the same as the digital elevation model (DEM). Two strengths of DHSVM are its explicit 3-D routing suitable for high-relief watersheds, and raster-based input and output. BGC offers a dynamic, interactive treatment of carbon and

nitrogen cycling through living plant tissue, litter, and soil states under local climatic and soil conditions. Its strength is biogeochemical cycling between atmosphere, vegetation, and soil. A coupling of the two models offers the prospect of having state-of-the-art hydrology and biogeochemistry in one grid-based model. The key state variables to both models are LAI and soil moisture content. BGC can provide a dynamic treatment of LAI, while DHSVM can provide soil moisture accounting that includes lateral movement of water.

The major challenges in linking these models are: 1) including the BGC functions in the DHSVM grid structure; 2) reducing the computational load of long "spin-up" times required by BGC in a grid context; 3) assessing model coupling effects on output. Answering the first challenge requires extensive use of pointers in the C programming language to keep the original model codes intact and modular as much as possible. The second challenge, high computational demand of running BGC for thousands of simulation years to achieve steady-state, was addressed by running the model on representative, idealized hillslope grids, rather than the DEM of an entire watershed. The third challenge, assessing effects of model coupling, was addressed through creating and testing a set of models with varying degrees of coupling. The limited spatial extent and simple geometry of the test grid also made it possible to compare the effects of the model coupling to the landscape features that are of primary interest, such as elevation, slope/aspect, and hillslope moisture movement.

2.3 Model Development and Application

2.3.1 Coupling the Code

The following steps were followed for coupling the two model codes:

1. Identify overlapping functions and variables.
2. Reconcile data structures, initialization requirements, and I/O methods.

3. Modify BGC functions to work within the DHSVM grid and time looping structures.

Coupling was done by degrees, starting with parallel, independent operation; progressing to passing of climate data, and finally to suppressing duplicative functions and sharing of core variables such as LAI, soil and snow moisture content.

The basic designs of DHSVM and BGC, and the insertion location of BGC into DSHVM for DHB, are shown in Figure 2.1. Most BGC hydrology functions are ignored in model structure options where DHSVM hydrology replaces BGC hydrology. BGC's radiation balance is retained in all model structures because it splits absorbed radiation into sun and shade fractions for photosynthesis, but the total absorbed shortwave radiation is the same in BGC and DHSVM. The BGC component also computes its own leaf-scale canopy conductance for photosynthesis purposes, even when canopy conductance and transpiration are computed in DHSVM.

Through various compile and run-time options, six different model structures are obtained and used for the experiment (Table 2.2). The options allowed the isolation and testing of four different effects on simulation output: 1) choice of vertical, 1-D hydrology parameterization (either BGC or DHSVM); 2) presence or absence of lateral water routing between cells; 3) zero or non-zero slope and aspect; and 4) choice of time step for DHSVM hydrology (24 or 3 hours). The option of lateral water routing in the case of BGC hydrology is implemented with a simple routing logic: all water percolating below the root zone in a cell is added to the root zone in the adjacent downslope cell before advancing the timestep. This simple, non-hydraulic approach represents an end member of high water availability within a cell while still moving water downslope. Solar radiation is the climate only input that varies between north, south, and zero slope model structures. Choice of time step controls the degree of averaging diurnal climate and hydrologic variables. For example, a 24-hour timestep leads to an absence of night with respect to solar radiation, and all precipitation occurs at once in the interception and throughfall algorithms. A 3-hour timestep is a convenient compromise between a daily timestep and the sub-minute timesteps that many of the processes follow in reality.

Figure 2.1 Major functions in DHB, a coupling of DHSVM and Biome-BGC. Underlined functions in BGC are replaced by like functions from DHSVM in model structures where DHSVM hydrology is specified.

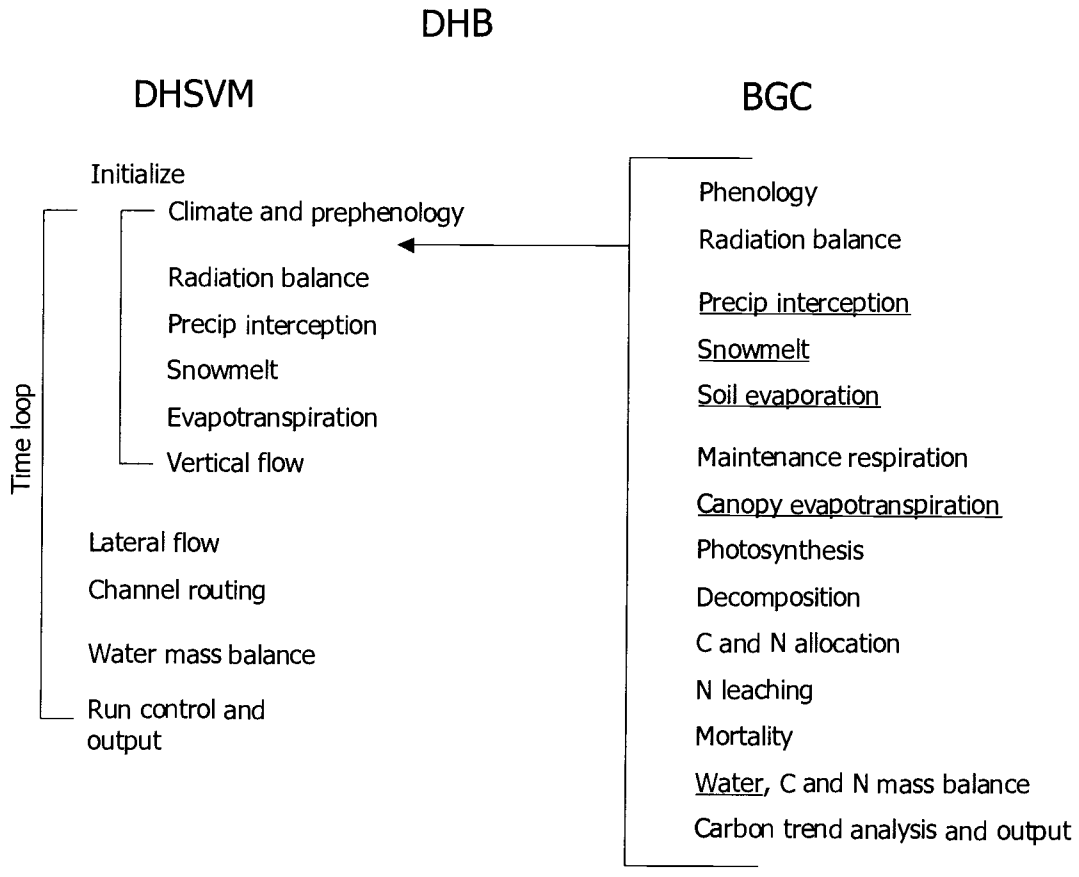

Some of the options, such as choice of 1-D hydrology parameterization, could be used in any grid or watershed application. The simple water routing option for BGC can only be used with the simplified one-cell-wide hillslope grids described in the next section. In addition to these model structure options, an elevation gradient is common to all of the simulations. To summarize, model output is a function of 1-D hydrology parameterization (including timestep), climate (through elevation, slope, and aspect), and contribution of upslope water (if any).

Model Structure Name	1-D Vertical Hydrology	Time-step	Slope and Aspect	2-D Lateral Flow Routing
Flat/BGC	BGC	Daily	None	None
Flat/DHSVM/24hr	DHSVM	Daily	None	None
Flat/DHSVM/3hr	DHSVM	3 hr	None	None
North/BGC	BGC	Daily	Yes	None
South/BGC	BGC	Daily	Yes	None
North/BGC/routing	BGC	Daily	Yes	Simple
South/BGC/routing	BGC	Daily	Yes	Simple
North/DHSVM/24hr	DHSVM	Daily	Yes	Hydraulic
South/DHSVM/24hr	DHSVM	Daily	Yes	Hydraulic
North/DHSVM/3hr	DHSVM	3 hr	Yes	Hydraulic
South/DHSVM/3hr	DHSVM	3 hr	Yes	Hydraulic

Table 2.2 Model structure options in DHB.

Consistency in common state variables and parameters is maintained by passing values within the model, and through selection of proper input values. For example, BGC describes soil texture on the basis of regression equations that convert percentages of sand, silt, and clay into properties such as porosity and field capacity (Cosby et al. 1984). Here a sandy loam is assumed, and the textural percentages are adjusted to yield a hydraulic soil description consistent with the DHSVM soil description, which is based on volumetric moisture contents. In all model structure options, LAI is determined dynamically by BGC and passed to DHVSM. In options where DHSVM hydrology replaces that in BGC, soil moisture content, snow water content, aerodynamic conductance, and percolation below the root zone are passed

from the DHSVM side to the BGC side of the model. These hydrologic quantities are needed in BGC for carbon and nitrogen cycling.

All simulations under current climate are spun-up from minimal carbon and nitrogen contents in soil. A BGC algorithm is used to "spike" the nitrogen input rate periodically and thereby reduce the time needed to achieve steady-state. The current climate vegetation and soil state are used as the initial conditions to simulate future scenarios.

2.3.2 Climate, soil, vegetation input

The test case for model application is the climate, soil, and vegetation of the American River basin, Washington. The American River is approximately 200 km^2 and is a headwater drainage on the east side of the Cascade Range, central Washington. The minimum, mean and maximum elevations of the basin are 850, 1470 and 2100 m, respectively, and mean slope is approximately 20 degrees. Land use is primarily wilderness area, with a highway and recreation corridor passing through the middle. Land cover is primarily mature conifer forest, with grand fir, mountain hemlock, and subalpine fir being the dominant species (Naches Ranger District 1998).

Climate data consists of daily minimum and maximum temperature, relative humidity, and precipitation from the Morse Lake meteorological station. Two daily lapse rates are derived for both temperature and precipitation (Mark Wigmosta, personal communication) from the Morse Lake, Bumping Ridge, and Bumping Lake stations (Table 2.3). The linear lapse rates are applied over the elevation ranges 850-1402m and 1402-2100m, respectively. For grid elevations less than 1402 m, the observation at Morse Lake is lapsed by applying lapse rate 1 over the elevation interval 1646 to 1402 m, and lapse rate 2 from 1402 m to the target elevation. The 3-hour time series of air temperature is created from the 24-hour data by applying a sine function . The 3-hour precipitation time series is created from dividing the 24-hour data by 8, making precipitation uniform throughout the day. The 24-hour and 3-hour

time series of relative humidity, solar radiation, and longwave radiation are developed from the measured variables using a sine function for temperature (Running et al. 1987), a humidity-based transmittance model for solar radiation (Bristow and Campbell 1984), and the Stefan-Boltzmann law for longwave radiation.

Name	Morse Lake	Bumping Ridge	Bumping Reservoir
Type	NRCS SNOTEL	NRCS SNOTEL	USBR
ID	21C17S	21C38S	BUM
Elev (m)	1646	1402	1036
Year installed	1978	1979	1909
Location	American River	Bumping River	Bumping River
Stations for lapse rate 1	x	x	
Stations for lapse rate 2		x	x

Table 2.3 Climate stations in proximity of American River watershed.

To generate current-climate vegetation from initial conditions of minimal carbon and nitrogen, the 7-year climate dataset is repeated in "spin-up" mode until steady-state is reached, as defined by a change in mean daily soil carbon of less than 5 gC/m2 between successive 98-year periods. Spin-up simulations with the American River climate range in length from 2300 to 4500 years, depending on elevation and aspect. The 7-year climate dataset includes wet and dry years, but the climate variability in relation to variability over longer periods was not evaluated.

Two future scenarios are also used as 7-year meteorological inputs. The first is a physical change in climate corresponding to a regional climate model $2xCO_2$ scenario (but with current CO_2 concentration); the second includes the same physical change and also the doubling in atmospheric CO_2 concentration. The future climate scenario is based on a "delta" approach involving alteration of observed climate to create a future climate. The deltas are obtained by differencing the current ("control") and $2xCO_2$ scenarios of the Regional Climate Model (RCM, (Leung and Ghan 1999a,b), which in turn is based on the National Center for Atmospheric Research (NCAR) Community Climate Model (CCM3, Kiehl et al. 1996). The mean differences between the current and future RCM scenarios for each month are applied to the

observed WY1990-96 record to create the future climate for model input. The monthly scalars are applied as differences for temperature, and ratios for all other meteorological variables. Mean annual increases in temperature and precipitation for the $2xCO_2$ scenario as applied to the American River are 2.7 C and 11 percent, respectively.

Vegetation under the future climate scenarios was simulated by using the steady-state under current climate state as the initial condition, and ramping up to the $2xCO_2$ climate linearly over a period of 98 years (Figure 2.2). (Ninety-eight is a multiple of seven and close to one hundred years, a useful assumption for the length of time until CO_2 doubles (Houghton et al. 1996). The future climate input file was recycled to fill the 98-year period, but with incremental changes in the parameters each year. After 98 years, the climate was assumed constant at the future scenario, and the model was run for three additional 7-year climate cycles (21 years). There is no apparent time lag between the end of climate ramping and the final mean LAI value, although interannual variability does increase for Flat/BGC. For model runs involving the future CO_2 effect, the CO_2 concentration was increased linearly over the 98 years from 350 ppm to 700 ppm. To simulate a hypothesized reduction in canopy conductance and increased water use efficiency, the stomatal conductance factor in the canopy conductance function was set to reduce linearly with increasing CO_2 concentration, to a maximum decrease of 20 percent at 2x CO_2. The 20 percent reduction in stomatal conductance has been used in previous modeling (VEMAP 1995) and is justified from empirical studies (Eamus 1991).

Figure 2.2 Example of LAI time series from current climate to future climate. First 7 years are current climate, followed by 98-year linear ramp to future climate, then 21 years at future climate. Model structure is Flat/BGC.

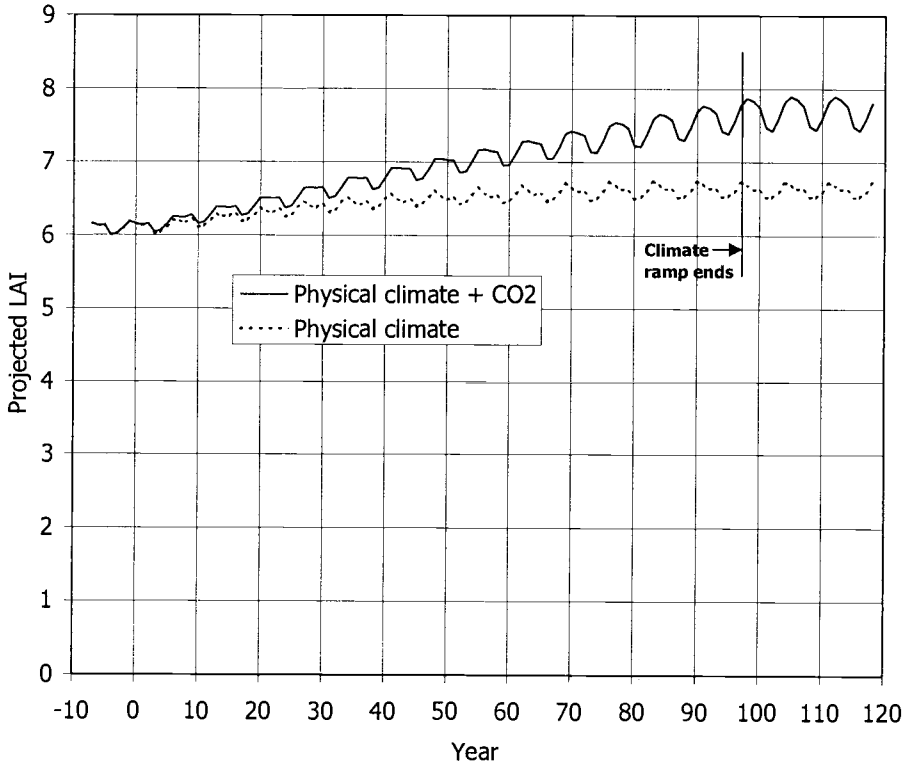

2.3.3 Idealized hillslope input

To facilitate testing of model coupling effects, and to minimize computational demand, idealized hillslope grids are created as proxies for the full watershed DEM (Figure 2.3). South-facing and north-facing grids of 1x26 cells, with bottom and top elevations corresponding to the minimum and maximum elevations of the watershed, are devised. The elevation change between cells is fixed at 50 m. The cell size used in the hillslope DEMs is set at 116 m to produce a slope of 23 degrees. This slope value is the mean of all slopes greater than 10 degrees in the watershed DEM. For "Flat" model structures, each cell has the same elevation as before, but zero slope for purposes of solar input. "Flat" model structures also involve no water routing.

Although a more realistic catena profile with convex top and concave bottom could be used for defining the elevations and slopes, the uniform slope assumption permits a clearer distinction of elevation and radiation loading effects in the results.

Figure 2.3 Idealized hillslope grid for DHB development. Sloping model structures have a 23 percent slope and either north or south aspect. Flat model structures have same elevations for each cell, but zero slope.

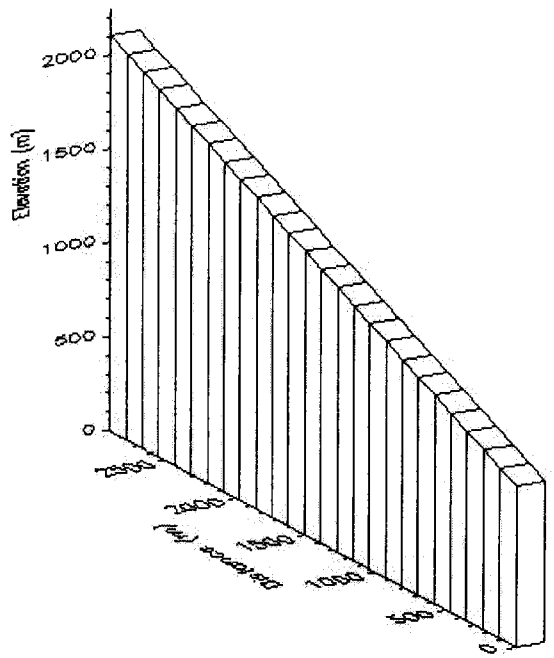

2.4 Results

2.4.1 Overview

Model output for evapotranspiration component fluxes, total evapotranspiration, soil moisture, snow water content, and LAI are presented and discussed below. All results come from the final 7-year climate cycle of the simulation. For current climate

simulations, this is the last cycle of a spin-up lasting on the order of 10^3 years; for future climate simulations, this final 7-year cycle consists of years 112-119. Because LAI is a dynamic variable, hydrologic results reflect differences in LAI as well as climate and physiology. Results from model structures with slope are averages of the north- and south-aspect simulations, unless noted otherwise.

Mean annual values of fluxes and state variables under current climate show that model structure has a large impact on predictions (Figure 2.4). The runoff ratio (runoff/precipitation) ranges from 0.43 to 0.74. The runoff ratio for the American River basin is approximately 0.52, based on observed streamflow and basin average precipitation estimated from climate station data. (It is emphasized that the idealized hillslope simulations reflect climate but not surface drainage density or variability in topography of the full watershed.) Model structures with downslope movement of water have the highest average soil moisture and ET (Figure 2.4a). Mean soil moisture is above field capacity (0.32) in model structures with routing, and not far below field capacity in model structures without routing, indicating the simulated soil is probably too wet compared to the actual watershed. Overall, model structures with routing have higher LAI, transpiration, and canopy evaporation than corresponding structures without water routing (Figure 2.4b). LAI ranges from 3 to 8 and is strongly correlated with soil moisture. These LAI values fall within the observed range for mature conifer forests in cool, wet PNW environments (Table 2.4). LAI falls within a narrow range among model structures with BGC hydrology, though the structure with routing results in a slight increase in LAI. In contrast, model structures with DHSVM hydrology have more variable LAI and proportions of ET components, because of different timesteps as well as presence or absence of water routing.

Figure 2.4 Mean annual hydrologic variables. (a) Runoff, evapotranspiration, soil moisture content. (b) Evapotranspiration components and projected leaf area index (LAI). All values are weighted means from the 1x26-cell grid, where the weights are based on relative areas of elevation bands in the American River basin.

(a)

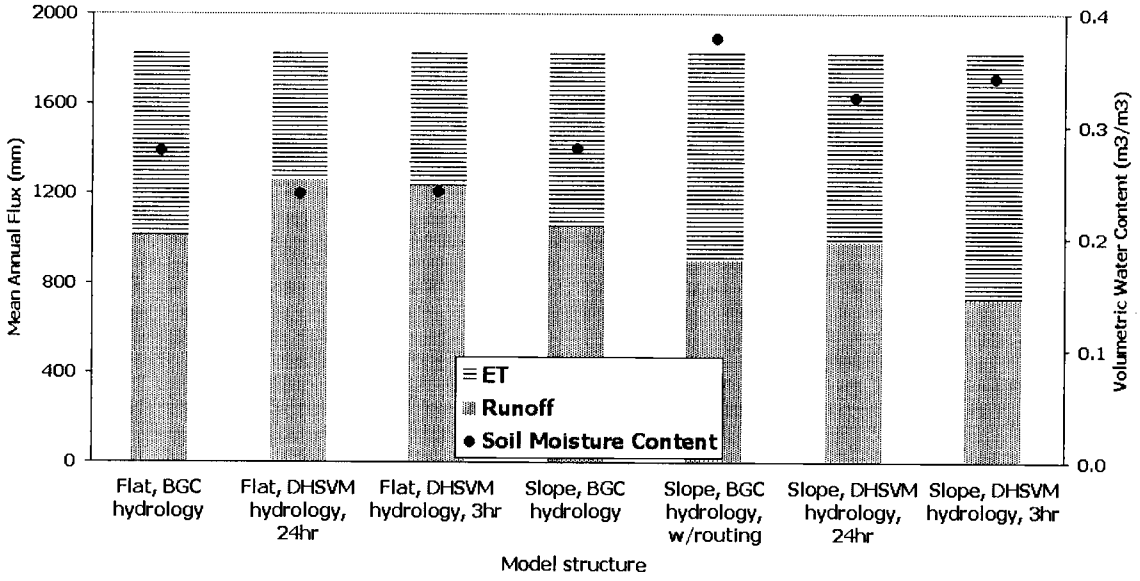

(b)

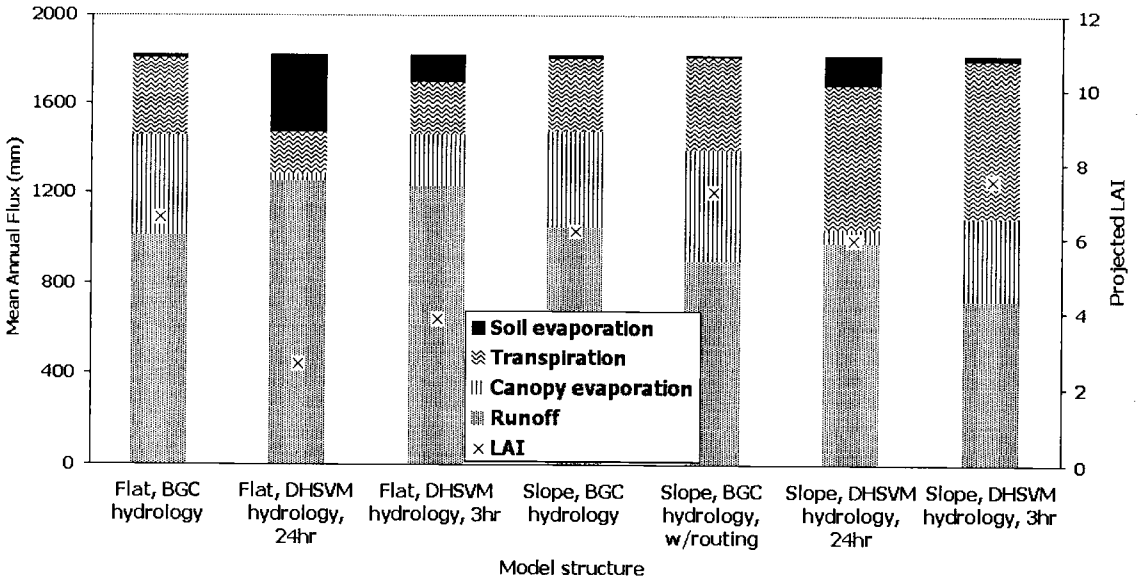

Projected LAI	Location	Elevation (m)	Tree types
7.8	Interior Coast Range, Oregon	365	Douglas fir and Grand fir
6.5	Western Cascades, Oregon	410	Douglas fir
9.6	Western Cascades, Oregon	1500	Douglas fir, with Western hemlock and Pacific silver fir
11.4	Western Cascades, Washington	<1200	Douglas fir with Western hemlock
11.9	Western Cascades, Oregon	360-1200	Douglas fir with Western hemlock
4.3	Western Cascades, Oregon	1590	Mountain hemlock

Table 2.4 Projected LAI values for mature conifer forests in the Pacific Northwest (Cannell, 1982).

2.4.2 Evapotranspiration

The three components of ET, canopy evaporation (from intercepted water), transpiration, and soil evaporation, have consistent proportions among model structures with BGC hydrology, but are variable among structures with DHSVM hydrology (Figure 2.4b). With BGC hydrology, canopy evaporation=55 percent, transpiration=44 percent, and soil evaporation=1 percent of ET. With DHSVM hydrology, use of different timesteps results in canopy evaporation ranging from 5 to 38 percent of ET, and soil evaporation ranging from 2 to 62 percent of ET. Among all model structures, canopy evaporation is greatest with BGC hydrology, and least with DHSVM hydrology at a 24-hr timestep. BGC hydrology tends to simulate more canopy evaporation than transpiration, while DHSVM does the opposite.

Transpiration and soil evaporation compete for available moisture in the entire root zone in BGC structures (which have only one soil layer), and in the top soil layer (out of four) in DHSVM. In DHSVM, transpiration also draws from the second and third soil layers. At a 24 hr timestep, transpiration is somewhat greater with BGC hydrology than DHSVM, because soil evaporation is so large in DHSVM. But

transpiration greatly increases in sloping DHSVM simulations, where downslope water routing provides extra moisture to grid cells with warmer, drier climates.

For soil evaporation, patterns opposite to transpiration are evident. BGC soil evaporation is much less than DSHVM at a 24 hr timestep, and comprises a very small fraction of total ET. No soil evaporation at all is predicted in BGC above elevation 1750 m because a permanent snowpack develops there with the BGC snowmelt algorithm (discussed further below). With DHSVM hydrology, soil evaporation is much greater with a 24 hr timestep than with a 3 hr timestep, because a 24 hr period allows a large amount of soil moisture to be removed prior to updating soil sorptivity and the related limit on subsequent evaporation. Competition between soil evaporation and transpiration is evident in the relative proportions; where one is up, the other tends to be down, especially if water routing is turned off.

Variability in total evapotranspiration is greatest at lower elevations within the hillslope grid (Figure 2.5). At higher elevations with colder climate, the range between simulations is much less. Flat/BGC results in a maximum ET at middle elevations because the combination of temperature and soil moisture conditions is optimal there. Slope/DHSVM/3hr results in maximum ET at low elevations, where temperatures are optimal and soil moisture is not as limiting due to subsurface inflow from upslope cells.

Under the two future climate scenarios, ET increases and runoff decreases in most model structures (Figure 2.6). Relationships between model structures are similar to those under current climate. LAI increases up to 30 percent for most model structures under the physical+CO_2 scenario, but increases are much smaller or negative under the physical-only scenario (Figure 2.6a). The physical-only scenario involves lower water use efficiency and increased competition from soil evaporation for available water compared to the physical+CO_2 scenario. For a given climate scenario, model structures with BGC hydrology have similar decreases in runoff and increases in ET. However, between climate scenarios, BGC soil evaporation is much lower, and canopy evaporation higher, in the physical+CO_2 scenario (Figure 2.6b). This reflects the increased LAI made possible by higher water use efficiency, and

increased shading of the ground surface by the denser canopy. Model structures with DHSVM hydrology exhibit greater variation within as well as between climate scenarios. Total ET increases 30 to 50 percent with climate change in the flat DHSVM model structures, but only 5 to 15 percent in DHSVM structures with slope and lateral routing.

Figure 2.5 Evapotranspiration versus elevation under current climate. Model structures: (1) Flat/BGC; (2) Flat/DHSVM/24hr; (3) Flat/DHSVM/3hr; (4) Slope/BGC; (5) Slope/BGC with routing; (6) Slope/DHSVM/24hr; (7) Slope/DHSVM/3hr.

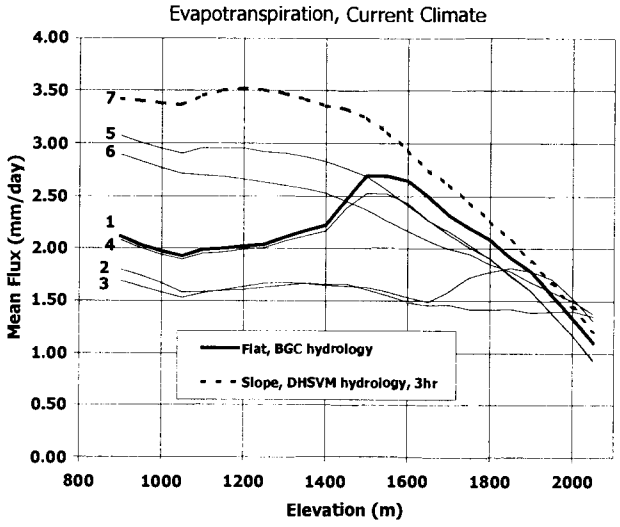

2.4.3 Snow Water Content

Monthly snow water content at elevation 1450 m reaches similar maximums between BGC and DHSVM, but melt occurs much earlier and faster with DHSVM (Figure 2.7a). DHSVM uses an energy balance approach, so a 24 hr timestep tends to raise mean temperatures during winter and spring, decreasing the amount of precipitation as snow and inhibiting refreezing at night during spring. The BGC parameterization has a more gradual snowmelt period. The BGC snowmelt function

Figure 2.6 Changes in mean annual fluxes and LAI under future climate scenarios. (a) Physical change only. (b) Physical + CO_2 change.

(a)

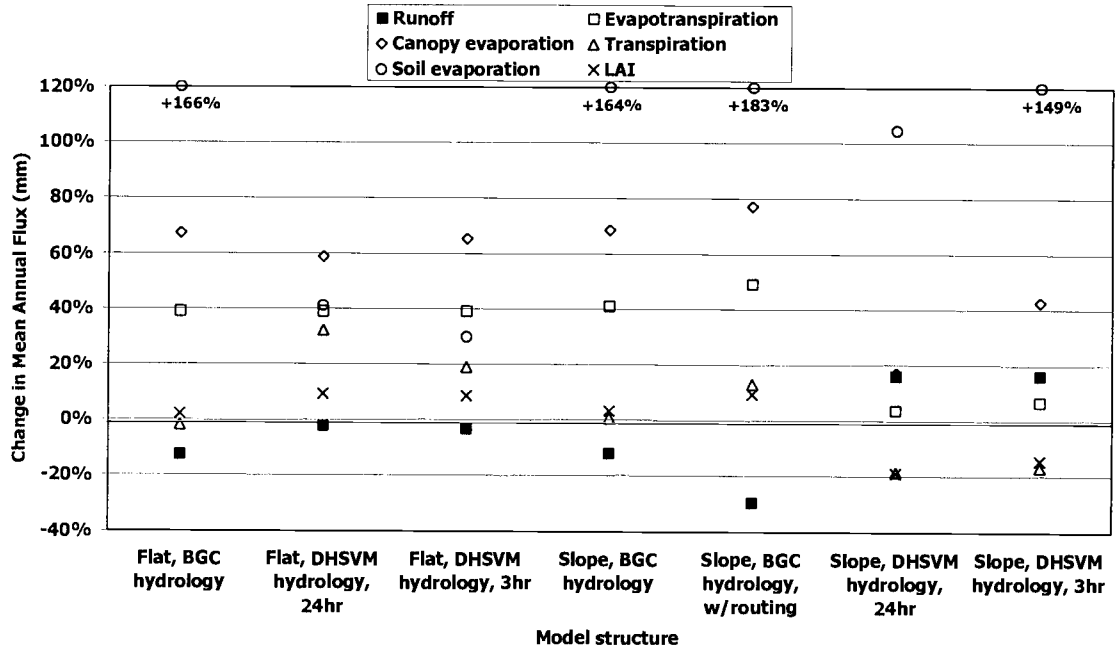

(b)

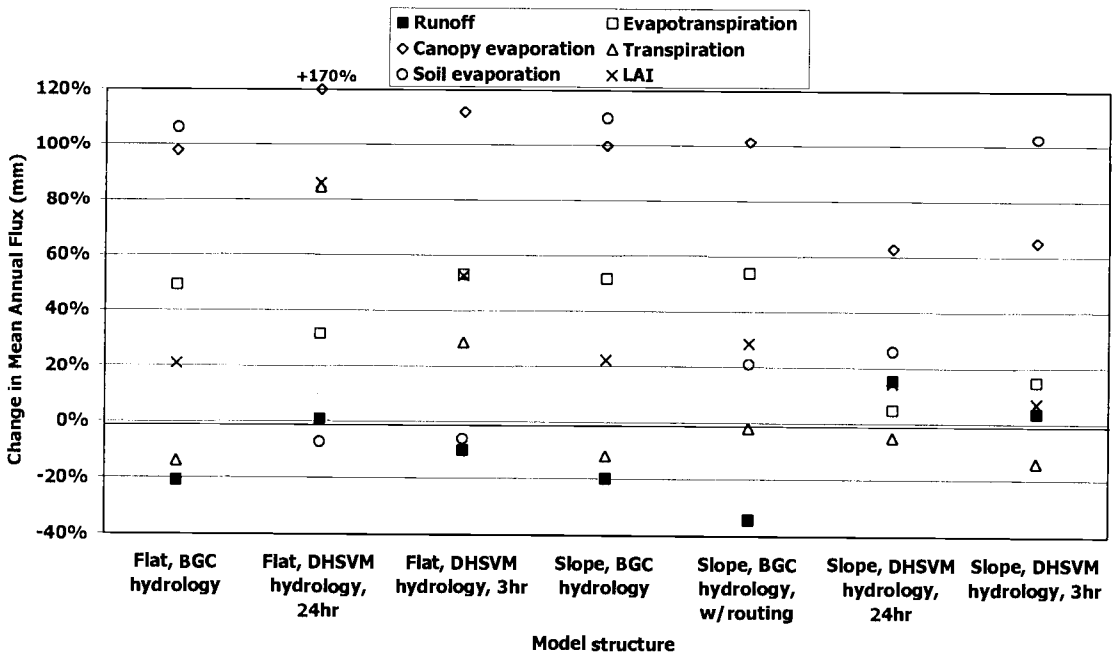

Figure 2.7 Snow water content, current climate. (a) SWE at 1450 m during CY1992. (b) Mean SWE versus elevation. Model structures: (1) Flat/BGC; (2) Flat/DHSVM/24hr; (3) Flat/DHSVM/3hr; (4) Slope/BGC; (5) Slope/BGC/routing; (6) Slope, DHSVM hydrology, 24hr; (7) Slope/DHSVM/3hr.

(a)

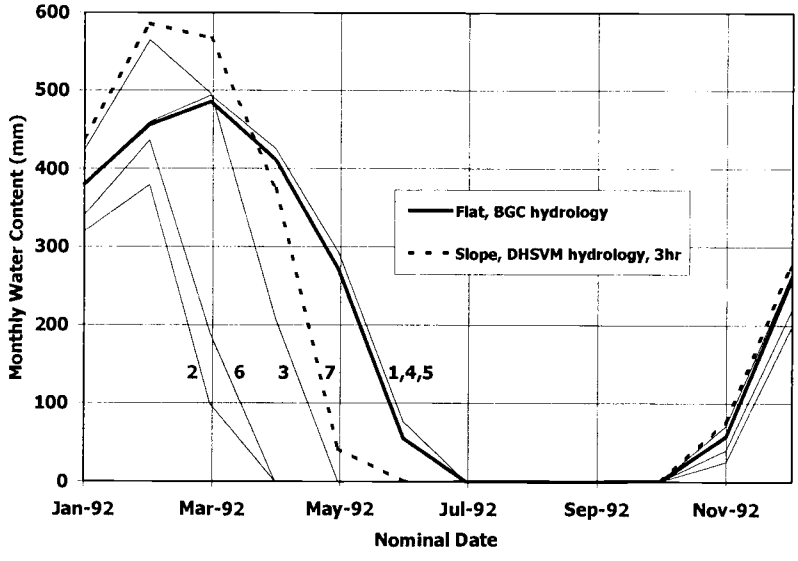

(b)

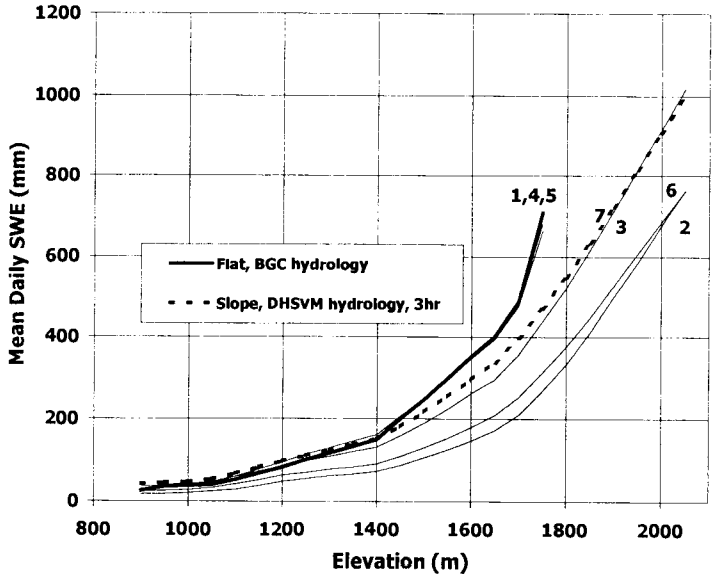

uses direct relationships of daily insolation and air temperature to compute daily melt, whereas the more complex DHSVM snowmelt function involves tracking cold and moisture content of a surface layer and an internal layer in the snowpack.

For low to medium elevations, model structures predict similar lapses in mean annual snow water content, but above 1750 m, BGC fails to melt the snowpack completely each year, resulting in erroneous interannual accumulation (Figure 2.7b). This error does not interfere with the BGC radiation balance, but it does result in erroneously high soil moisture. For Flat/BGC, this does not affect LAI, because vegetation development is limited by temperature rather than soil moisture above 1600 m, as corroborated by model structures with DHSVM hydrology. However, the excess soil moisture at high elevations does increase LAI at low elevations in Slope/BGC/routing.

2.4.4 Soil Water Content

Daily soil water content exhibits a wide range of behavior according to hydrologic parameterization (Figure 2.8a). Moisture contents in all simulations are at field capacity or above during winter, but Flat/BGC begins seasonal drying earlier than Slope/DHSVM/3hr (Table 2.5). Runs with water routing pass most of winter and spring at saturation, and Slope/BGC/routing never drops below field capacity because of the permanent snowpack above 1750 m.

Viewed in elevation profile, simulations with routing have soil moisture content near or above field capacity across all cells (Figure 2.8b). Simulations without routing are much drier, especially at low elevations. Obviously, the idealized hillslope is unrealistically wet because no mid-slope surface drainage exists to remove some of the flow, as would happen in a real hillslope. Slope/BGC/routing is the wettest because of the snow problem.

Figure 2.8 Root zone soil water content, current climate. (a) Daily water content during year 1992, at elevation 1450 m. (b) Mean water content versus elevation. Model structures: (1) Flat/BGC; (2) Flat/DHSVM/24hr; (3) Flat/DHSVM/3hr; (4) Slope/BGC; (5) Slope/BGC/routing; (6) Slope/DHSVM/24hr; (7) Slope/DHSVM/3hr.

(a)

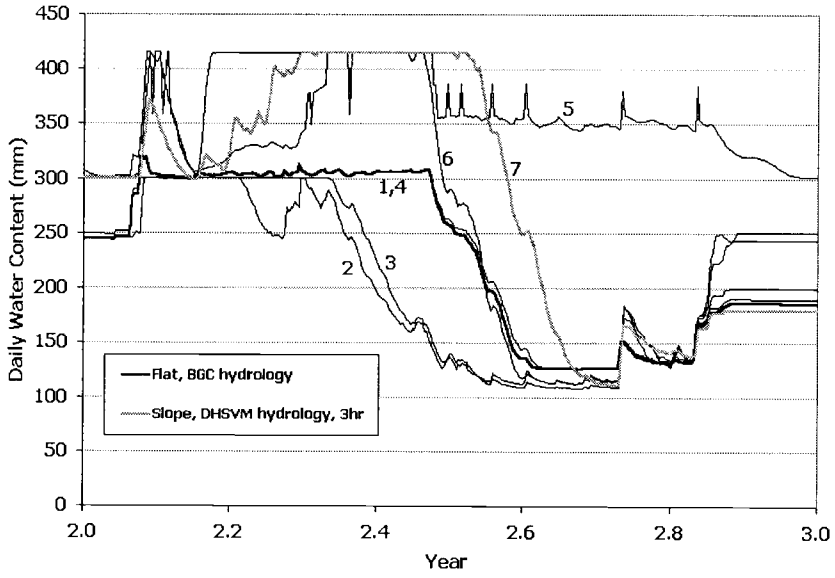

(b)

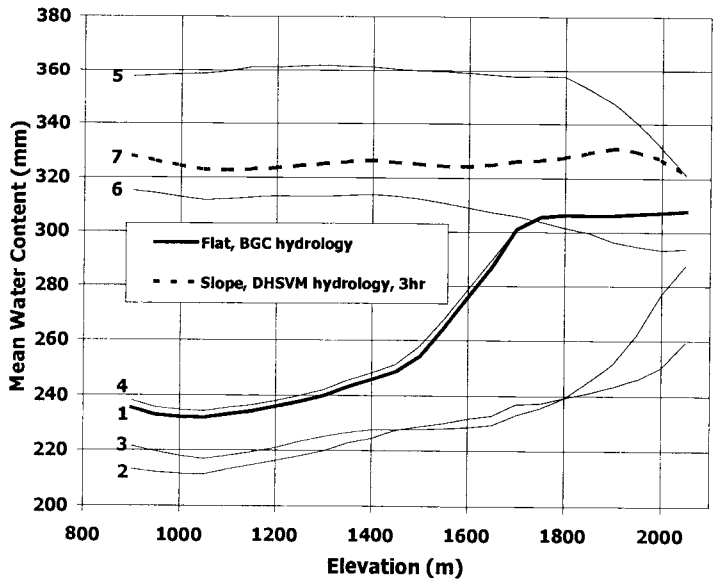

Moisture Content	(%)	(mm)
Saturation	44	435
Field capacity	32	315
Wilting point	13	129

Table 2.5 Soil moisture thresholds. Root zone thickness is 0.95 m.

2.4.5 Leaf Area Index

The evergreen lifeform and simple evergreen phenology in BGC lead to relatively small seasonal and interannual range in LAI, less than 10% of the mean for most simulations (Figure 2.9). As with some of the fluxes, results from DHSVM without routing are distinctly different from the other model structures. Complete time series from current climate through future scenarios indicate that interannual variability of LAI changes with climate (Figure 2.10). Structures with higher LAI tend to have increased variability, while structures with low LAI tend to have decreased variability. Under the physical-only scenario, Flat/BGC predicts a small increase in LAI, while Slope/DHSVM/3hr predicts a small decrease (Figure 2.10a). Under the physical+CO_2 scenario, both model structures predict increased LAI (Figure 2.10b).

Variation in LAI with elevation reflects temperature and soil moisture regime, as determined by lapsed climate and availability of water from upslope cells. Temperature and soil moisture conditions are the controls on vegetation that vary with elevation, and soil moisture also varies with model structure. Warmer temperatures favor vegetation development only if soil moisture is adequate, so too much competition from soil evaporation or lack of water inflow from upslope cells will result in lower LAI. LAI variability between model structures is most pronounced at low to medium elevations where soil moisture is most variable (Figure 2.11a). Slope/DHSVM/3hr has one-third more leaf area than Flat/BGC at low elevations.

Figure 2.9 Daily LAI, current climate. Model structures: (1) Flat/BGC; (2) Flat/DHSVM/24hr; (3) Flat/DHSVM/3hr; (4) Slope/BGC; (5) Slope/BGC/routing; (6) Slope/DHSVM/24hr; (7) Slope/DHSVM/3hr.

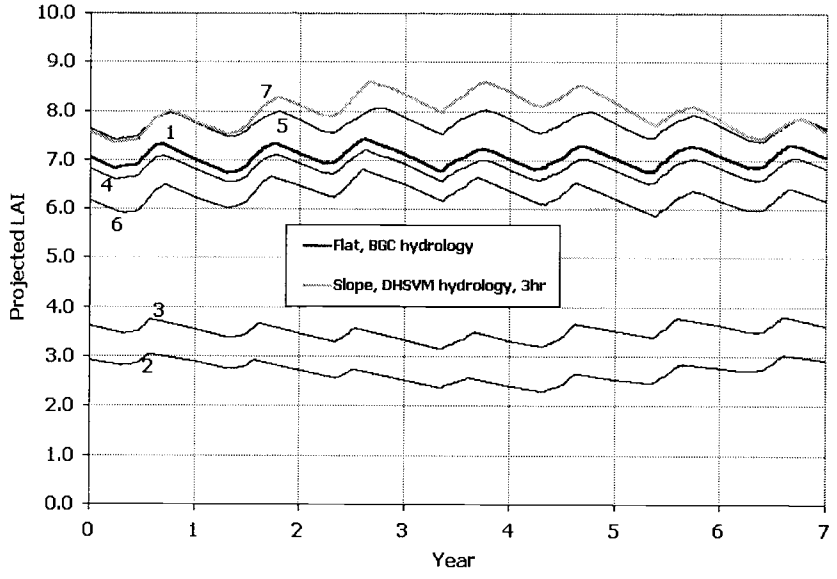

Flat/BGC simulates maximum LAI at middle elevations, where the combination of temperature and soil moisture is optimum for vegetation. At high elevations, soil moisture is excessive in Flat/BGC because of the permanent snowpack problem, but temperature is limiting for both model structures, and LAI values are similar. LAI in Flat/DHSVM is much lower (<4) at most elevations, although at high elevations Flat/DHSVM/3hr is similar to other model structures. This is because the 3 hr timestep allows the high-elevation snowpack to last up to 2 months longer than at a 24 hr timestep, maintaining soil moisture longer into the growing season.

Under the physical-only future climate, the main impact on LAI is an increase at upper elevations, and a decrease at lower elevations (Table 2.6). Simulations with BGC hydrology are especially sensitive to the temperature increase of the future climate, resulting in LAI increases of over 50 percent at upper elevations. The mean change for the physical-only climate scenario, weighted by areas of elevation bands in the American basin, ranges from +2 to +9 percent for all model structures except

Figure 2.10 Mean annual LAI, complete time series. Years –7 to –1 are current climate. (a) With future physical climate. (b) With future physical+CO_2 climate. Model structures: (1) Flat/BGC; (2) Flat/DHSVM/24hr; (3) Flat/DHSVM/3hr; (4) Slope/BGC; (5) Slope/BGC/routing; (6) Slope/DHSVM/24hr; (7) Slope/DHSVM/3hr.

(a)

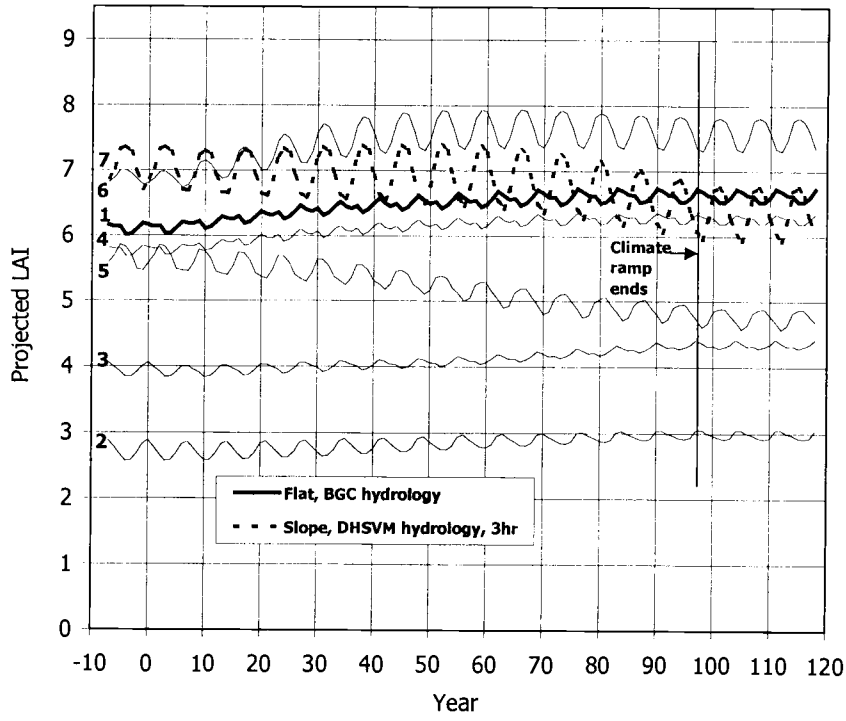

(b)

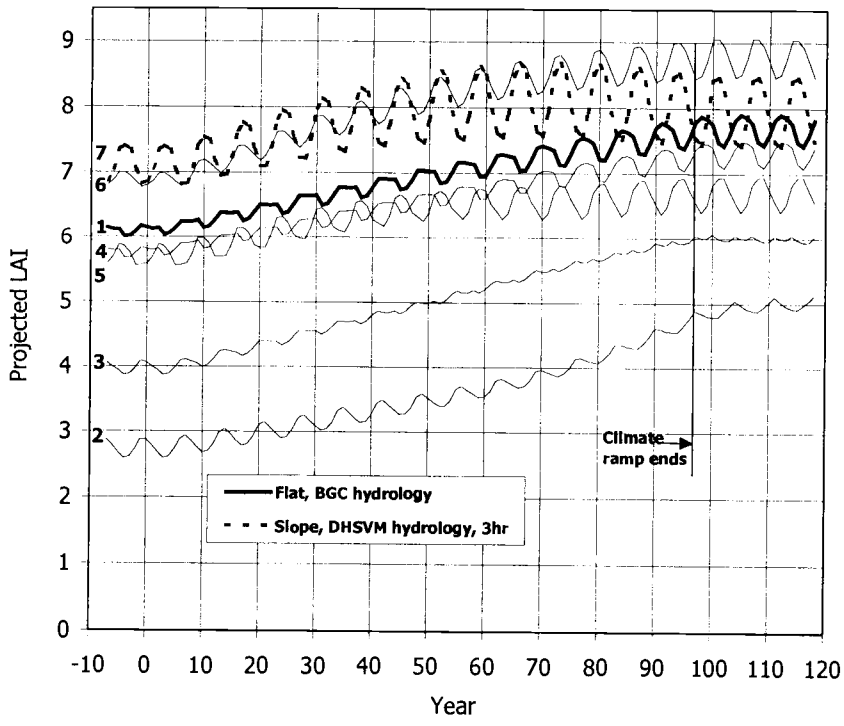

Figure 2.11 Leaf area index (LAI) versus elevation. (a) Current climate. (b) Future climate, physical+CO_2. Model structures: (1) Flat/BGC; (2) Flat/DHSVM/24hr; (3) Flat/DHSVM/3hr; (4) Slope/BGC; (5) Slope/BGC/routing; (6) Slope/DHSVM/24hr; (7) Slope/DHSVM/3hr.

(a)

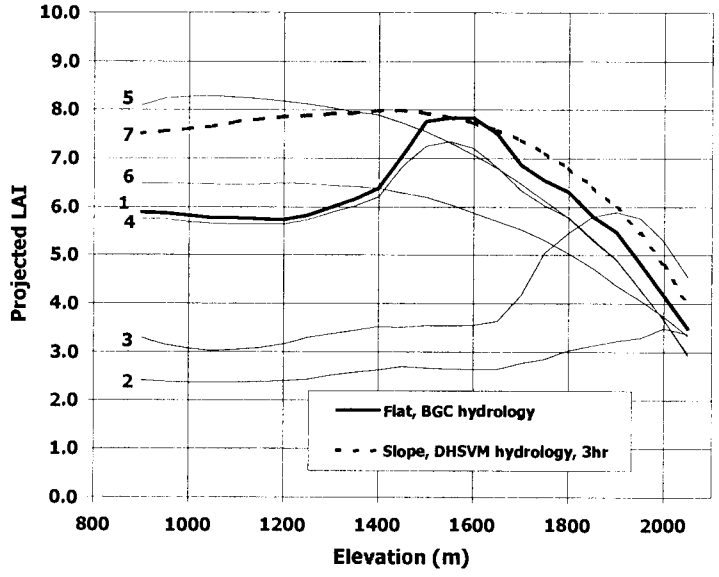

(b)

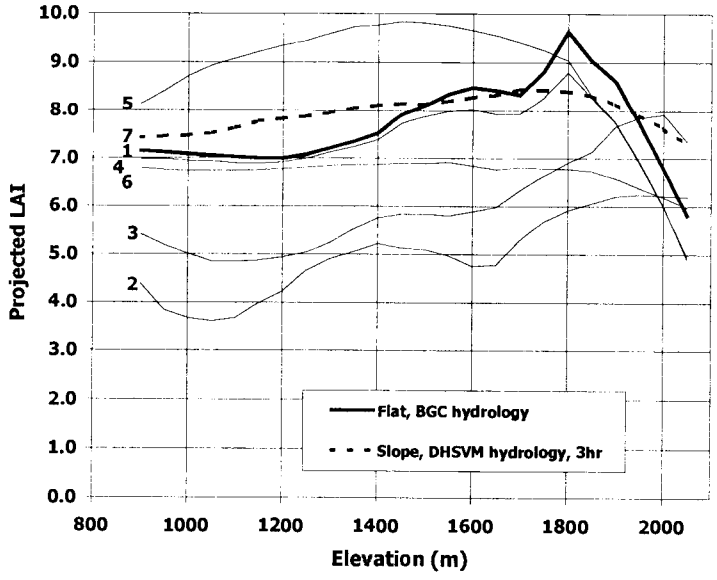

Figure 2.12 Effects of model structure on LAI. (a) Choice of vertical 1-D hydrology parameterization. (b) Aspect and hydrology time step.

(a)

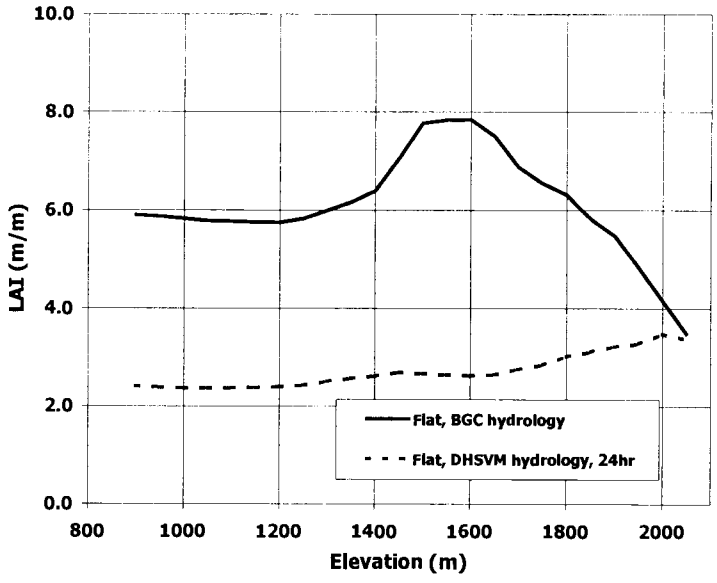

(b)

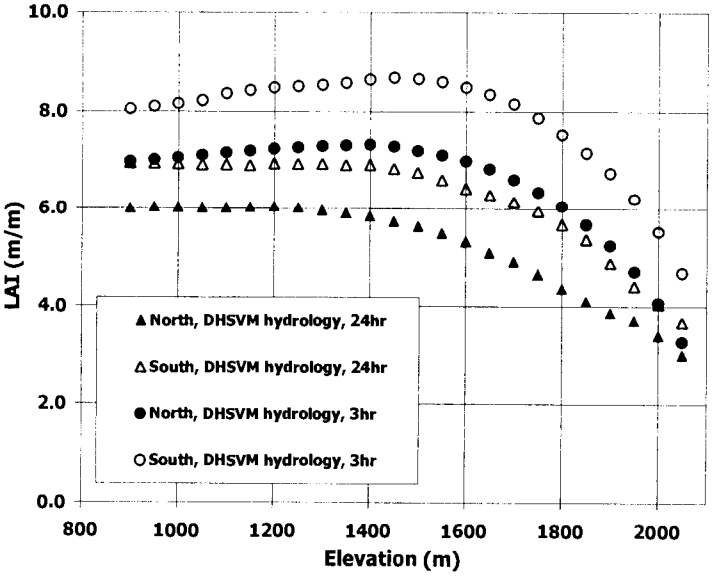

Figure 2.13 More effects of model structure on LAI. (a) Water routing and aspect. (b) Climate change.

(a)

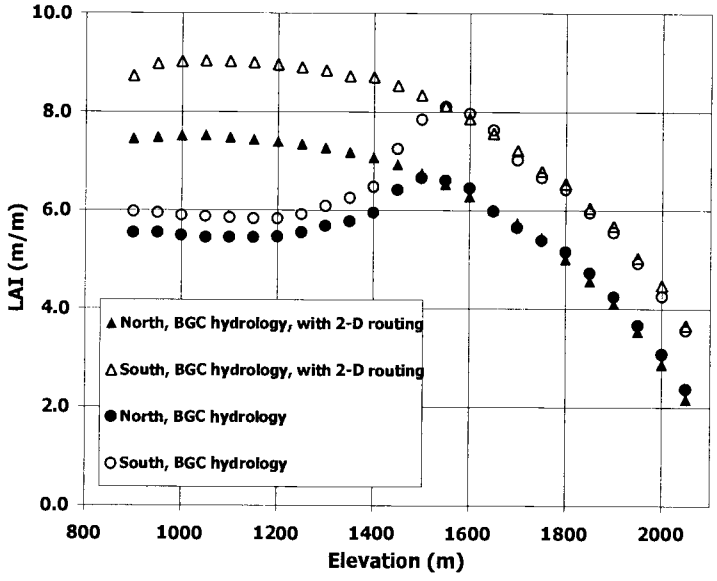

(b)

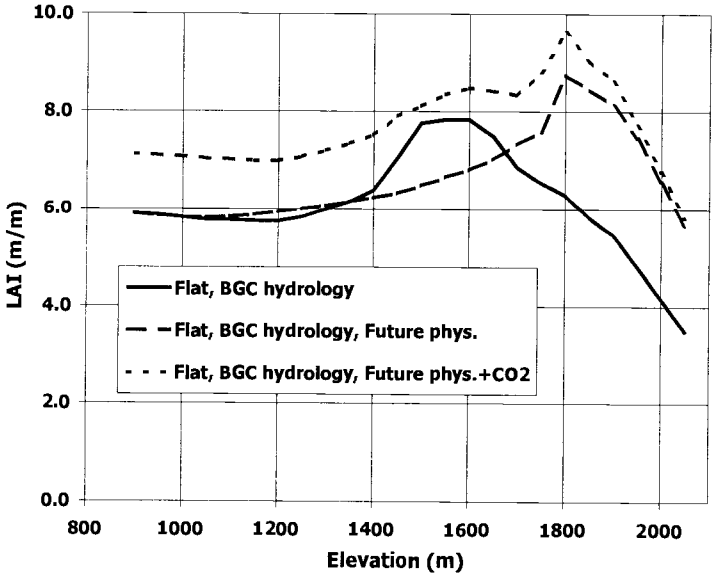

DHSVM with routing structures, which have decreases in LAI of –15 and –19 percent (Table 2.6). The negative response for Slope/DHSVM structures is due to lower soil moisture caused by earlier snowmelt and increased competition from soil evaporation. The unfavorable snowpack and soil evaporation under future physical climate are less important for the Flat/DHSVM structures, where base LAI is much lower and benefits from the modest increase in precipitation.

LAI Change, Current to Future Climate			
Model structure	*	Current to Future Physical	Current to Future Phys.+ CO_2
Flat/BGC	(a)	2%	21%
Flat/DHSVM/24hr	"	9%	86%
Flat/DHSVM/3hr	"	9%	53%
Slope/BGC	"	3%	22%
Slope/BGC/routing	"	9%	28%
Slope/DHSVM/24hr	"	-19%	14%
Slope/DHSVM/3hr	"	-15%	7%
Elevation 900 m	(b)	-10%	20%
Elevation 1450 m	"	-6%	25%
Elevation 2050 m	"	47%	74%
* (a) = weighted mean by elevation; (b) = mean across simulations			

Table 2.6 LAI change from current to future climate.

Under the future physical+CO_2 scenario, LAI increases from current climate in all elevations and model structures except low to medium elevations in Slope/DHSVM/3hr, where it is unchanged (Figure 2.11b). All model structures experience an increase in mean LAI (Table 2.6). The programmed 20 percent reduction in stomatal conductance at double the current concentration of CO_2 boosts water use efficiency of the vegetation and mitigates the summer soil drought compared to current climate or future physical-only climate. The upper elevations experience a particularly big increase in LAI, to levels found at the low to medium elevations under current climate.

Some specific model structure effects on LAI are now discussed. Choice of 1-D hydrology parameterization results in dramatically different LAI profiles under

current climate (Figure 2.12a), highlighting the importance of the soil moisture budget on vegetation simulation. Within the DHSVM hydrology parameterization, timestep can make a difference as well, although the effect is less than the difference between hydrology parameterizations (Figure 2.12b). Separating results from north- and south-facing slopes indicates that LAI is predicted to be higher on south-facing slopes because of higher solar input there (Figure 2.12b). This model prediction conflicts with common field observations that south-facing slopes are drier and have less dense vegetation than north-facing slopes in temperate latitudes of the northern hemisphere. The discrepancy is largely because the model distributes air temperature on the basis of elevation only and does not account for variation in local insolation. Also, simulation results are for steady-state, which requires ~1000 more years to attain on the south-facing than north-facing slope. If the model simulations were stopped during a period of regrowth following disturbance, the difference in LAI between slopes would be less. The presence of water routing sharply increases soil moisture and LAI at low elevations, but not at high elevations, where vegetation is limited by temperature rather than moisture (Figure 2.13a). The addition of water routing is more important for the south-facing slope because of greater competition from soil evaporation there relative to the north slope. The effect of climate scenario on LAI is most evident at upper elevations, and the LAI maximum in Flat/BGC increases and shifts upward in elevation under the future climate scenarios (Figure 2.13b).

2.4.6 Sensitivity of LAI to Nitrogen Input Rate and Soil Thickness

This paper is primarily concerned with a sensitivity analysis at the level of model structures rather than individual parameters within those structures. The large number of parameters in the coupled model structures makes a formal sensitivity analysis of them very difficult, if not impossible. This section describes a limited sensitivity analysis for two key individual parameters, nitrogen input rate and soil thickness. Nitrogen input rate is important because LAI and biomass in natural systems are commonly limited by available mineralized nitrogen as well as water and energy.

BGC takes this into account by controlling maximum photosynthesis rate with leaf nitrogen content. Soil thickness is critical because of the direct relationship with water holding capacity and resistance to seasonal drought. Water and N limitations are directly linked through the processes of soil leaching and decomposition of plant litter, which tend to decrease and increase availability of mineral N, respectively.

The base case nitrogen input value is 0.0005 kg $N/m^2/yr$. The alternate inputs for this analysis are unlimited nitrogen, i.e. completely satisfy the uptake demand; and 0.00025 kg $N/m^2/yr$ (-50%). For the base and low-input cases, the input is constant in time. For soil thickness sensitivity analysis, the two alternate inputs used for comparison with the base case value of 1.0 m are 0.5 m (-50%), and 1.5 m (+50%). As with all previous runs, the grid was assumed to have uniform soil thickness and root zone properties. Sensitivities to these parameters are analyzed for model structures Flat/BGC and Slope/DSHVM/3hr only.

Leaching of mineral N in Flat/BGC is normally an important removal process, so providing unlimited N increases LAI in that model structure (Figure 2.14). The increase is greatest under current climate (+17%), and less under the two future scenarios (+2 and +9%, respectively). Slope/DHSVM/3hr is saturated in mineral nitrogen after spin-up because of incomplete leaching, so N is already unlimiting and LAI does not increase in that structure. Halving the nitrogen input rate also affects Flat/BGC more, resulting in LAI reductions of -18, -7, and –14 percent for current, future/physical, and future/physical+CO_2, respectively. The reductions in Slope/DHSVM/3hr are less than 5 percent. Under the future physical+CO_2 scenario, sensitivity of Flat/BGC to N input rate is less because soil moisture is more limiting to LAI than N.

LAI from soil thickness changes under current climate shows significant sensitivity to water storage capacity at low to medium elevations (Figure 2.15). As with nitrogen, the largest impacts are in BGC, but DHSVM simulations are affected in the same qualitative way. The mean LAI increases for Flat/BGC and Slope/DHSVM/3hr are +18% and +7%, respectively. The corresponding LAI decreases for reducing soil thickness are –30% and –17%.

Figure 2.14 Effect of nitrogen input rate on LAI. (a) Current climate. (b) Future physical+CO_2 climate. (1) Flat/BGC, unlimited N; (2) Flat/BGC base case; (3) Flat/BGC –50% N; (4) Slope/DHSVM/3hr, unlimited N; (5) Slope/DHSVM/3hr, base case; (6) Slope/DHSVM/3hr, -50% N.

(a)

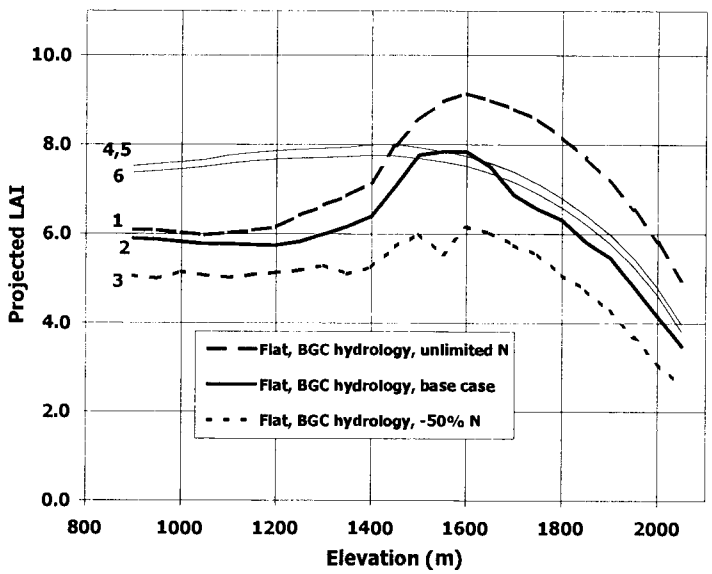

(b)

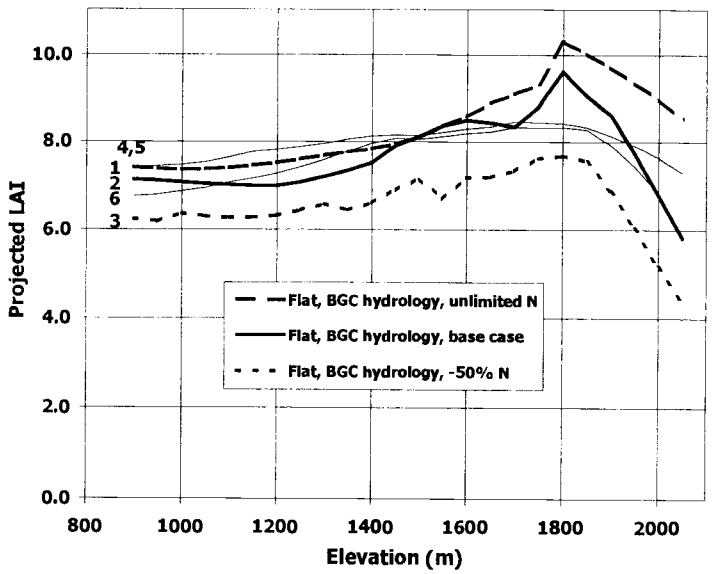

Figure 2.15 Effect of soil thickness on LAI, current climate. (1) Flat/BGC, +50% thickness; (2) Flat/BGC base case; (3) Flat/BGC –50% thickness; (4) Slope/DHSVM/3hr, +50% thickness; (5) Slope/DHSVM/3hr, base case; (6) Slope/DHSVM/3hr, -50% thickness.

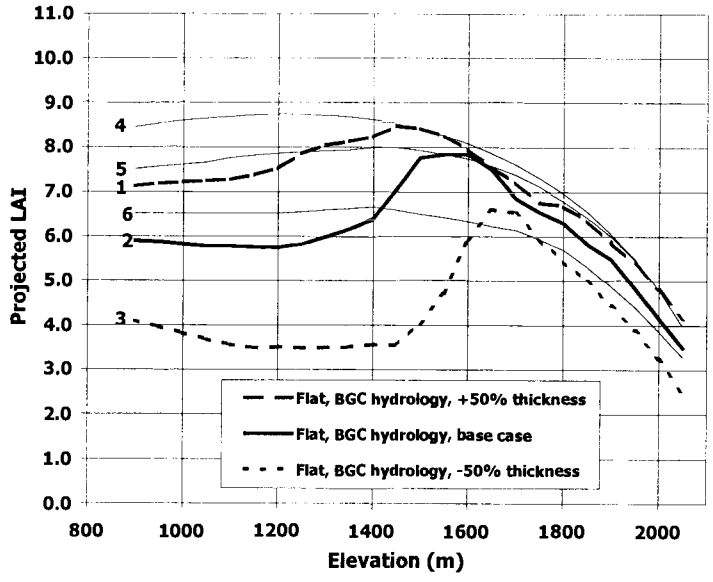

2.5 Discussion

2.5.1 Hydrology Simulation Problems

Several aspects of the simulated water balance differ from typical field observations and require further analysis and model improvement. These include temporal distribution of precipitation, rates of ET and its components, snow ablation, and soil moisture content. Because the model application involves an idealized hillslope and not a measured field setting, a detailed critique using integrating variables such as runoff ratio is not possible. Nevertheless, the model structures should provide outputs that are reasonable for the setting. For each water balance component in question, the mean annual values are considered first, followed by consideration of progressively smaller timescales to expose the fundamental problems.

The variety of spatial and temporal scales at which hydrologic processes act is a fundamental difficulty for creating process-based models. The difficulty begins with precipitation—how does one adequately distribute 24 hr measurements over the course of the day? One important consequence of precipitation distribution from a modeling perspective is the amount of canopy interception and evaporation from water stored on the leaf. Most field studies of canopy evaporation from interception storage are based on monthly to annual timescales. Mature PNW conifer forest in a cool, wet environment loses about 15 percent of annual precipitation to canopy evaporation (Rothacher 1963); mature evergreen beech forest in a somewhat warmer climate loses about 29 percent (Rowe 1983). Simulated annual interception losses are 24 percent for Flat/BGC and 20 percent for Slope/DHSVM/3hr. Thus, both models appear to simulate too much canopy evaporation for the American River climate. Waring and Running (1998) estimate maximum evaporation from a wet forest as 6 mm d^{-1}. Field observations at a daily timestep are not readily available because most studies of evapotranspiration from forests have only considered transpiration and a wet understory, and not an overstory that is repeatedly rewetted during the day. Compared to the above estimate, maximum daily canopy evaporation in Flat/BGC is a whopping 29 mm, while DSHVM has a more reasonable value of 7.5 mm. The problem for BGC canopy evaporation lies in both the interception model and potential evaporation rates.

The BGC hydrology parameterization takes a conceptually simple approach to interception. Daily total precipitation is input to the land surface all at once. To compensate for the sudden deluge on days with high rainfall, a large interception storage capacity and a simple bucket model for vertical subsurface flow are used. The problem with specifying a daily interception capacity is that it becomes more of a tuning parameter and less of a physical one. Interception capacity in BGC4.1.1 is computed as k * precipitation * all-sided LAI, where k is a coefficient. The intent of making interception proportional to precipitation is to recognize that rainfall total and duration are correlated, especially in the PNW where large frontal systems dominate delivery of precipitation. A larger rainfall is assumed to occupy a larger part of the

day, and therefore a larger interception capacity is meant to substitute for repeated evaporation and replenishment of interception storage during the day. Appropriate values for coefficient k depend on climate, with higher values suited to climates with lower rainfall intensities. This study used the default value of k=0.041 LAI^{-1} day^{-1} provided with BGC4.1.1 for the climate of Missoula, Montana. It should be noted that the first version of BGC contained a different approach that apparently made interception inversely proportional to precipitation, but no equation was given (Running and Coughlan 1988).

The default k and interception equation lead to huge interception capacities in the case of the American River. For example, the 0.90 percentile of daily rainfall is 19 mm. Assuming all-sided LAI=16.9, corresponding interception capacity=13 mm (Table 2.7). Maximum daily rainfall in the current climate is 143 mm, which leads to a BGC interception capacity of 99 mm! Observed storage capacities include 1.5 mm for an evergreen beech forest (Rowe 1983), 1.3 mm for a mature Douglas-fir forest (Rothacher 1963), and 1.1 mm in a juvenile Sitka spruce plantation (Teklehaimanot and Jarvis 1991). The simulated capacities in BGC must be reduced by placing limits on k, or by using an approach like that of Running and Coughlan (1988). A minor compensating consideration for BGC is the absence of day-to-day storage of intercepted water, so the excess water not evaporated from the canopy during the day is released to the soil. Even though the interception capacity is too large in BGC, it is also the limiting factor for daily canopy evaporation on most days in BGC, indicating that potential evaporation rates are also a problem.

Interception in DHSVM has a different problem. In that model, interception capacity is computed as k * projected LAI. The default value of the coefficient k is 0.1 mm LAI^{-1}, so the interception capacity per timestep with the LAI value corresponding to above is 0.65 mm. This value is much closer than BGC's version to the actual instantaneous storage capacity of vegetation, and does place an upper limit on canopy evaporation on most days. Canopy evaporation is maximized when a subdaily timestep is used because precipitation is evenly allocated throughout the day and

Variable	BGC	DHSVM	Literature (see text)
Interception capacity per timestep (mm)	13(1)	0.65	1.3
Maximum daily wet canopy evaporation (mm)	29	7.5	6
Mean wet evaporation rate (mm h^{-1})	2.2	2.0	
Maximum wet evaporation rate (mm h^{-1})	6.7	5.7	30
Mean aerodynamic conductance, G_A (mm s^{-1})	550	657	100
Maximum aerodynamic conductance, G_A (mm s^{-1})	652	657	300
Maximum daily transpiration (mm)	7.3	15	4.5
Mean canopy conductance, G_S (mm s^{-1})	1.9	33	21
Maximum canopy conductance, G_S (mm s^{-1})	5.2	96	35
Maximum daily soil evaporation (mm)	0.7	0.27	1
Maximum daily evapotranspiration (mm)	30	18	6
Mean daily evapotranspiration (mm)	2.3	3.9	

Table 2.7 Comparison of BGC and DHSVM evapotranspiration variables. Values are area-weighted means by elevation of American River basin. Subdaily flux rates are based on LAI and insolation conditions in Flat/BGC, and daily average climate variables common to all model structures. Daily total fluxes are from South/BGC and South/DSHVM/3hr, respectively. (1) For 0.9 percentile rainfall.

interception storage can empty and refill with each subdaily timestep. When DHSVM hydrology is applied at too large a timestep (e.g., daily), interception may be underestimated. Thus, BGC addresses the timestep issue with empirical adjustment, while DHSVM uses a conceptual model that is closer to the physical process. The DHSVM equation is more conservative, but should be used with multiple timesteps per day.

Interception capacity is one aspect of the canopy water balance; the other is evaporation rate. Both hydrology parameterizations use similar versions of the Penman-Monteith equation for potential evaporation from a wet surface, and the mean 7-year potential evaporation rates are approximately 2 mm hr^{-1} (Table 2.7). Teklehaimanot and Jarvis (1991) directly measured evaporation from a wet canopy at 1-minute intervals, and found an average rate of 30 mm hr^{-1}, so the simulated maximum rates of about 6 mm hr^{-1} are feasible for short time intervals but probably not for an entire day. More field measurements are needed to clarify reasonable

subdaily interception and evaporation patterns. Large aerodynamic (boundary layer) conductance, G_A, is a contributing factor to high canopy evaporation rates. Teklehaimanot and Jarvis (1991) found maximum G_A=300 mm s^{-1}, or about half of the simulated values (Table 2.7). Other field studies have found maximum G_A to be about 200 mm s^{-1} (Kelliher et al. 1993). The high simulated values of G_A in BGC and DHSVM result in part from multiplying leaf-level conductance by LAI, which may not be justified without an upper limit.

Thus, excessive canopy evaporation in BGC is made possible by large interception capacity, and high potential rates applied over the entire daylight period. Similar potential rates occur in DHSVM, but canopy evaporation is limited by interception capacity in that model. Opportunity to refill the canopy 8 times per day causes DHSVM canopy evaporation to be much greater at a 3-hour timestep than a 24-hr timestep.

Considering transpiration next, the model performance situation is reversed. BGC produces a maximum daily transpiration that is 60 percent greater than observed values, but DHSVM's maximum transpiration is 200 percent greater (Table 2.7, Kelliher et al. 1993). DHSVM's maximum transpiration is double its maximum canopy evaporation, indicating that without an analogue to interception capacity to limit the flux, transpiration rates are able to become unrealistically large. In addition to having high G_A, DHSVM has canopy (stomatal) conductance (G_S) that is an order of magnitude greater than in BGC. The BGC values appear to be too low, while the mean value in DHSVM (33 mm s^{-1}) is above reported maximum values (21 mm s^{-1}, Kelliher et al. 1995). The maximum value in DHSVM (96 mm s^{-1}) is too high in part because the leaf-level conductance is scaled by LAI without an upper limit. Beyond LAI values of about 3, G_S is determined primarily by leaf-level conductance (Kelliher et al. 1995).

The last ET component to be considered is evaporation from soil. Maximum observed values in forests are about 1 mm d^{-1} (Kelliher et al. 1993), or slightly more than the simulated values (Table 2.7). Both BGC and DHSVM use the Penman-Monteith equation as a starting point, with BGC estimating surface conductance as a

function of time since last rainfall, and DHSVM limiting potential evaporation from soil by a sorptivity approach (Wigmosta et al. 1994). However, at a 24 hr timestep the sorptivity-based approach in DHSVM breaks down because soil moisture is not updated frequently enough. Further application of DHSVM hydrology at a 24 hr timestep would require the soil evaporation function to be modified or replaced with a new approach.

Maximum daily evapotranspiration, the sum of the three above components, reflects mainly canopy evaporation in the case of BGC, and transpiration in the case of DHSVM. One more factor producing high ET in both models is the simultaneous simulation of precipitation and evapotranspiration through the entire timestep. In reality, during periods of precipitation essentially no ET takes place. Both models do preclude simultaneous canopy evaporation and transpiration, and DHSVM also limits total land surface ET to the potential rate for a wet canopy.

The approach to simulating snow ablation in the two hydrology parameterizations involves tradeoffs that are similar to those in ET. DHSVM's approach is based on a detailed energy balance, and is fundamentally geared toward a subdaily timestep. If a daily timestep is used, then averaging air temperature and solar radiation causes too little precipitation as snowfall, and too little refreezing during the long springtime freeze-thaw period that is characteristic of PNW mountain watersheds. On the other hand, the simple snowmelt equation in BGC yielded incomplete melting above 1750 m elevation in the model, producing a permanent snowpack. Obviously, the BGC snowmelt function requires replacement or new coefficients for future applications in climates like the American River.

Soil moisture content is an important control for transpiration and soil evaporation, which in turn affect the amount of precipitation that leaves the hillslope as runoff. Model structures with lateral flow routing simulate a soil that is above field capacity on average (Figure 2.8b). In the case of BGC with routing, this is largely caused by the supply of moisture from the excessive snowpack, especially the permanent snow zone above 1750 m. In the case of DHSVM with routing, average soil moisture is somewhat less, but still unrealistically high. One cause is the uniform

slope and lack of midslope channels to intercept subsurface flow in the hillslope model; channels and valleys would exist in a real hillslope to divert some of the flow. The assumption of a relatively thin soil (1.0 m) overlying an impermeable surface also tends to keep soil moisture high. This problem could be addressed by making soil thicker or including a separate water table aquifer in the model. Gradients for subsurface flow are based on topography and are therefore high, but it is possible that soil transmissivity is too low to adequately move water downslope. However, values for all of these hydraulic properties were adopted from a previous calibration of DHSVM to the full watershed (Wigmosta, personal communication), so they do have some basis in model performance at a larger scale.

For model structures without routing, soil is drier on average, except for BGC in the permanent snowpack elevations (Figure 2.8b). At low elevations, mean volumetric soil moisture content is a reasonable 0.25 in BGC, and about 0.23 in DHSVM (field capacity=0.32). DHSVM hydrology includes a quasi-Richards equation approach for continued drainage below field capacity, whereas in BGC only transpiration and soil evaporation remove water below field capacity. As a result of this and higher DHSVM transpiration, flat DHSVM structures approach wilting point about 2 months earlier than BGC (Figure 2.8a), shortening the growing season in low to medium elevations and causing LAI to be much smaller with flat DHSVM than with other structures.

2.5.2 Significance of LAI Variability

LAI is significantly affected by all the experiment factors, but the relative sensitivities for just Flat/BGC and Slope/DHSVM/3hr are different compared to the whole collection of model structures (Table 2.8). The various combinations of model structure result in a wide range of soil moisture and LAI conditions, but when the structures that are most consistent with the original development are used (i.e., Flat/BGC and Slope/DHSVM/3hr), environmental factors, especially soil moisture availability, are most sensitive. When all model structures are considered, the effect

of model structure itself is most important, followed by lapsed climate. However, if just Flat/BGC and Slope/DHSVM/3hr are considered, the effect of model structure is much less, and soil thickness and lapsed climate are most important. Climate change and nitrogen input have a medium effect, and aspect and interannual variation are less important. This is encouraging from a model development perspective and indicates that future work should focus on BGC hydrology without routing, and DHSVM hydrology with routing and a subdaily timestep.

LAI is water-limited at low elevations, temperature-limited at high elevations, and insolation-limited at all elevations. At higher elevations, the presence of water routing does not increase LAI, and at low elevations the difference between Flat/BGC and Slope/DHSVM/3hr is modest. The importance of lapsed climate to LAI suggests that Flat/BGC would be the preferred structure of the two where simulation of vegetation under current climate is the primary objective. This daily-timestep model structure is much more efficient to run than Slope/DHSVM/3hr with its subdaily timestep and variable aspect assumption. However, the BGC interception and snowmelt functions do not work correctly in the test case climate and would need to be modified or replaced. Also, the different responses of Flat/BGC and Slope/DHSVM/3hr under the climate change scenarios, especially the physical-only scenario, indicate that both structures should be exercised in climate change applications, until uncertainty in the component models is reduced. If hydrology is the focus, then DHSVM at a subdaily timestep is superior in most respects, particularly in ET and snowpack dynamics. DHSVM G_S and transpiration need to be reduced, however. Simulated dependence of LAI on terrain position and soil moisture status awaits validation with field data to better indicate its potential value in landscape analysis. The significance of LAI variation on mean watershed hydrology also needs to be determined.

All Model Structures		Flat/BGC and Slope/DHSVM/3hr Model StructuresOnly	
Factor	% Difference Between Max, Min	Factor	% Difference Between Max, Min
Model structure	246	Soil thickness	136
Lapsed climate	186	Lapsed climate	123
Climate change	77	N input rate	92
Aspect	68	Climate change	83
Interannual	30	Aspect	42
		Model structure	39
		Interannual	18

Table 2.8 Relative sensitivity of LAI to simulation factors. Ranking is based on largest difference observed between minimum and maximum values. Sensitivity to N input rate and soil thickness was tested only for Flat/BGC and Slope/DHSVM/3hr. Model structure includes choice of 1-D hydrology parameterization, timestep, slope, and lateral routing.

2.6 Conclusions

The set of grid-based hydrology-biogeochemistry models preserve structure options and allow comparison of various environmental and operational effects on vegetation and hydrology. One reason to start out with a set of coupled models is to compare strengths and weaknesses of the previously published component models. Another reason is to find a model structure that can efficiently simulate vegetation change over a representative cross-section of terrain. The vegetation change scenario can then be used with a stand-alone hydrology model for analysis of a full watershed.

The link between vegetation state, expressed as LAI, and hydrologic fluxes is strong. Flux rates for ET and its components, especially canopy evaporation and transpiration, follow those of LAI, so if variation in LAI across space or time is significant, so is variation in ET. The two model structures that are closest to the assumptions of the original developers, Flat/BGC and Slope/DHSVM/3hr, are superior in terms of overall simulation of LAI and hydrology. Although field data

from the test case watershed are lacking, simulated LAI from the two best model structures is consistent with other observations from the PNW. Both model structures simulate soil that is too wet, however. Flat/BGC does so because its snowmelt function yields a permanent snowpack at high elevations, which leads to excess soil moisture during summer. Slope/DHSVM/3hr has soil that is too wet because of the limited soil thickness and lack of midslope interception by surface channels. These problems with DHSVM are mainly input specifications, however. Introducing quickflow mechanisms to move some soil moisture down the hillslope would also decrease soil moisture to more reasonable levels in DHSVM.

Under the physical-only climate change scenario, Flat/BGC simulated a slight increase in mean LAI, while Slope/DHSVM/3hr simulated a decrease. Both model structures simulated increases in LAI under the physical+CO_2 scenario. Canopy evaporation dramatically increased under both scenarios for all model structures, due to increased rainfall and warmer temperatures, while transpiration generally decreased, particularly with the CO_2 effect included. Under current climate, the optimal combination of water and energy availability is found at low to medium elevations. Under the future/physical scenario, high elevation LAI increases, while lower elevation LAI decreases or remains constant. With the CO_2 effect added, LAI increases over all elevations, suggesting that existing forests may grow more dense and expand to higher elevations.

For many applications in forest settings, the difference in LAI results between Flat/BGC and Slope/DHSVM/3hr model structures would be unimportant compared to overall model error. However, the interception and snowmelt problems in BGC suggest that coupling BGC vegetation functions to DHSVM hydrology leads to the best overall model. Future development of DHB will focus on making the existing code more efficient and practical for use on a large grid.

2.7 Acknowledgments

Support for this research was provided by the US EPA Regional Hydrologic Vulnerability to Climate Change Program, the U.S. Forest Service, and the Department of Bioresource Engineering, Oregon State University. I thank Mark Wigmosta for providing American River data, and Ed Llewellyn for programming assistance. Biome-BGC version 4.1 was provided by the Numerical Terradynamic Simulation Group (NTSG) at the University of Montana. NTSG assumes no responsibility for the proper use of Biome-BGC by others.

2.8 References

Abbott, M.B. 1986a. An Introduction to the European Hydrological System—Systeme Hydrologique Europeen, "SHE"—1: History and Philosophy of a Physically-Based, Distributed Modelling System. Journal of Hydrology 87, 45-59.

Abbott, M.B. 1986b. An Introduction to the European Hydrological System—Systeme Hydrologique Europeen, "SHE"—2: Structure of a Physically-Based, Distributed Modelling System. Journal of Hydrology 87, 61-77.

Band, L.E., P. Patterson, R. Nemani, and S.W. Running. 1993. Forest ecosystem processes at the watershed scale: Incorporating hillslope hydrology. Agricultural and Forest Meteorology 63, 93-126.

Beven, K. 1997. TOPMODEL: A Critique. Hydrological Processes 11, 1069-1085.

Bristow, K.L. and G.S. Campbell. 1984. On the relationship between incoming solar radiation and daily maximum and minimum temperature. Agricultural and Forest Meteorology 31, 159-166.

Cosby, B.J., G.M. Hornberger, R.B. Clapp, and T.R. Ginn. 1984. A statistical exploration of the relationships of soil moisture characteristics to the physical properties of soils. Water Resources Research 20, 682-690.

Daly, C., D. Bachelet, J.M. Lenihan, R.P. Neilson, W.J. Parton, and D.S. Ojima. 2000. Dynamic simulation of tree-grass interactions for global change studies. Ecological Applications 10(2): 449-469.

Dickinson, R.E., A. Henderson-Sellers, C. Rosenzweig, P.J. Sellers. 1991. Evapotranspiration models with canopy resistance for use in climate models, a review. Agriculture and Forest Meteorology 54, 373-388.

Eamus, D. 1991. The interaction of rising CO_2 and temperatures with water use efficiency. Plant, Cell and Environment 14, 843-852.

Feddes, R.A., P.J. Kowalik, H. Zaradny. 1978. Simulation of Field Water Use and Crop Yield. Wiley and Sons, New York, 188 p.

Houghton, J.T., L.G. Meira Filho, B.A. Callander, N. Harris, A. Kattenberg, and K. Maskell (Editors). 1996. Climate Change 1995: The Science of Climate Change. Contribution of Working Group I to the Second Assessment Report of the Intergovernmental Panel on Climate Change. Cambridge University Press, Cambridge, U.K.

Kelliher, F.M., R. Leuning, and E.-D. Schulze. 1993. Evaporation and canopy characteristics of coniferous forests and grasslands. Oecologia 95, 153-163.

Kelliher, F.M., R. Leuning, M.R. Raupach, E.-D.Schulze. 1995. Maximum conductances for evaporation from global vegetation types. Agricultural and Forest Meteorology 73, 1-16.

Kiehl, J.T., J.J. Hack, G.B. Bonan, B.A. Boville, B.P. Briegleb, D.L. Williamson, and P.J. Rasch. 1996. Description of the NCAR Community Climate Model (CCM3).

Leavesley, G.H., R.W. Lichty, B.M. Troutman, and L.G. Saindon. 1983. Precipitation-Runoff Modeling System: User's Manual: U.S. Geological Survey Water-Resources Investigations Report 83-4238, 207 p.

Leavesley, G.H., P.J. Restrepo, S.L. Markstrom, M. Dixon, and L.G. Stannard. 1996. The modular modeling system - MMS: User's manual: U.S. Geological Survey Open File Report 96-151, 200 p.

Leung, L.R. and S.J. Ghan. 1999a. Pacific Northwest Climate Sensitivity Simulated by a Regional Climate Model Driven by a GCM. Part II: $2xCO_2$ Simulations. Journal of Climate 12(7), 2031-2058.

Leung, L.R. and S.J. Ghan. 1999b. Pacific Northwest Climate Sensitivity Simulated by a Regional Climate Model Driven by a GCM. Part I: Control Simulations. Journal of Climate 12(7), 2010-2030.

Mackay, D.S. and L.E. Band. 1997. Forest ecosystem processes at the watershed scale: dynamic coupling of distributed hydrology and canopy growth. Hydrological Processes 11, 1197-1217.

Parton, W.J., D.S. Schimel, C.V. Cole, and D.S. Ojima. 1987. Analysis of factors controlling organic matter levels in Great Plains grasslands. Soil Science of America Journal 51:1173-1179.

Rothacher, J. 1963. Net Precipitation under a Douglas-fir Forest. Forest Science 9(4), 423-429.

Rowe, L.K. 1983. Rainfall interception by an evergreen beech forest, Nelson, New Zealand. Journal of Hydrology 66, 143-158.

Running, S.W. and J.C. Coughlan. 1988. A general model of forest ecosystem processes for regional applications I. Hydrological balance, canopy gas exchange and primary production processes. Ecological Modelling 42, 125-154.

Running, S.W., R.R.Nemani, and R.D.Hungerford. 1987. Extrapolation of synoptic meteorological data in mountainous terrain, and its use for simulating forest evapotranspiration and photosynthesis. Canadian Journal of Forest Research 17, 472-483.

Running, S.W. and S.T. Gower. 1991. FOREST-BGC, A general model of forest ecosystem processes for regional applications II. Dynamic carbon allocation and nitrogen budgets. Tree Physiology 9, 147-160.

Tague, C.L. and L.E. Band. 2000. Evaluating explicit and implicit routing for watershed hydro-ecological models of forest hydrology at the small catchment scale. Hydrological Processes (in press).

Teklehaimanot, Z. and P.G. Jarvis. 1991. Direct measurement of evaporation of intercepted water from forest canopies. Journal of Applied Ecology 28, 603-618.

Vertessy, R., E. O'Loughlin, E. Beverly and T. Butt. 1994. Australian experiences with the CSIRO Topog model in land and water resources management. In: Proceedings of UNESCO International Symposium on Water Resources Planning in a Changing World, Karlsruhe, Germany, June 28-30, 1994, pp. III-135-144.

Waring, R.H. and S.W. Running. 1998. Forest Ecosystems, 2nd ed. Academic Press, San Diego, 370 pp.

Wigmosta, M.S., L.W. Vail, and D.P. Lettenmaier. 1994. A distributed hydrology-vegetation model for complex terrain. Water Resources Research 30, 1665-1679.

3 LEAF AREA AND PHYSIOLOGY EFFECTS IN CLIMATE CHANGE ANALYSIS OF A CASCADE WATERSHED

Scott R. Waichler

For submittal to Journal of the American Water Resources Association

3.1 Abstract

Potential climate change impacts on water resources include altered vegetation and evapotranspiration. Vegetation density, commonly expressed as leaf area index (LAI), may change with physical climate and atmospheric CO_2 concentrations, and feedback to the regional water balance. Another potential effect is reduction of stomatal conductance and transpiration under an enriched atmosphere. A distributed hydrology model is used in a 2x3 factorial experiment involving LAI and climate inputs, respectively. The test case watershed has a cool, wet environment with high base LAI. Feedbacks of LAI and reduced stomatal conductance to the water balance are minor in comparison to the direct physical impacts of increase temperature and precipitation and reduced snowpack. Precipitation, streamflow, and evapotranspiration all increase with relative magnitudes varying with LAI and climate assumptions. Increased LAI is offset by reduced stomatal conductance, so the outcome of the most complex treatment of climate change (variable LAI with CO_2 effect included) is similar to the simplest treatment (uniform LAI with no CO_2 effect). In a drier watershed with lower base LAI, the feedback effect of LAI on hydrology would probably be more significant.

3.2 Introduction

Analysis of potential climate change impacts at the watershed scale is a growing area of research in water resources. Most watershed modeling concerned with climate change has focused on the physical climate change, particularly precipitation and temperature regimes. For the Pacific Northwest (PNW) region of the U.S., the most significant and commonly identified direct impact on water resources is increased air temperature. One $2xCO_2$ scenario from a regional climate model resulted in a 2.7 degree increase in mean annual temperature for the American River basin located in the Cascade Range, Washington (Leung and Wigmosta 1999). A more severe

increase in temperature was found for winter months, and the overall impact was a marked reduction in snowpack formation, and earlier snowmelt.

In addition to the direct effects of physical climate change on hydrology, there are also potential second-order effects related to altered vegetation density and function. After precipitation, evapotranspiration is the most important flux affecting streamflow and soil moisture regimes. Transpiration and canopy interception generally increase with leaf area density and stomatal conductance, so changes in these may affect total evapotranspiration and therefore streamflow. If leaf area increases due to warmer temperatures in mountainous regions, evapotranspiration may increase and streamflow may decrease. Leaf area may also increase in response to an atmosphere enriched in CO_2 because of reduced stomatal conductance and increased water use efficiency in environments with seasonal drought. A larger leaf area would potentially lead to greater amounts of canopy evaporation (from intercepted precipitation), but total transpiration might decrease under the assumption of decreased stomatal conductance.

This paper investigates vegetation impacts on hydrology for the American River basin, using the process-based, distributed hydrology model DHSVM (Wigmosta et al. 1994). Simulations that take the LAI and CO_2 effects into account are compared to results from a previous study that considered only the direct physical effects of climate change (Leung and Wigmosta 1999).

3.3 Method

3.3.1 American River Basin

The American River basin is a 200 km^2 Cascade watershed that heads along the Pacific Crest and lies in the eastern, rain shadow side (Figure 3.1). It is part of the Yakima-Columbia drainage system. The basin ranges in elevation from 850 to 2100 m and has a mean slope of about 20 degrees (Figure 3.2). Basin average annual

Figure 3.1 Location of American River, Washington.

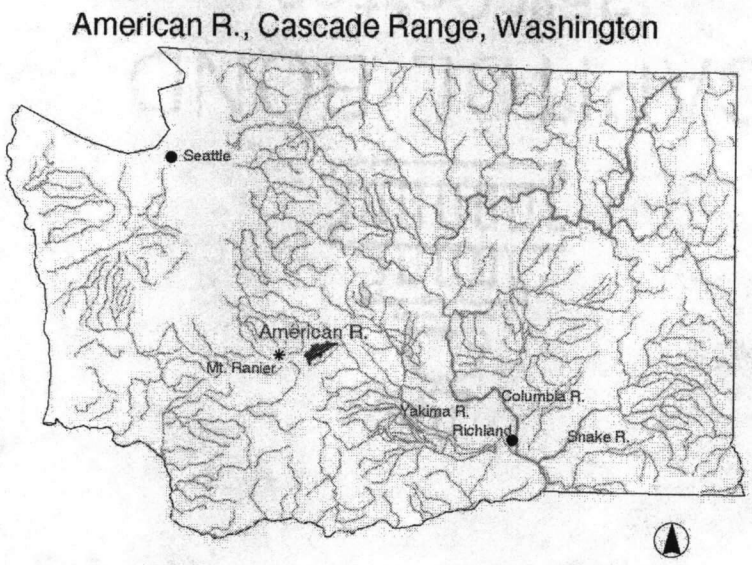

Figure 3.2 American River digital elevation model (DEM).

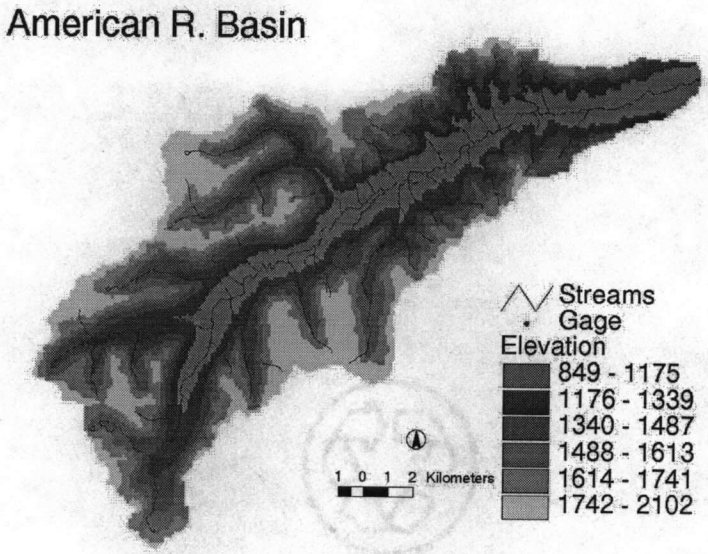

precipitation is approximately 1800 mm. Land use is primarily wilderness area, with a state highway corridor traversing the middle. Land cover is primarily mature conifer forest dominated by grand fir, mountain hemlock, and subalpine fir (Naches Ranger District 1998). Multiple runoff peaks typically occur during the year. The largest is caused by spring snowmelt, and others are caused by winter rain-on-snow in the middle elevation transition zone, and rain at the lower elevations.

3.3.2 Climate Scenarios

Three scenarios, each comprising 7 years of climate input for the model, are used to evaluate impact of climate and vegetation change on the hydrology of the basin. The current climate scenario is based on daily observations at climate and SNOTEL stations in the basin (Waichler, in submission [Ch. 2]). Two future climate scenarios based on a $2xCO_2$ atmosphere are used: 1) physical change (meteorologic inputs) only (Future/phys); and 2) physical change + CO_2 effect (Future/phys+CO_2). The physical climate is based on a "delta" approach involving alteration of the observed current climate to create a future climate input. The deltas are obtained by differencing the control and $2xCO_2$ scenarios of the Regional Climate Model (RCM, Leung and Ghan 1999a,b), which in turn is based on the National Center for Atmospheric Research (NCAR) Community Climate Model (CCM3, Kiehl et al. 1996). The mean differences between the control and future RCM scenarios for each month (Table 3.1) are applied to the observed WY1990-96 record to create the future climate for model input. The monthly scalars are applied as differences for temperature, and as ratios for all other meteorological variables. Current climate is based on daily observations of minimum and maximum air temperature, precipitation, and relative humidity at the Morse Lake SNOTEL station for WY1990-96 (Wigmosta, personal communication). Two daily lapse rates for temperature and precipitation were derived from the Morse Lake, Bumping Ridge, and Bumping Lake stations (Waichler, in submission [Ch. 2]). Future mean annual air temperature is 2.7 C higher than current, and annual precipitation increases about 11 percent (Figure 3.3). The CO_2 effect is defined as a

20 percent reduction in stomatal conductance, reducing transpiration in the model, as computed by the Penman-Monteith equation (Wigmosta et al 1994).

Figure 3.3 Air temperature and precipitation versus elevation.

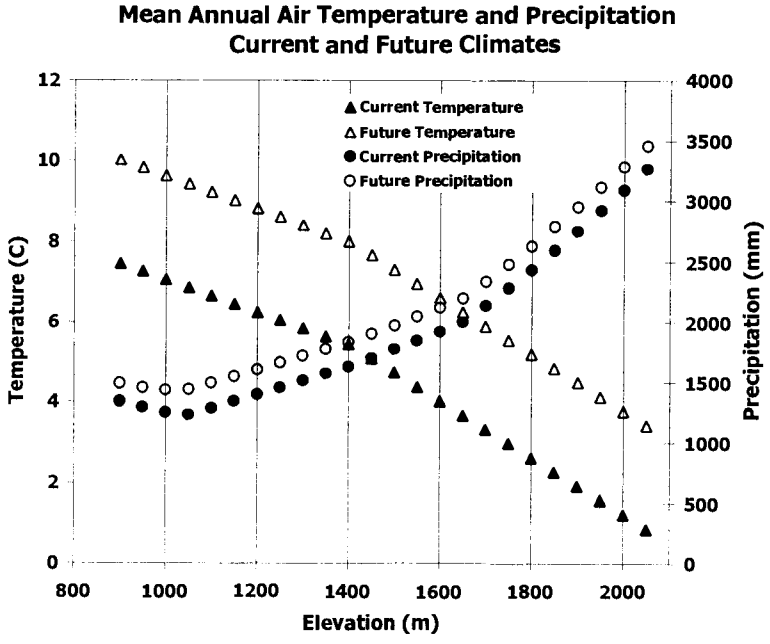

3.3.3 Leaf Area Scenarios

The current and future climate scenarios were used previously to generate representative leaf area index values for the American River basin (Waichler, in submission [Ch. 2]). A set of Distributed Hydrology-Biogeochemistry model (DHB) structures was previously applied to idealized north- and south-facing hillslopes, and LAI values were generated for conifer vegetation type at 50 m intervals within the elevation range of the watershed. The LAI output from a model structure based on DHSVM hydrology at a 3 hr timestep and BGC carbon and nitrogen cycling at a daily timestep are used here.

Month	Tmin	Tmax	Precip	Shortwave Radiation	Longwave Radiation	Relative Humidity
Oct	1.5	0.8	19.6%	-10.0%	3.7%	2.0%
Nov	5.1	3.3	11.5%	-12.1%	10.2%	0.0%
Dec	6.2	3.4	18.7%	-9.2%	10.8%	-0.9%
Jan	0.6	1.2	-10.3%	4.4%	1.8%	0.1%
Feb	4.1	3.7	-0.3%	-1.6%	7.7%	-0.5%
Mar	6.0	3.3	22.7%	-3.8%	9.8%	-1.6%
Apr	3.7	2.3	21.5%	-6.5%	6.9%	-1.8%
May	2.4	2.4	-4.1%	-1.5%	4.7%	-7.6%
Jun	2.9	1.7	19.3%	-4.8%	5.5%	-0.3%
Jul	1.5	1.6	-10.0%	-0.7%	2.8%	-5.2%
Aug	1.4	0.3	98.3%	-5.0%	3.5%	9.6%
Sep	1.9	1.1	7.5%	-5.1%	4.8%	6.4%

Table 3.1 Monthly scalars for generating future climate from current climate.

LAI values were distributed from the idealized hillslope results to the full watershed using elevation, slope, and aspect classifications based on the digital elevation model. Eighteen LAI classes are used to represent the watershed, corresponding to 6 elevation bands, and 3 slope/aspect classes (Table 3.2). For north and south aspect classes, the LAI value assigned to each class is from the mean elevation of the range; for low-slope/east/west classes, the mean of the north and south values for the elevation was assigned to the class. Actual LAI distribution in the watershed is unknown, but simulated LAI values are consistent with plot-scale measurements for forests in similar environments (Cannell 1982).

The resulting mean LAI values for the full watershed and low- and high-elevation subbasins under the three climate scenarios are given in Table 3.3. The basin experiences a 15 percent decrease in leaf area under the Future/phys scenario because of decreased soil moisture during the growing season. If the CO_2 effect is included, the increased water use efficiency results in more primary productivity and a 7 percent increase in LAI. At lower elevations, LAI is primarily limited by soil moisture and LAI decreases under both future scenarios. At higher elevations where

vegetation growth is limited by both temperature and water, LAI increases 14 percent under Future/phys, and 40 percent under Future/phys+CO_2.

Class	Elevation (m)	Slope and Aspect	% Basin Area
1	849-1049	Slope>10 degrees, Aspect NW-NE ("North")	1.3%
2	1050-1249	"	4.0%
3	1250-1449	"	5.4%
4	1450-1649	"	6.4%
5	1650-1849	"	5.2%
6	1850-2102	"	1.4%
7	849-1049	Slope>10 degrees, Aspect SW-SE ("South")	1.1%
8	1050-1249	"	7.0%
9	1250-1449	"	9.8%
10	1450-1649	"	11.8%
11	1650-1849	"	10.5%
12	1850-2102	"	3.1%
13	849-1049	Slope<10 degrees, or Aspect SW-NW, NE-SE	3.4%
14	1050-1249	"	7.4%
15	1250-1449	"	6.1%
16	1450-1649	"	8.0%
17	1650-1849	"	6.3%
18	1850-2102	"	1.8%

Table 3.2 LAI classes and rationale for assigning values to American River, based on digital elevation model.

Watershed	Mean Elevation (m)	Current LAI	Future/ phys LAI	Future/ phys+CO_2 LAI	Change, Current to Future/phys	Change, Current to Future/ phys+CO_2
Entire basin	1469	7.7	6.6	8.2	-15%	+7%
Low subbasin	1027	7.7	6.0	7.6	-22%	-1%
High subbasin	1953	5.6	6.4	7.9	+14%	+40%

Table 3.3 Mean projected LAI under current and future climate scenarios. (Waichler, in submission [Ch. 2]).

Each scenario for watershed analysis therefore includes both the climate assumption and the corresponding LAI distribution that is consistent with that climate.

This is in contrast to the previous study by Leung and Wigmosta (1999), which assumed a uniform LAI value of 7.0 across the basin and for all climate scenarios. The uniform and mean simulated LAI values are similar, and the vegetation modeling supports the choice of LAI by Leung and Wigmosta (1999), who had started with a literature value and adjusted it somewhat during calibration. Although some canopy thinning at lower elevations and denser growth at higher elevations are predicted, changes in the mean basin value under future climates are modest.

3.3.4 Hydrologic Model

The Distributed Hydrology-Soil-Vegetation Model (DHSVM, Wigmosta et al. 1994) is a process-based hydrology model that computes vertical 1-D fluxes and 2-D water routing in a grid structure. Major modeled processes are canopy interception, evaporation, transpiration, canopy and ground snow accumulation and melt, vertical unsaturated water flow, and horizontal saturated groundwater flow. Major inputs are regular grids of elevation, soil type, soil thickness, and vegetation type, look-up tables of soil and vegetation biophysical parameter values, and time series tables of the climate variables air temperature, precipitation, wind speed, relative humidity, solar radiation, and longwave radiation.

For this study, climate input is provided via a time series file corresponding to the Morse Lake station, and local climate data is mapped to each cell during the model run using the vertical lapse rates for temperature and precipitation. No variation in climate based on horizontal position is assumed. Incoming solar radiation is adjusted according to topographic slope and aspect. A grid resolution of 100 m, and a timestep of 3 hours are used here. Except for treatment of future climate scenarios and LAI, all of the input parameters are the same as those used by Leung and Wigmosta (1999). The rest of this paper explores the hydrologic significance of the climate and leaf area scenarios.

3.4 Results

Mean daily streamflow at the watershed outlet is the primary data available for evaluating model performance. Both the simulation with uniform LAI and the simulation with variable LAI overpredict annual streamflow for WY1990-96, by 7 and 10 percent, respectively (Table 3.4). Under the future climate scenarios, ET and streamflow both increase in response to the warmer and wetter climate, while snow water content decreases. The increases in streamflow and evapotranspiration depend on LAI as well as the climate scenario. The relative increases between Future/phys and Future/phys+CO_2 switch depending on LAI scenario. If LAI is held constant, there is a smaller increase in evapotranspiration under Future/phys+CO_2, because water is conserved with the CO_2 effect. On the other hand, if LAI is allowed to increase with the future/phys+CO_2 climate, the larger increase in evapotranspiration occurs with the CO_2 effect.

		Uniform LAI			Variable LAI		
			Difference from Current			Difference from Current	
Variable	Observed	Current Climate	Future/ Phys	Future/ Phys+CO_2	Current Climate	Future/ Phys	Future/ Phys+CO_2
Temperature (C)	3.7	3.7	+2.7		3.7	+2.7	
Precipitation (mm)	1813	1813	+11%		1813	11%	
Streamflow (mm)	937	1007	+2%	+6%	1032	+8%	+1%
Evapotranspiration (mm)		830	+25%	+20%	804	+18%	+26%
Snow water equivalent (mm)		279	-79%	-79%	275	-79%	-78%

Table 3.4 Mean basin hydrologic flux and state variables. Future values represent increase or decrease over current climate for the particular LAI assumption (in degrees for temperature, percentages for others).

Following the annual results, the ability of the model to replicate daily streamflow is reasonable but not outstanding. One year from the 7-year hydrograph indicates that the simulations with uniform and variable leaf area are similar (Figure 3.4). Both simulations underpredict fall baseflow and some storm peaks, and

overpredict streamflow during spring snowmelt. For the entire 7-year period, R^2=0.77, and Nash and Sutcliffe (1970) efficiency=0.68. Further calibration beyond what was done in the previous study was attempted, but did not achieve significant gains. The direction of these flow regime errors is not consistent and the errors are opposite in sign during other years. Streamflow averaged by month over the 7 years shows that most of the simulated excess flow occurs during December-May, especially March and April, indicating that simulated precipitation is excessive (Figure 3.5). Despite the modest performance in simulating historical flow, the modeling exercise still provides an opportunity to examine relative differences between scenarios for a variety of hydrologic properties.

Figure 3.4 Daily streamflow, WY1991.

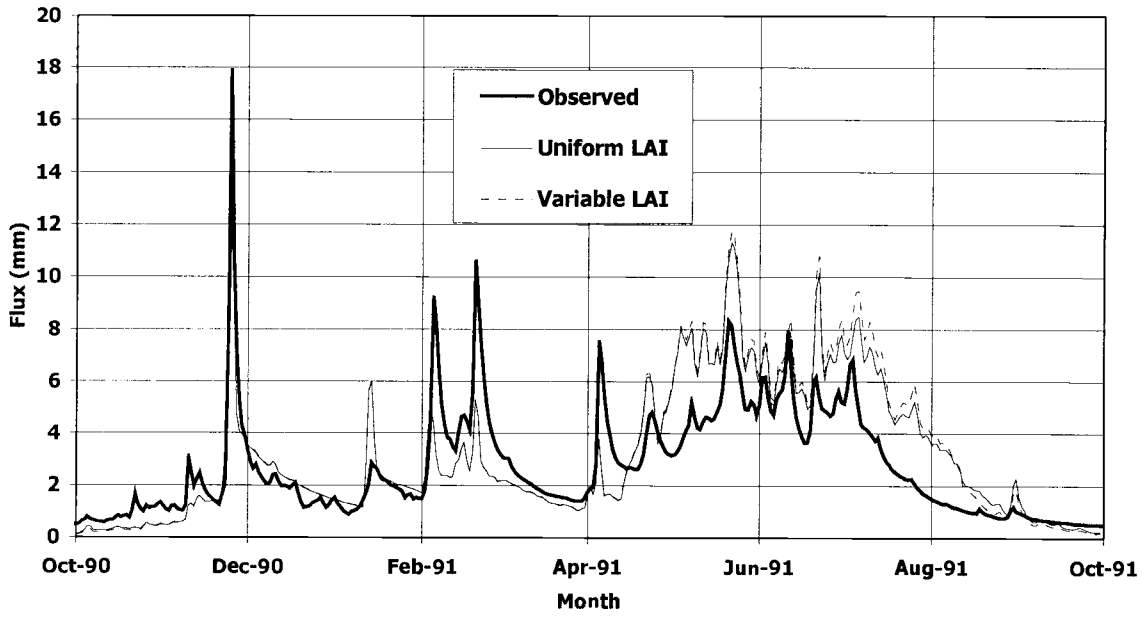

Figure 3.5 Mean monthly streamflow, WY1990-96.

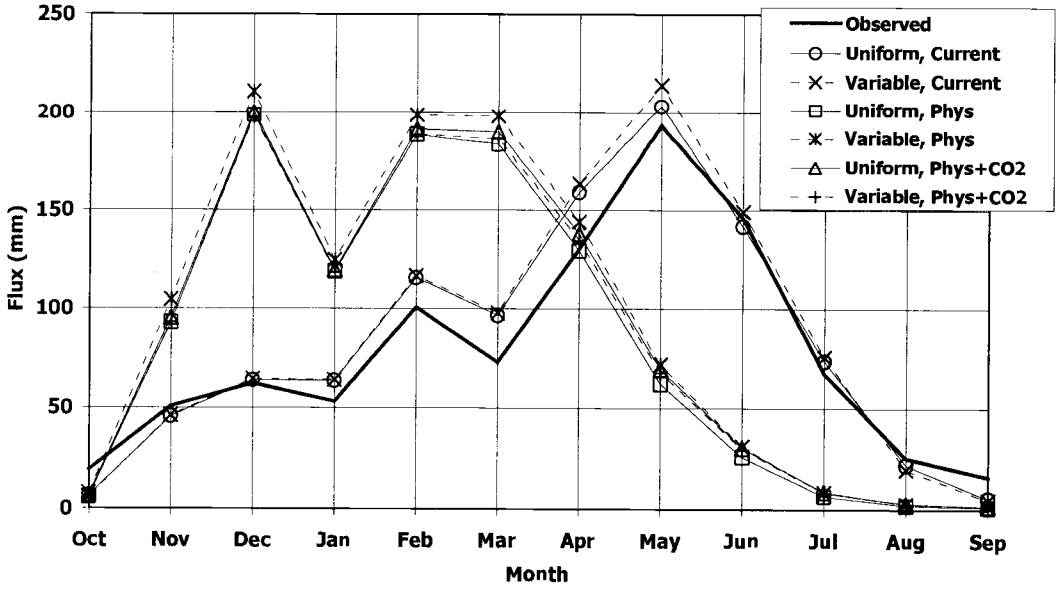

3.4.1 Monthly Averages, Full Basin

The major impact of the future scenarios on streamflow is a shift in the peak flow months from spring to winter (Figure 3.5). Under the warmer temperatures, winter snow accumulation is greatly reduced (Figure 3.6), and spring, summer, and early fall flows are much less, as was shown by Leung and Wigmosta (1999). Compared to this direct physical climate effect, the LAI and the CO_2 effects are minor. The odd-looking streamflow decrease for January in the future simulations is due to an anomaly in the RCM climate scenario for that month—mean temperature is close to observed climate, and precipitation is less (Table 3.1). The seasonal pattern in soil moisture also shows a shift to earlier in the year, with the period of soil drought beginning about 1-1/2 months earlier, and ending about the same time as current climate (Figure 3.7).

Although the major climate change effect is the direct physical one, some differences caused by the LAI and CO_2 effects are apparent in the component fluxes of evapotranspiration. Canopy evaporation (from intercepted water) is the predominant ET component, and depends on LAI. The qualitative difference between LAI decreasing under future physical climate, or increasing with the CO_2 effect included, leads to distinct canopy evaporation responses in the variable LAI simulations (Figure 3.8). Under the uniform LAI assumption, canopy evaporation is identical for both future climates because stomatal control plays no role in evaporation from a wet leaf surface.

The shift in timing and shape of monthly transpiration under the future climate scenarios indicates the growing season will start earlier, tail off more quickly, and end about one month earlier (Figure 3.9). Among the future scenarios, Uniform/physical has the largest transpiration flux because leaf area and water use efficiency are maintained from current climate.

Figure 3.6 Mean monthly snow water content, WY1990-96.

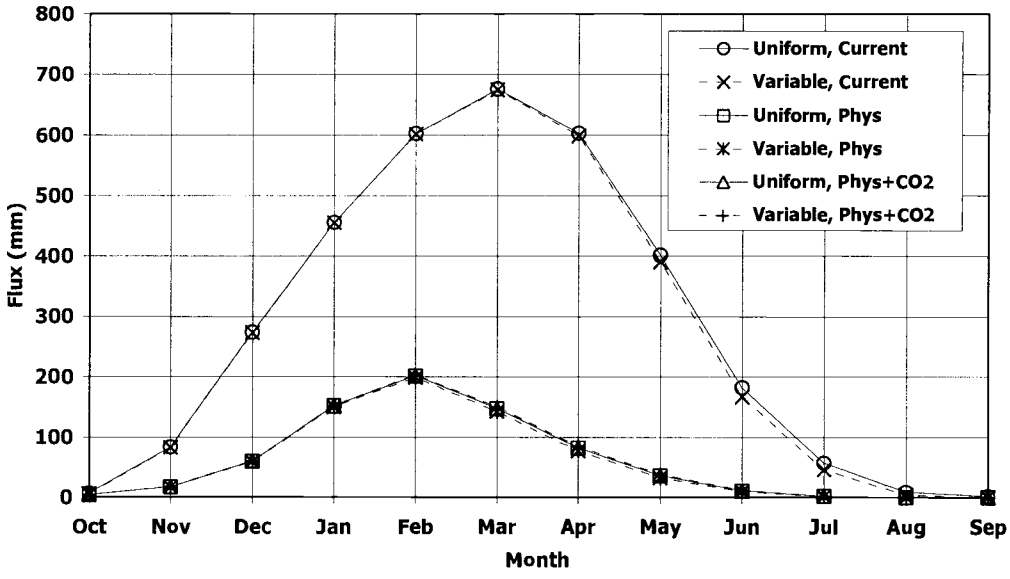

Figure 3.7 Mean monthly root zone soil water content, WY 1990-96.

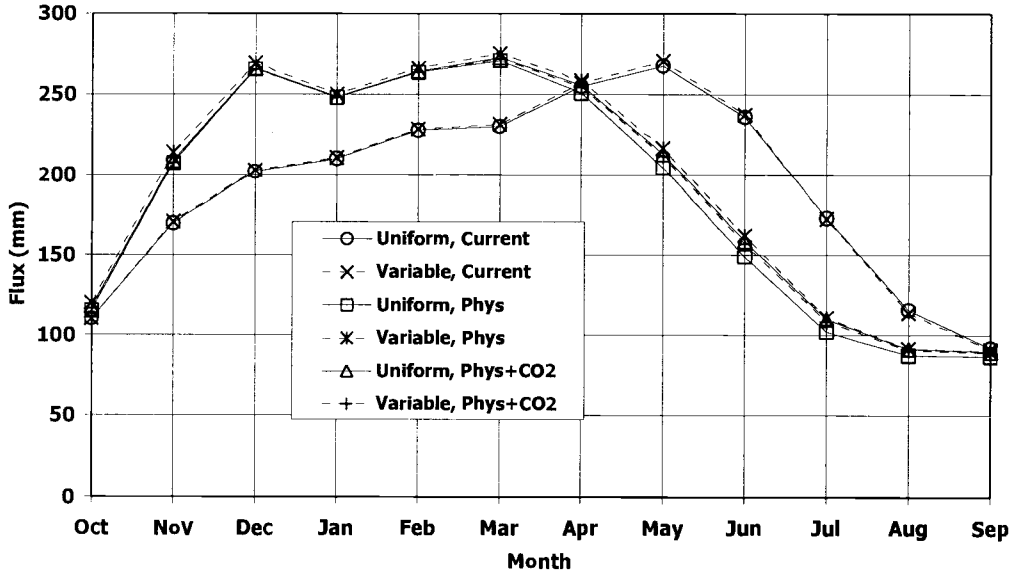

Figure 3.8 Mean monthly canopy evaporation, WY 1990-96.

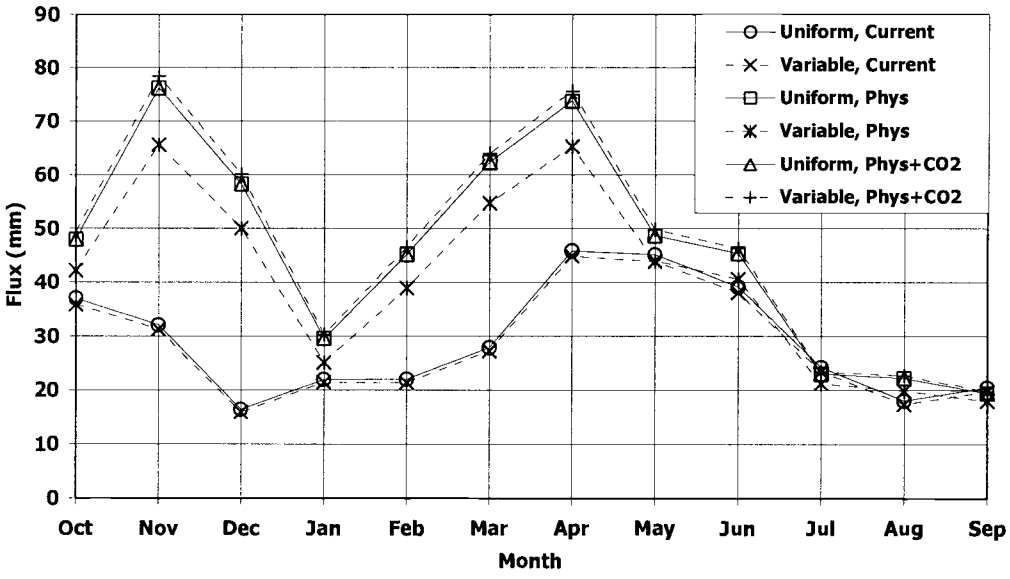

Figure 3.9 Mean monthly transpiration, WY 1990-96.

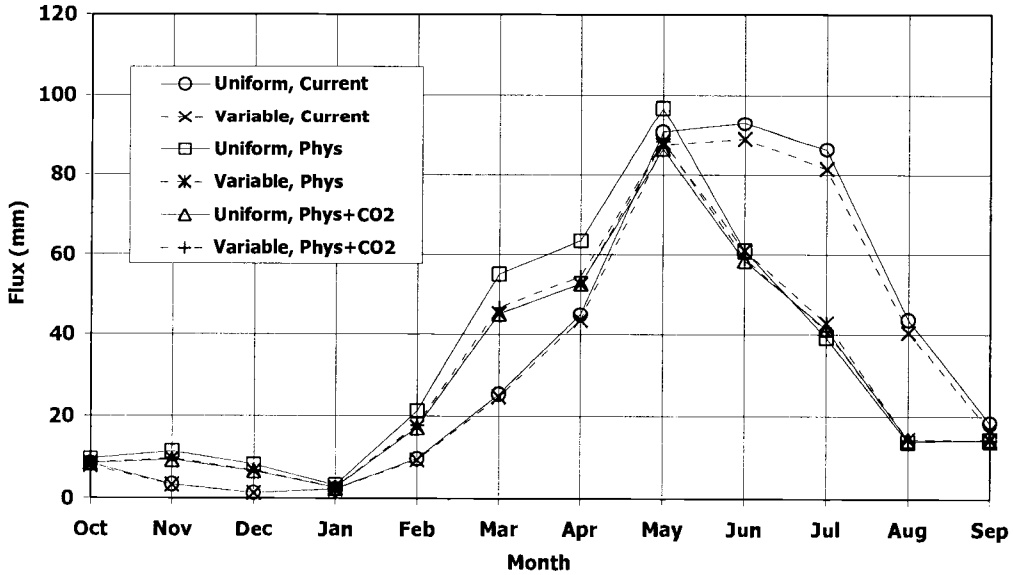

Soil evaporation is greatest under the Variable/physical scenario because this scenario has the lowest LAI, so more radiation is able to reach the ground surface, and there is less competition from transpiration for available soil moisture (Figure 3.10). Reflecting the net effect of the previous fluxes, total evapotranspiration is greatest under the Uniform/physical scenario, and least under the Variable/physical scenario (Figure 3.11).

3.4.2 Monthly Averages in Low- and High-Elevation Subbasins

Climate lapsing with elevation results in very different hydrologic responses between low- and high-elevation subbasins. Maximum ET occurs in May at low elevation, but in July at high elevation (Figure 3.12, 3.13). Variable LAI is much lower than the uniform value at high elevation, resulting in lower ET for Variable/current. Under the future physical+CO_2 scenario, Uniform and Variable LAI result in similar ET because of compensating changes in the ET component fluxes. At low elevation there is much less runoff per unit area, and most of it occurs during the winter (Figure 3.14). In contrast, high elevation runoff is modest until snowmelt begins in earnest during April (Figure 3.15). Most of the climate change impact on streamflow occurs as a result of altered conditions at higher elevations.

Figure 3.10 Mean monthly soil evaporation, WY 1990-96.

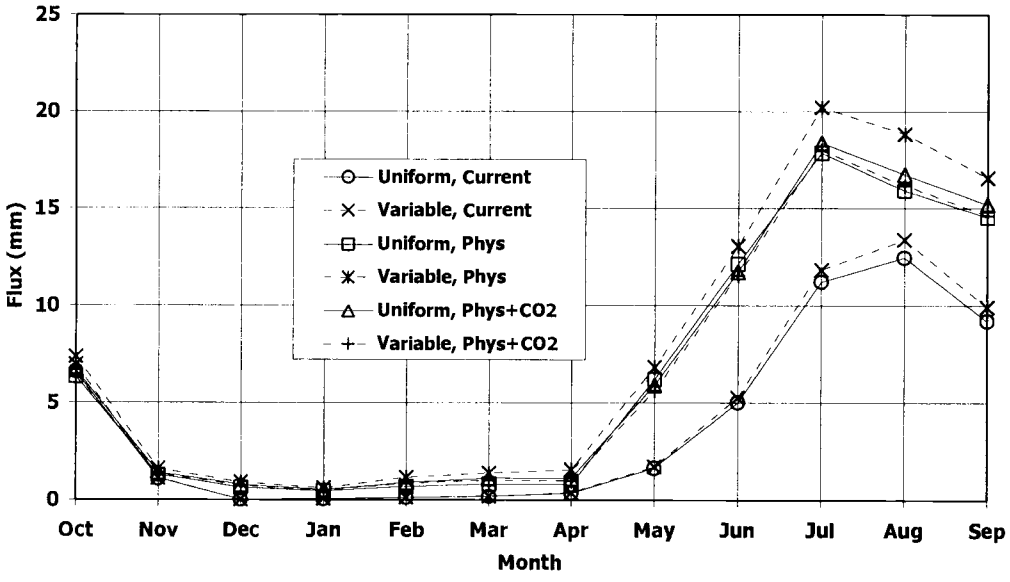

Figure 3.11 Mean monthly evapotranspiration, WY-1990-96.

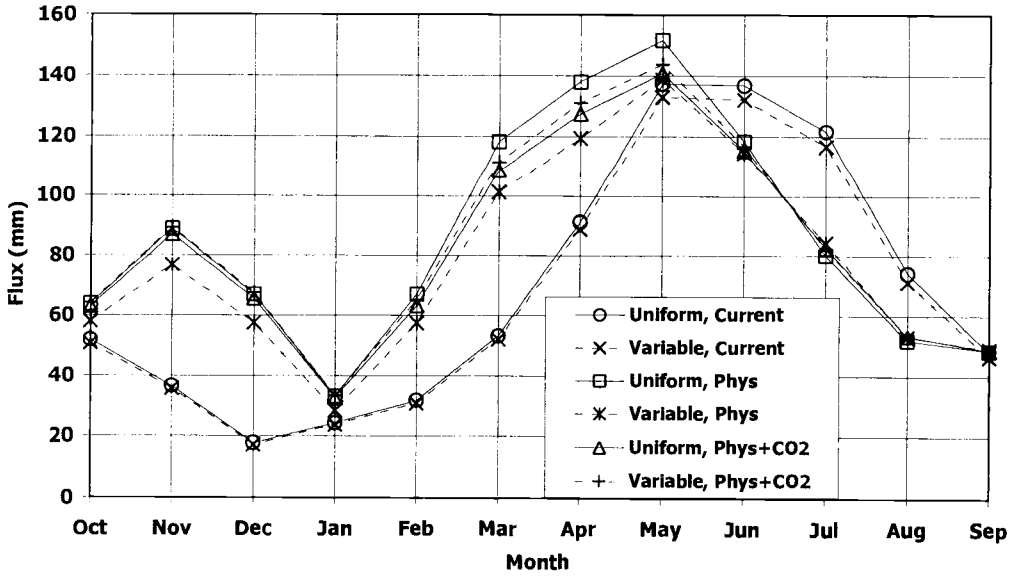

Figure 3.12 Mean monthly evapotranspiration, low elevation subbasin, WY1990-96.

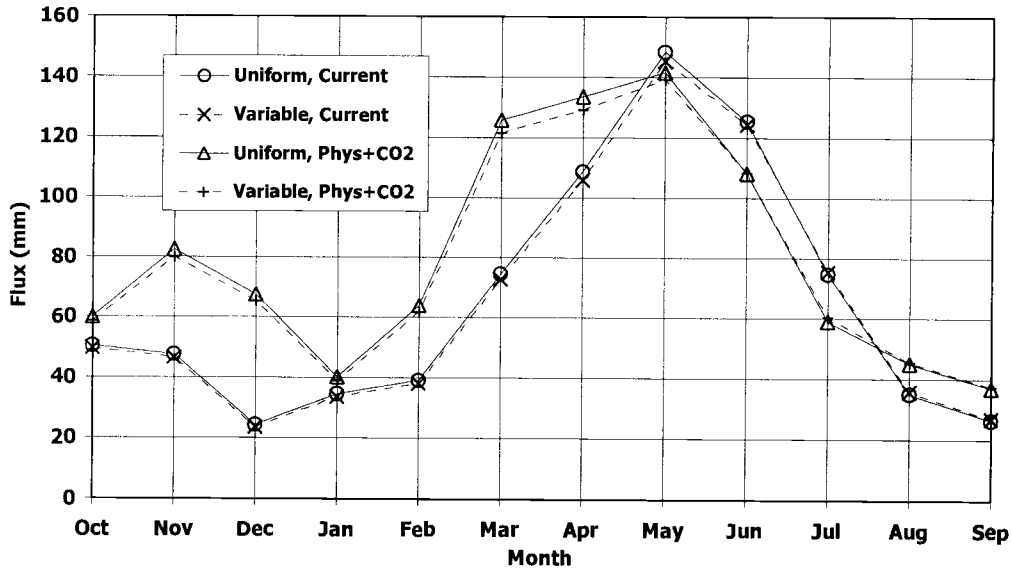

Figure 3.13 Mean monthly evapotranspiration, high elevation subbasin, WY1990-96.

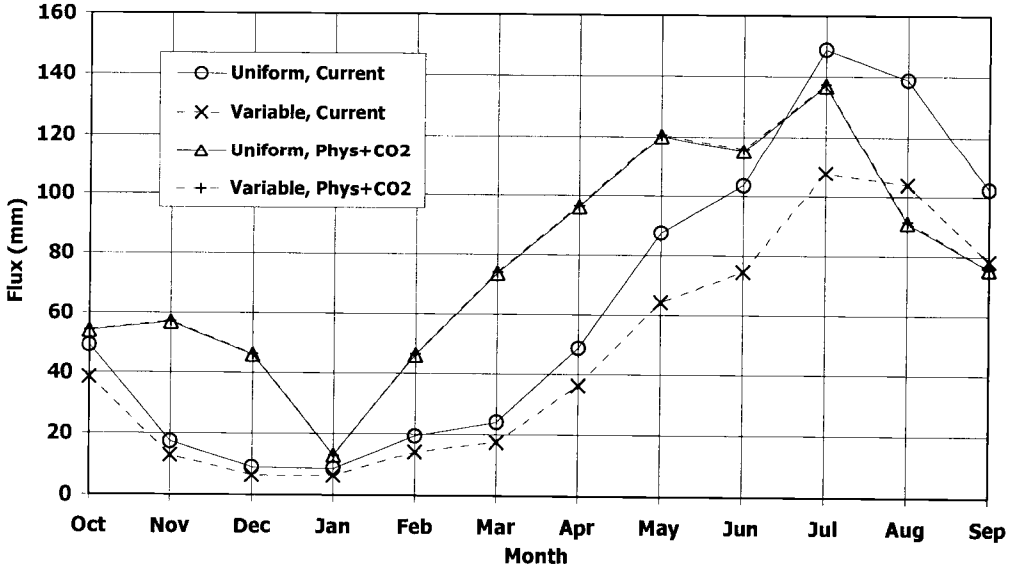

Figure 3.14 Mean monthly streamflow, low elevation subbasin, WY1990-96.

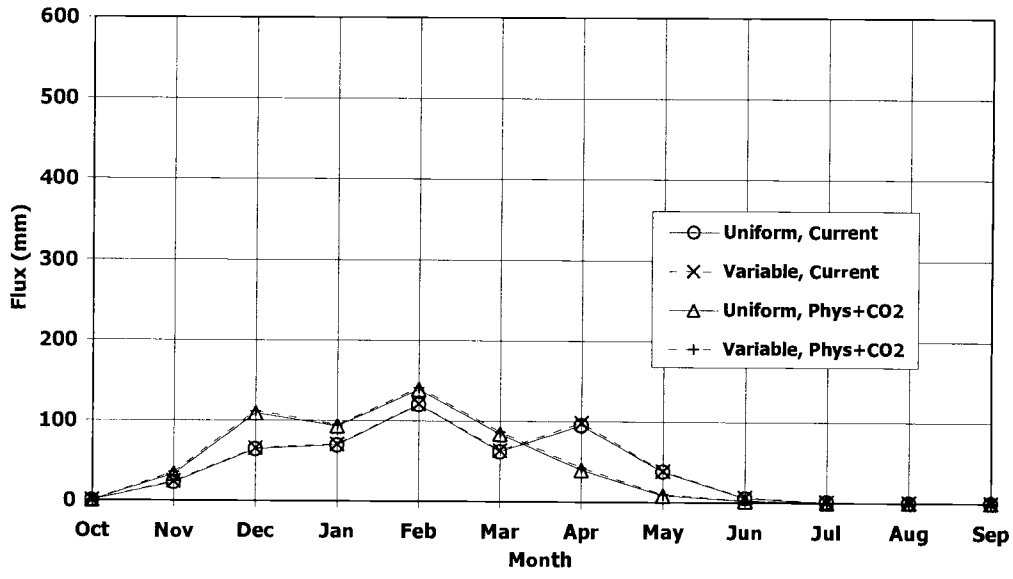

Figure 3.15 Mean monthly streamflow, high elevation subbasin, WY1990-96.

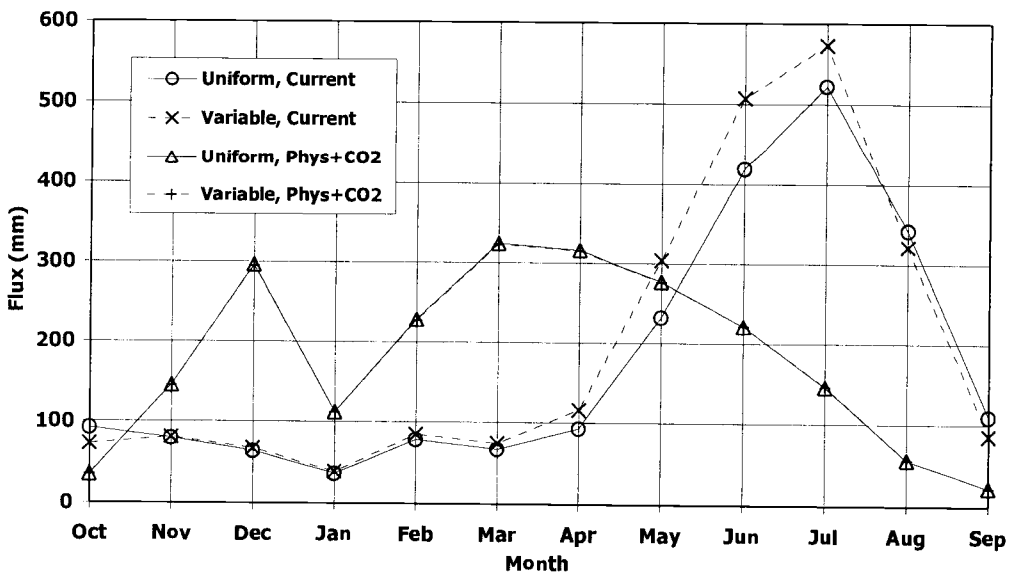

3.5 Discussion

The over prediction of streamflow for current climate is probably caused by error in the precipitation field. The simple approach for distributing precipitation, based on lapsing values vertically from a single station, may lead to significant error in the basin mean. The Morse Lake weather station is located in the western part of the basin, so a horizontal gradient in precipitation caused by the rain shadow effect is likely, and would result in decreased mean basin precipitation. Future modeling will likely use horizontal lapse rates derived from monthly PRISM precipitation output for the state of Washington (Daly et al. 1994), which would tend to decrease precipitation. However, it should also be noted that no adjustment for undercatch was made to the data, which would increase input precipitation.

Given that model simulation of historical streamflow is only fair, the main value of the simulations is to generate hypotheses and suggest methodology improvements for future work, rather than prediction of climate change impacts. The differences in streamflow and evapotranspiration between the Uniform and Variable LAI cases are probably much smaller than the uncertainty of the physical climate and CO_2 change. One could conclude that for this type of montane PNW watershed, the direct climate change impacts are much more significant than second-order effects due to altered LAI. This is especially apparent in the across-the-board reduction in mean snow water equivalent. However, if uncertainty of the climate input can be reduced, the variability in LAI across the watershed and with climate would merit additional attention. The relative increases in streamflow and ET depend on LAI as well as climate scenario. Among the scenario pairs, Uniform/physical and Variable/physical+CO_2 yield similar ET and streamflow response; as do Uniform/physical+CO_2 and Variable/physical. These pairs of similar response result from two compensating mechanisms: reduced transpiration per LAI, and higher LAI. The decrease in stomatal conductance is offset by the increase in leaf area. This symmetry would probably not hold as well in environments with lower LAI. In drier environments such as grassland or savannah, where LAI<3, changes in LAI would be proportionally greater, and have more hydrologic impact than they do in this forest

setting. If extended to drier climates, a similar analysis of hydrology would probably yield greater sensitivity to LAI variability.

The LAI scenarios for this study were generated previously by another model over a limited spatial domain. To the extent that LAI variation within the watershed is significant, its simulation in the future would benefit from application of a model like DHB to the entire basin so that LAI conforms more exactly to local environmental conditions. This approach would generate LAI and hydrologic fluxes in a fully dynamic way over the entire watershed. The results here suggest that such detail is not warranted for the American River setting, with its humid climate and relatively narrow range of LAI values.

The partitioning of ET into its components under current climate is similar to field observations under current climate, but shifts under climate change. For example, canopy evaporation is 19 percent of precipitation (42% of ET) for the Uniform/current simulation, while transpiration is 48 percent. Mature PNW conifer forest in a cool, wet environment loses about 15 percent of annual precipitation to canopy evaporation (Rothacher 1963); mature evergreen beech forest in a somewhat warmer climate loses about 29 percent (Rowe 1983). The increased LAI under Variable/physical+CO_2 results in canopy evaporation becoming more dominant, at 28 percent of precipitation (56% of ET).

Vegetation change is of interest for many other reasons apart from hydrology of course, for example wildlife habitat, timber resources and carbon cycling. The drive for integrated assessments that delve into areas such as these will encourage more study of regional hydrology-vegetation interaction.

3.6 Conclusions

Previously, Leung and Wigmosta (1999) identified a shift to warmer temperatures and the resulting change to snowpack and streamflow timing as being the most significant impacts of a future GCM/RCM climate scenario on the American River watershed. This study asks whether leaf area and physiology changes in

response to the future climate and an atmosphere enriched in CO_2 could potentially change the basic assessment for this watershed. Even though mean LAI decreases 15 percent under physical climate change only, and increases 7 percent under climate change that includes a CO_2 effect on vegetation, the direct physical effect of climate change predominates in terms of hydrologic impact. In response to increased precipitation and temperatures, streamflow and evapotranspiration increase under all LAI assumptions. The effect of higher LAI on ET is offset by reduced transpiration if a CO_2 effect on stomatal conductance is included. In applications to drier watersheds where base LAI is lower, the feedback effect of LAI on hydrology would probably be more significant.

3.7 Acknowledgments

Support for this research was provided by the US EPA Regional Hydrologic Vulnerability to Climate Change Program, the U.S. Forest Service, and the Department of Bioresource Engineering, Oregon State University. I thank Mark Wigmosta for providing American River data and valuable insights into DHSVM.

3.8 References

Cannell, M.G.R. 1982. World Forest Biomass and Primary Production Data. Academic Press, London. 391 pp.

Daly, C., R.P. Neilson, and D.L. Phillips. 1994. A statistical-topographic model formapping climatological precipitation over mountainous terrain. Journal of Applied Meteorology 33: 140-158.

Kiehl, J.T., J.J. Hack, G.B. Bonan, B.A. Boville, B.P. Briegleb, D.L.Williamson, and P.J.Rasch. 1996. Description of the NCAR Community Climate Model (CCM3).

Leung, L.R. and S.J. Ghan. 1999a. Pacific Northwest Climate Sensitivity Simulated by a Regional Climate Model Driven by a GCM. Part II: $2xCO_2$ Simulations. Journal of Climate 12(7), 2031-2058.

Leung, L.R. and S.J. Ghan. 1999b. Pacific Northwest Climate Sensitivity Simulated by a Regional Climate Model Driven by a GCM. Part I: Control Simulations. Journal of Climate 12(7), 2010-2030.

Leung, L.R. and M.S. Wigmosta. 1999. Potential climate change impacts on mountain watersheds in the Pacific Northwest. Journal of the American Water Resources Association 35, 1-9.

Wigmosta, M.S., L.W. Vail, and D.P. Lettenmaier. 1994. A distributed hydrology-vegetation model for complex terrain. Water Resources Research 30, 1665-1679.

4 SUMMARY

Climate change in the Pacific Northwest may substantially alter current vegetation distributions and hydrology in the region. Two of the commonly cited climate impacts are increased mean annual temperature in the range of 2-4 C, and increased precipitation in the range of 5-15 percent. Altered temperature has the larger impact on vegetation, according to the literature and the simulations done here. A warmer climate would result in shifting vegetation zones, and high-elevation parkland could be substantially replaced by closed forest. Altered temperature also would have the larger impact on hydrology because of the critical role played by the snowpack reservoir in the region's water resources. This study examined the potential interaction of vegetation and hydrology under climate change through the development and application of a new hydrology-biogeochemistry model (DHB) to the American River, a Cascade watershed.

DHB unites an advanced three-dimensional, grid-based hydrology model (DHSVM) with a leading biogeochemistry model (Biome-BGC). The purpose of the coupling is similar to that of patch-based RHESSys: provide a realistic landscape soil moisture distribution to simulation of vegetation, and provide realistic, space- and time-varying vegetation to simulation of hydrology. Both of the original models simulate vertical 1-D hydrologic processes, so overlapping functionality is handled such that alterations to model sensitivity are made clear. This prototype version of DHB preserves options for model structure, including the choice of DHSVM or BGC vertical 1-D hydrology, presence or absence of 2-D water routing, and length of hydrology timestep. To obtain the clearest signal from each of the parameterization options, DHB is applied to a simple grid representing an idealized hillslope and climate conditions from the American River. The idealized hillslope also permits a straightforward comparison of effects due to lapsed climate (by elevation), different radiation loading (by aspect), and a simple water-routing scheme. Leaf area index (LAI) and major hydrologic properties vary with model parameterization as much as they do by elevation or aspect. However, reasonable LAI values are produced by

model versions with BGC hydrology or DHSVM hydrology with 2-D water routing. In the American River climate, LAI is water-limited at low to medium elevations, and temperature-limited at high elevations. Model structures with downslope, 2-D water routing have higher mean soil moisture and support more LAI in the moisture-limited elevations. A 3-hr timestep in DHSVM hydrology leads to more LAI than a 24-hr timestep because snowmelt and soil evaporation are more favorable for growing season transpiration at 3-hr. South-facing slopes have higher steady-state LAI than north-facing slopes in the model. Model structures with DHSVM 1-D hydrology but no water routing are inadequate for simulating vegetation and hydrology simultaneously. Model structures with BGC hydrology are also inadequate in their current form because they have erroneous interception and snowmelt functions.

Two future climate scenarios were used in the simulations. The first includes physical effects only, which are obtained from previously published regional climate scenarios. The second includes physiological effects that may result from doubling CO_2 concentration in the atmosphere with resulting reduction in stomatal conductance. Among model parameterizations there is some variation in the qualitative response of mean LAI to a $2xCO_2$ physical climate change scenario, but all versions predict increased mean LAI under a future scenario that includes the CO_2 physiological effect. The largest increases took place at high elevation, suggesting that sparse forest in alpine areas could become much denser under climate change.

The large number of parameters in DHB makes a formal sensitivity analysis very difficult, if not impossible. Two key parameters, soil thickness and nitrogen input rate, were tested in a simple scheme and found to have sensitivity similar to choice of model parameterization. As expected, LAI had a positive relationship to both nitrogen input rate (where the system was not already saturated), and soil thickness (because of soil water holding capacity).

The simple hillslope simulations provided a way to evaluate model sensitivity and efficiently generate representative LAI scenarios consistent with the American River terrain and climate. Next, the potential impact of changing LAI and physiology under climate change was explored in the context of the full watershed using DHSVM

as a stand-alone hydrology model. LAI results from the Slope/DHSVM/3hr simulation on the simple hillslope grid were mapped to the full American River watershed using a classification scheme based on the DEM. Six elevation bands and three slope/aspect types for a total of 18 classes were used to classify the watershed and assign LAI values from the DHB hillslope results. Mean basin LAI decreased 15 percent under the future, physical only scenario, but increased 7 percent when CO_2 effects on physiology were included. The major hydrologic impact of the climate change at the watershed scale is reduced snowpack and altered runoff timing. In comparison with the direct physical effects, LAI and physiology change are relatively minor in overall impact on hydrology. Under the future scenarios, precipitation, streamflow, and evapotranspiration all increase, the amount of increases varying somewhat with LAI and climate assumptions. Increased LAI and decreased stomatal conductance are partially compensating mechanisms that make the outcome of the most complex treatment of climate change similar to the least complex treatment in this already dense forested environment. In drier environments such as grassland or savannah, changes in LAI would be proportionally greater, and have more hydrologic impact than they do in this forest setting. If extended to drier areas, a similar analysis of hydrology would probably yield greater sensitivity to LAI variability. Besides its hydrologic role, vegetation change is of interest for many other reasons as well of course, such as wildlife habitat, regional timber inventory, and carbon cycling. The drive for integrated assessments that delve into areas such as these will encourage more study of hydrology and vegetation interaction.

The best modeling strategy for such assessments will depend on needs, data availability, and even computing power, which still lags model requirements for many applications. Greater model complexity lends greater confidence that fundamental processes are being simulated, but at a cost of greater computational load and input requirements. Perhaps more application of models like DHB and RHESSys in formal comparisons, similar to the global vegetation modeling community's effort in VEMAP (Vegetation/Ecosystem Modeling and Analysis Project), would be a wise activity in the development of integrated watershed models. The most scientific and engineering

utility will be provided by integrated models when 1) the vegetation state is important for non-hydrology reasons; 2) it is less dense than closed forest; or 3) it is anticipated to change a great deal. Simpler watershed modeling schemes without integration may be more appropriate when these conditions are not met, or the grid resolution is larger than hillslope scales.

BIBLIOGRAPHY

Abbott, M.B. 1986a. An Introduction to the European Hydrological System—Systeme Hydrologique Europeen, "SHE"—1: History and Philosophy of a Physically-Based, Distributed Modelling System. Journal of Hydrology 87, 45-59.

Abbott, M.B. 1986b. An Introduction to the European Hydrological System—Systeme Hydrologique Europeen, "SHE"—2: Structure of a Physically-Based, Distributed Modelling System. Journal of Hydrology 87, 61-77.

Band, L.E., D.S. Mackay, I.F. Creed, R. Semkin, and D. Jeffries. 1996. Ecosystem processes at the watershed scale: Sensitivity to potential climate change. Limnology and Oceanography 41, 928-938.

Band, L.E., P. Patterson, R. Nemani, and S.W. Running. 1993. Forest ecosystem processes at the watershed scale: Incorporating hillslope hydrology. Agricultural and Forest Meteorology 63, 93-126.

Band, L.E., D.L. Peterson, S.W. Running, J. Coughlan, R. Lammers, J. Dungan, and R.Nemani. 1991. Forest ecosystem processes at the watershed scale: Basis for distributed simulation. Ecological Modelling 56, 171-196.

Beven, K. 1997. TOPMODEL: A Critique. Hydrological Processes 11, 1069-1085.

Bristow, K.L. and G.S. Campbell. 1984. On the relationship between incoming solar radiation and daily maximum and minimum temperature. Agricultural and Forest Meteorology 31, 159-166.

Cannell, M.G.R. 1982. World Forest Biomass and Primary Production Data. Academic Press, London. 391 pp.

Cosby, B.J., G.M. Hornberger, R.B. Clapp, and T.R. Ginn. 1984. A statistical exploration of the relationships of soil moisture characteristics to the physical properties of soils. Water Resources Research 20, 682-690.

Daly, C., D. Bachelet, J.M. Lenihan, R.P. Neilson, W.J. Parton, and D.S. Ojima. 2000. Dynamic simulation of tree-grass interactions for global change studies. Ecological Applications 10(2): 449-469.

Daly, C., R.P. Neilson, and D.L. Phillips. 1994. A statistical-topographic model formapping climatological precipitation over mountainous terrain. Journal of Applied Meteorology 33: 140-158.

Dickinson, R.E., A. Henderson-Sellers, C. Rosenzweig, P.J. Sellers. 1991. Evapotranspiration models with canopy resistance for use in climate models, a review. Agriculture and Forest Meteorology 54, 373-388.

Dooge, J.C.I. 1992. Hydrologic models and climate change. Journal of Geophysical Research 97, 2677-2686.

Eamus, D. 1991. The interaction of rising CO_2 and temperatures with water use efficiency. Plant, Cell and Environment 14, 843-852.

Eamus, D. 1996a. Responses of field grown trees to CO_2 enrichment. Commonwealth Forestry Review 75(1), 39-47.

Eamus, D. 1996b. Tree responses to CO_2 enrichment: CO_2 and temperature interactions, biomass allocation and stand-scale modeling. Tree Physiology 16, 43-47.

Fagre, D.B., P.L. Comanor, J.D. White, F.R. Hauer, and S.W. Running. 1997. Watershed responses to climate change at Glacier National Park. Journal of the American Water Resources Association 33, 755-765.

Feddes, R.A., P.J. Kowalik, H. Zaradny. 1978. Simulation of Field Water Use and Crop Yield. Wiley and Sons, New York, 188 p.

Franklin, J.F., F.J. Swanson, M.E. Harmon, D.A. Perry, T.A. Spies, V.H. Dale, A. McKee, W.K. Ferrell, J.E. Means, S.V. Gregory, J.D. Lattin, T.D. Schowalter, and D. Larsen. 1992. Effects of Global Climatic Change on Forests in Northwestern North America.

Gleick, P.H. and E.L. Chalecki. 1999. The impacts of climatic changes for water resources of the Colorado and Sacramento-San Joaquin River basins. Journal of the American Water Resources Association 35(6), 1429-1441.

Hamlet, A.F., and D.P. Lettenmaier. 1999. Effects of climate change on hydrology and water resources in the Columbia River basin. Journal of the American Water Resources Association 35(6), 1597-1623.

Hay, L.E., R.J.L. Wilby, and G.H. Leavesley. 2000. A comparison of delta change and downscaled GCM scenarios for three mountainous basins in the United States. Journal of the American Water Resources Assoc. 36(2), 387-397.

Hicks, B.J., R.L. Beschta, and R.D. Harr. 1991. Long-term changes in streamflow following logging in Western Oregon and associated fisheries implications. Water Resources Bulletin 27, 217-226.

Houghton, J.T., L.G. Meira Filho, B.A. Callander, N. Harris, A. Kattenberg, and K. Maskell (Editors). 1996. Climate Change 1995: The Science of Climate Change. Contribution of Working Group I to the Second Assessment Report of the Intergovernmental Panel on Climate Change. Cambridge University Press, Cambridge, U.K.

Hurd, B., N. Leary, R. Jones, J. Smith. 1999. Relative regional vulnerability of water resources to climate change. Journal of the American Water Resources Association 35(6), 1399-1409.

Jones, J.A. and G.E. Grant. 1996. Peak flow responses to clearcutting and roads in small and large basins, western Cascades, Oregon. Water Resources Research 32, 959-974.

Kelliher, F.M., R. Leuning, and E.-D. Schulze. 1993. Evaporation and canopy characteristics of coniferous forests and grasslands. Oecologia 95, 153-163.

Kelliher, F.M., R. Leuning, M.R. Raupach, E.-D.Schulze. 1995. Maximum conductances for evaporation from global vegetation types. Agricultural and Forest Meteorology 73, 1-16.

Keppeler, E.T. and R.R. Ziemer. 1990. Logging effects on streamflow: Water yield and summer low flows at Caspar Creek in northwestern California. Water Resources Research 26, 1669-1679.

Kiehl, J.T., J.J. Hack, G.B. Bonan, B.A. Boville, B.P. Briegleb, D.L. Williamson, and P.J. Rasch. 1996. Description of the NCAR Community Climate Model (CCM3).

Kite, G. 1998. Integration of forest ecosystem and climatic models with a hydrologic model. Journal of the American Water Resources Association 34, 743-753.

Kremer, R.G. and S.W. Running. 1996. Simulating seasonal soil water balance in contrasting semi-arid vegetation communities. Ecological Modelling 84, 151-162.

Leavesley, G.H. 1994. Modeling the effects of climate change on water resources-a review. Climatic Change 28, 159-178.

Leavesley, G.H., R.W. Lichty, B.M. Troutman, and L.G. Saindon. 1983. Precipitation-Runoff Modeling System: User's Manual: U.S. Geological Survey Water-Resources Investigations Report 83-4238, 207 p.

Leavesley, G.H., P.J. Restrepo, S.L. Markstrom, M. Dixon, and L.G. Stannard. 1996. The modular modeling system - MMS: User's manual: U.S. Geological Survey Open File Report 96-151, 200 p.

Leung, L.R. and S.J. Ghan. 1999a. Pacific Northwest Climate Sensitivity Simulated by a Regional Climate Model Driven by a GCM. Part II: $2xCO_2$ Simulations. Journal of Climate 12(7), 2031-2058.

Leung, L.R. and S.J. Ghan. 1999b. Pacific Northwest Climate Sensitivity Simulated by a Regional Climate Model Driven by a GCM. Part I: Control Simulations. Journal of Climate 12(7), 2010-2030.

Leung, L.R. and M.S. Wigmosta. 1999. Potential climate change impacts on mountain watersheds in the Pacific Northwest. Journal of the American Water Resources Association 35, 1-9.

McCabe, G.J., and D.M. Wolock. 1999. *Journal of the American Water Resources Association* 35(6), 1473-1484.

Mackay, D.S. and L.E. Band. 1997. Forest ecosystem processes at the watershed scale: dynamic coupling of distributed hydrology and canopy growth. Hydrological Processes 11, 1197-1217.

Miles, E.L., A.K. Snover, A.F. Hamlet, B. Callahan, D. Fluharty. 2000. Pacific Northwest Regional Assessment: The impacts of climate variability and climate change on the water resources of the Columbia River basin. Journal of the American Water Resources Association 36(2), 399-420.

Naches Ranger District. 1998. Bumping/American Watershed Analysis. Wenatchee National Forest, U.S. Forest Service.

Neilson, R.P. 1995. A model for predicting continental-scale vegetation distribution and water balance. Ecological Applications 5, 362-385.

Neilson, R.P., and R.J. Drapek. 1998. Potentially complex biosphere responses to transient global warming. Global Change Biology 4, 505-521.

Neilson, R.P. and S.W. Running. 1996. Global dynamic vegetation modelling: coupling biogeochemistry and biogeography models. Pages 451-465 in B. Walker and W. Steffen, editors. Global Change and Terrestrial Ecosystems. Cambridge University Press, Cambridge.

Nemani, R., L. Pierce, S. Running, and L. Band. 1993. Forest ecosystem processes at the watershed scale: sensitivity to remotely-sensed Leaf Area Index estimates. International Journal of Remote Sensing 14, 2519-2534.

Nemani, R.R. and S.W. Running. 1989. Testing a theoretical climate-soil-leaf area hydrologic equilibrium of forests using satellite data and ecosystem simulation. Agricultural and Forest Meteorology 44, 245-260.

Pan, Y.D., J.M. Melillo, A.D. McGuire, D.W. Kicklighter, L.F. Pitelka, K. Hibbard, L.L. Pierce, S.W. Running, D.S. Ojima, W.J. Parton, and D.S. Schimel. 1998. Modeled responses of terrestrial ecosystems to elevated atmospheric CO_2: a comparison of simulations by the biogeochemistry models of the

Vegetation/Ecosystem Modeling and Analysis Project (VEMAP). Oecologia 114, 389-404.

Parton, W.J., D.S. Schimel, C.V. Cole, and D.S. Ojima. 1987. Analysis of factors controlling organic matter levels in Great Plains grasslands. Soil Science of America Journal 51:1173-1179.

Rothacher, J. 1963. Net Precipitation under a Douglas-fir Forest. Forest Science 9(4), 423-429.

Rowe, L.K. 1983. Rainfall interception by an evergreen beech forest, Nelson, New Zealand. Journal of Hydrology 66, 143-158.

Running, S.W. 1994. Testing FOREST-BGC ecosystem process simulations across a climatic gradient in Oregon. Ecological Applications 4, 238-247.

Running, S.W., R.R.Nemani, and R.D.Hungerford. 1987. Extrapolation of synoptic meteorological data in mountainous terrain, and its use for simulating forest evapotranspiration and photosynthesis. Canadian Journal of Forest Research 17, 472-483.

Running, S.W. and J.C. Coughlan. 1988. A general model of forest ecosystem processes for regional applications I. Hydrological balance, canopy gas exchange and primary production processes. Ecological Modelling 42, 125-154.

Running, S.W. and S.T. Gower. 1991. FOREST-BGC, A general model of forest ecosystem processes for regional applications II. Dynamic carbon allocation and nitrogen budgets. Tree Physiology 9 147-160.

Running, S.W. and R.R. Nemani. 1991. Regional hydrologic and carbon balance responses of forests resulting from potential climate change. Climatic Change 19, 349-368.

Sendek, K.H., R.M. Rice, and R.B. Thomas. 1990. Logging effects on streamflow: Storm runoff at Caspar Creek in northwestern California. Water Resources Research 26, 1657-1667.

Storck, P.A., L. Bowling, P. Wetherbee, and D.P. Lettenmaier. 1998. Application of a GIS based distributed hydrologic model for the prediction of forest harvest effects of peak flow in the Pacific Northwest. Hydrological Processes 12, 889-904.

Tague, C.L. and L.E. Band. 2000a. Evaluating explicit and implicit routing for watershed hydro-ecological models of forest hydrology at the small catchment scale. Hydrological Processes (in press).

Tague, C.L. and L.E. Band. 2000b. Simulating the impact of road construction and forest harvesting on hydrologic response. Earth Surface Processes and Landforms (in press).

Teklehaimanot, Z. and P.G. Jarvis. 1991. Direct measurement of evaporation of intercepted water from forest canopies. Journal of Applied Ecology 28, 603-618.

Thornton, P.E. 1998. Regional ecosystem simulation: combining surface- and satellite-based observations to study linkages between terrestrial energy and mass budgets. Ph.D. thesis, University of Montana (Missoula).

Urban, D.L., M.E. Harmon, and C.B. Halpern. 1993. Potential response of Pacific Northwestern forests to climatic change, effects of stand age and initial composition. Climatic Change 23, 247-266.

VEMAP. 1995. Vegetation/ecosystem modeling and analysis project: Comparing biogeography and biogeochemistry models in a continental-scale study of terrestrial ecosystem responses to climate change and CO_2 doubling. Global Biogeochemical Cycles 9(4), 407-437.

IPCC. 1998. The Regional Impacts of Climate Change, An Assessment of Vulnerability, North America, Chapter 8. D.S. Shriner and R.B. Street, eds. Volume eds.: R.T. Watson, M.C. Zinyowera, R.H. Moss, and D.J. Dokken. A special report of IPCC Working Group II. Cambridge University Press, 517 p.

Vertessy, R., E. O'Loughlin, E. Beverly and T. Butt. 1994. Australian experiences with the CSIRO Topog model in land and water resources management. In: Proceedings of UNESCO International Symposium on Water Resources Planning in a Changing World, Karlsruhe, Germany, June 28-30, 1994, pp. III-135-144.

Waring, R.H. and S.W. Running. 1998. Forest Ecosystems, 2nd ed. Academic Press, San Diego, 370 pp.

Wemple, B.C., J.A. Jones, and G.E. Grant. 1996. Channel network extension by logging roads in two basins, western Cascades, Oregon. Water Resources Bulletin 32(6), 1195-1207.

White, J.D., S.W. Running, P.E. Thornton, R.E. Keane, K.C. Ryan, D.B. Fagre, and C.H. Key. 1998. Assessing simulated ecosystem processes for climate variability research at Glacier National Park, USA. Ecological Applications 8, 805-825.

Wigmosta, M.S., L.W. Vail, and D.P. Lettenmaier. 1994. A distributed hydrology-vegetation model for complex terrain. Water Resources Research 30, 1665-1679.

Wolock, D.M. and G.J. McCabe. 1999. Estimates of runoff using water-balance and atmospheric general circulation models. Journal of American Water Resources Association 35(6), 1341-1350.

APPENDICES

Appendix A1 General Considerations for Coupling DHSVM and BGC

"Hydrologic modeling is concerned with the accurate prediction of the partitioning of water among the various pathways of the hydrological cycle" (Dooge, 1992). This partitioning takes its simplest form in the basic water balance equation:

$$Q = P - ET +- S$$

where Q is runoff, P is precipitation, ET is evapotranspiration, and S is the change in storage. Every hydrologic and watershed model has this equation at heart, with additional complexity in the details according to modeling purpose, data availability, and spatial and temporal scales. Process-based, distributed-parameter models are the most suitable for coupling with biologic or chemical models, with the major limitation being data availability commensurate with the fine-scale resolution of the model (Leavesley, 1994).

Similar equations could be written for carbon and nitrogen:

$$ES = PSN - R - L \qquad \text{(carbon)}$$

and

$$ES = DEP - DN - L \qquad \text{(nitrogen)}$$

where ES is ecosystem storage, PSN is photosynthesis, R is respiration, L is leaching, DEP is nitrogen deposition and fixation, DN is denitrification. In the carbon and nitrogen equations, the storage term on the left-hand-side is emphasized. All of the terms are represented in BGC except L for carbon.

Appendix A2 Specific Issues in Coupling DHSVM and BGC

BGC v4.1 is designed for transient simulation and thus requires long spin-up times to achieve a steady-state vegetation when initial conditions are significantly different from the end state. While this is of no consequence for point model simulations, it is a serious limitation for incorporating BGC into a grid and processing thousands or tens of thousands of cells. At least 2500 years of simulated time were usually needed to achieve steady-state from "scorched earth" initial conditions consisting of minimal carbon and nitrogen pools. This time can be shortened somewhat by starting with significant carbon and nitrogen pools in soil, but limited testing showed that accidentally starting a grid cell with too much organic matter may require a long decay time to get down to the steady-state level. Addressing this issue further would be a fruitful area of model development.

Another logistical problem relevant to model coupling is storage of climate data in BGC. Daily climate and phenology information for an entire climate cycle are held in memory, rather than read in during the model run. The climate timeseries must be read in during initialization to support two functions: the generation of moving average temperature data, and daily phenology information. Both requirements stem from statistical studies of ecosystem as a function of long-term climate. The phenology module uses average climate and regression relationships from White et al. (1997) to define leaf-on and leaf-off dates. If climate at a given location is determined during the model run, as it is in DHSVM, then for a large grid one must either do some preprocessing, or use a different phenology scheme. An earlier version of DHB implemented a model phenology that eliminated the need to look forward, and was based solely on climate for today and previous days. However, problems with the results prompted the author to take a simpler approach that retained as much as possible of the existing model structure and logic. For this study, I decided it would be better to use it as is and try to obtain some information that would be helpful in going about its elimination in a future model engineering effort.

Both DHSVM and BGC simulate vertical 1-D hydrology with a process orientation, but their parameterizations are quite different. Some of the areas where

BGC hydrology differs from DHSVM are explained in Chapter 2. Other differences are listed in Table A-1.

Component	DHSVM	BGC
Interception	As rain or snow; day-to-day storage	As rain only, no overnight storage
Snow	Energy balance for both canopy and ground	Degree-day approach for ground only
Aerodynamic conductance	Computed using logarithmic and exponential profiles of wind speed	Default constant value
Canopy conductance	Factors: soil temperature, photosynthetically-active radiation (PAR), vapor pressure deficit, volumetric moisture content. CO_2 added for this study	Factors: minimum air temperature, PAR for sun and shade canopy fractions, vapor pressure deficit, matric potential, CO_2.
Projected LAI	Used for interception and radiation balance	Used for canopy conductance and radiation absorption
All-sided LAI	Used for canopy conductance	Used for interception

Table A-1 More differences between DHSVM and BGC vertical 1-D hydrology.

The C programming required to couple the models included the following tasks:

- New data structures were added to BGC to hold the existing structures in logical groups: Pointer structure for passing variables by reference; Grid structure for persistent spatial variables, Temporary structure for replaceable spatial variables, and Global structure for constants.
- Memory allocation and variable translation functions were added.
- Some vegetation properties in DHSVM were changed from constants in a look-up table to spatial variables.
- Runtime control for spin-up and climate ramping were added to DHSVM.
- A simple, non-hydraulic 2-D routing option was added to BGC.
- New hydrologic variables were added to DHSVM to facilitate direct comparison with BGC.
- BGC's main function was altered to be callable by DHSVM; and the function call and associated coded were added to DHSVM's main function.